Monitoring Survey at the Massachusetts Bay Disposal Site
September/October 2012

Disposal Area Monitoring System DAMOS

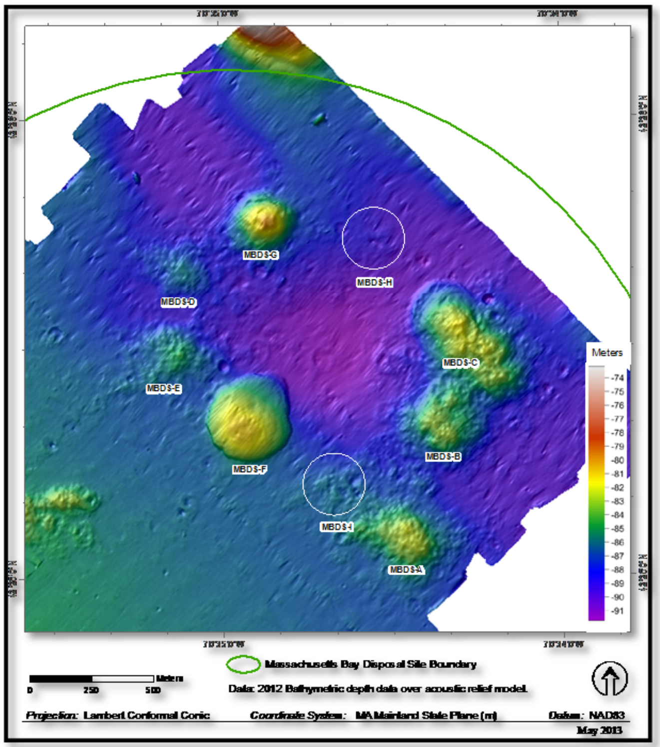

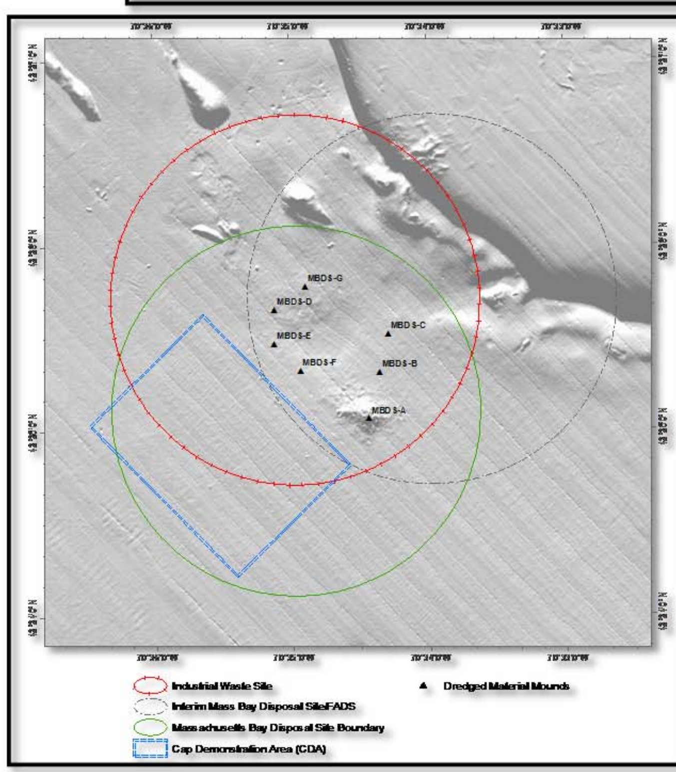

D A M O S
DISPOSAL AREA MONITORING SYSTEM

Contribution 195
December 2013

US Army Corps of Engineers®
New England District

This report should be cited as:

Carey, D. A.; Hickey, K.; Germano, J. D.; Read, L. B.; Esten, M. E. 2013. Monitoring Survey at the Massachusetts Bay Disposal Site September/October 2013. DAMOS Contribution No. 195. U.S. Army Corps of Engineers, New England District, Concord, MA, 87 pp.

REPORT DOCUMENTATION PAGE

form approved
OMB No. 0704-0188

1. AGENCY USE ONLY (LEAVE BLANK)

2. REPORT DATE
December 2013

3. REPORT TYPE AND DATES COVERED
FINAL REPORT

4. TITLE AND SUBTITLE
Monitoring Survey at the Massachusetts Bay Disposal Site September/October 2012

5. FUNDING NUMBERS

6. AUTHOR(S)
Drew A. Carey, Ken Hickey, Joseph D. Germano, Lorraine B. Read, Marie Evans Esten

7. PERFORMING ORGANIZATION NAME(S) AND ADDRESS(ES)
Battelle|Environmental Solutions
397 Washington Street
Duxbury, MA 02332

DAMOSVision
215 Eustis Avenue
Newport, RI 02840

8. PERFORMING ORGANIZATION REPORT NUMBER
DV-2013-003

9. SPONSORING/MONITORING AGENCY NAME(S) AND ADDRESS(ES)
US Army Corps of Engineers-New England District
696 Virginia Rd
Concord, MA 01742-2751

10. SPONSORING/MONITORING AGENCY REPORT NUMBER
Contribution No. 195

11. SUPPLEMENTARY NOTES
Available from DAMOS Program Manager, Evaluation Branch
USACE-NAE, 696 Virginia Rd, Concord, MA 01742-2751

12a. DISTRIBUTION/AVAILABILITY STATEMENT
Approved for public release; distribution unlimited

12b. DISTRIBUTION CODE

13. ABSTRACT
A monitoring survey was conducted in September and October 2012 at the Massachusetts Bay Disposal Site (MBDS) as part of the Disposal Area Monitoring System (DAMOS) Program. The 2012 monitoring effort involved a high-resolution acoustic survey to characterize seafloor topography and dredged material distribution, as well as sediment-profile imaging (SPI) and plan-view imaging (PV) surveys to provide additional physical characterization and to assess benthic recolonization. The results of the 2012 surveys were used to document changes at MBDS since the previous survey in 2007 and the subsequent placement of over 1.5 million m^3 of dredged material at the site.

The high-resolution acoustic survey consisted of multibeam bathymetric, acoustic backscatter and side-scan sonar data acquisition. The survey was conducted over a 2,000 × 3,000 m area that incorporated the portion of MBDS including the active mounds (G, H, and I) and a capping demonstration area. The bathymetric data revealed three features on the seafloor: the MBDS-G mound increased in height from 3 m to 8 m but retained a similar footprint to that seen in 2007; the MBDS-H mound accumulated less than 1 m in height and had a small footprint detectable in backscatter (ca. 125 m in diameter); the MBDS-I mound accumulated less than 1 m in height but had a large footprint detectable in backscatter (ca. 1000 × 750 m). The size and extent of the MBDS-G mound was similar to that expected from placement of nearly 1.5 million m^3 of dredged material in 90-m water depths. The limited height of the MBDS-H and MBDS-I mounds were attributed to placement of small volumes (ca. 100,000 m^3 and 50,000 m^3 respectively) of dredged material with high water content that formed thin layers surrounding the placement locations. The high-resolution acoustic data were used to support selection of SPI/PV station locations in areas of active placement of dredged material.

SPI and PV images were collected from MBDS and three reference areas. Evidence of Stage 3 successional status was present in most replicate images from all survey stations. These findings suggest that the benthic community at the disposal site had recovered and was equivalent to reference area benthic communities. Evidence of deep deposit-feeding infauna was present throughout the disposal site, and the aRPD depths within the disposal site boundary were similar and statistically equivalent compared to those found in the ambient areas.

In summary, the placement of approximately 1.5 million m^3 of dredged material created one mound with the size and extent expected from placement of this volume in 90-m water depths and two smaller deposits with minimal bathymetric signatures. In addition, MBDS has experienced full recovery of the benthic community in the year and a half since cessation of dredged material placement activities. Given the complete recovery of the benthic infaunal community, it is predicted that the effects from any future disposal operations at MBDS would be transient and the infaunal community would quickly re-establish itself within a time frame of 12-18 months following completion of disposal operations.

14. SUBJECT TERMS DAMOS, Massachusetts Bay Disposal Site, Dredged Material Monitoring, Acoustic Survey, Sediment-Profile/Plan-View Survey

15. NUMBER OF TEXT PAGES: 87

16. PRICE CODE

17. SECURITY CLASSIFICATION OF REPORT Unclassified

18. SECURITY CLASSIFICATION OF THIS PAGE

19. SECURITY CLASSIFICATION OF ABSTRACT

20. LIMITATION OF ABSTRACT

MONITORING SURVEY AT THE MASSACHUSETTS BAY DISPOSAL SITE SEPTEMBER/OCTOBER 2012

CONTRIBUTION #195

December 2013

Contract No. W912WJ-12-D-0004
Report No. DV-2013-003

Submitted to:
New England District
U.S. Army Corps of Engineers
696 Virginia Road
Concord, MA 01742-2751

Prepared by:
Drew A. Carey
Ken Hickey
Joseph D. Germano
Lorraine B. Read
Marie Evans Esten

Submitted by:
DAMOSVision
215 Eustis Avenue
Newport, RI 02840

Frontispiece

Mystic River Navigation Project

The Mystic River Navigation Project is one of many urban harbors with material that has been dredged and placed at the Massachusetts Bay Disposal Site. The Mystic River has a long history of industrial use and flows through parts of Boston (the Charlestown area), Chelsea, Medford, Everett, and Somerville. The upper section of the river is upstream of the Amelia Earhart Dam in the Medford/Somerville area and is used extensively by recreational boaters. The lower Mystic River serves shipping and commercial interests.

The navigational dredging project consisted of a 5.5-mile-long channel extending from Boston Inner Harbor at the Mystic River Bridge (U.S. Route 1, the cantilever bridge in the background of this photo) to the Craddock Bridge on Main Street in Medford, near Medford Square (after USACE 2013).

Note on units of this report: As a scientific contribution, information and data are presented in the metric system. However, given the prevalence of English units in the dredging industry of the United States, conversions to English units are provided for general information in Section 1. A table of common conversions can be found in Appendix E.

TABLE OF CONTENTS

LIST OF TABLES

LIST OF FIGURES

Page

Page

Page

EXECUTIVE SUMMARY

A monitoring survey was conducted in September and October 2012 at the Massachusetts Bay Disposal Site (MBDS) as part of the Disposal Area Monitoring System (DAMOS) Program. The 2012 monitoring effort involved a high-resolution acoustic survey to characterize seafloor topography and dredged material distribution, as well as sediment-profile imaging (SPI) and plan-view imaging (PV) surveys to provide additional physical characterization and to assess benthic recolonization. The results of the 2012 surveys were used to document changes at MBDS since the previous survey in 2007 and the subsequent placement of over 1.5 million m^3 of dredged material at the site.

The high-resolution acoustic survey consisted of multibeam bathymetric, acoustic backscatter and side-scan sonar data acquisition. The survey was conducted over a 2,000 × 3,000 m area that incorporated the portion of MBDS including the active mounds (G, H, and I) and a capping demonstration area. The bathymetric data revealed three features on the seafloor: the MBDS-G mound increased in height from 3 m to 8 m but retained a similar footprint to that seen in 2007; the MBDS-H mound accumulated less than 1 m in height and had a small footprint detectable in backscatter (ca. 125 m in diameter); the MBDS-I mound accumulated less than 1 m in height but had a large footprint detectable in backscatter (ca. 1000 × 750 m). The size and extent of the MBDS-G mound was similar to that expected from placement of nearly 1.5 million m^3 of dredged material in 90-m water depths. The limited height of the MBDS-H and MBDS-I mounds were attributed to placement of small volumes (ca. 100,000 m^3 and 50,000 m^3 respectively) of dredged material with high water content that formed thin layers surrounding the placement locations. The high-resolution acoustic data were used to support selection of SPI/PV station locations in areas of active placement of dredged material.

SPI and PV images were collected from MBDS and three reference areas. Evidence of Stage 3 successional status was present in most replicate images from all survey stations. These findings suggest that the benthic community at the disposal site had recovered and was equivalent to reference area benthic communities. Evidence of deep deposit-feeding infauna was present throughout the disposal site, and the aRPD depths within the disposal site boundary were similar and statistically equivalent compared to those found in the ambient areas.

In summary, the placement of approximately 1.5 million m^3 of dredged material created one mound with the size and extent expected from placement of this volume in 90-m water depths and two smaller deposits with minimal bathymetric signatures. In addition, MBDS has experienced full recovery of the benthic community in the year and a half since cessation of dredged material placement activities. Given the complete recovery of the benthic infaunal community, it is predicted that the effects from any future disposal operations at MBDS would be transient and the infaunal community would quickly re-establish itself within a time frame of 12-18 months following completion of disposal operations.

1.0 INTRODUCTION

A monitoring survey was conducted at the Massachusetts Bay Disposal Site (MBDS) in September and October 2012 as part of the U.S. Army Corps of Engineers (USACE) New England District (NAE) Disposal Area Monitoring System (DAMOS) Program. DAMOS is a comprehensive monitoring and management program designed and conducted to address environmental concerns surrounding the placement of dredged material at aquatic disposal sites throughout the New England region. An introduction to the DAMOS Program and MBDS, including brief descriptions of previous dredged material disposal and site monitoring activities, is provided below.

1.1 Overview of the DAMOS Program

The DAMOS Program features a tiered management protocol designed to ensure that any potential adverse environmental impacts associated with dredged material disposal are promptly identified and addressed (Germano et al. 1994). For over 35 years, the DAMOS Program has collected and evaluated disposal site data throughout New England. Based on these data, patterns of physical, chemical, and biological responses of seafloor environments to dredged material disposal activity have been documented (Fredette and French 2004).

DAMOS monitoring surveys fall into two general categories: confirmatory studies and focused studies. Confirmatory studies are designed to test hypotheses related to expected physical and ecological response patterns following placement of dredged material on the seafloor at established, active disposal sites. The data collected and evaluated during these studies provide answers to strategic management questions in determining the next step in the disposal site management process. Focused studies are periodically undertaken within the DAMOS Program to evaluate inactive or historical disposal sites and contribute to the development of dredged material placement and capping techniques. The resulting information is used to guide the management of disposal activities at each site. The 2012 MBDS investigation was a confirmatory study featuring monitoring of an area that had recently received dredged material.

Two primary goals of DAMOS confirmatory monitoring surveys are to document the physical location and stability of dredged material placed into the aquatic environment and to evaluate the biological recovery of the benthic community following placement of the dredged material. Several survey techniques are employed in order to characterize these responses to dredged material placement. Sequential acoustic monitoring surveys (including bathymetric and acoustic backscatter measurements) are made to characterize the height and spread of discrete dredged material deposits or mounds created at open water sites as well as the accumulation/consolidation of dredged material into confined aquatic disposal (CAD) cells. Sediment-profile imaging (SPI) surveys, and more recently the addition of plan-view imaging (PV) as part of the survey, are performed to provide further physical characterization of the material and to support evaluation of seafloor (benthic) habitat conditions and recovery over time. Each type of data collection activity is conducted periodically at disposal sites, and the conditions found after a defined period of disposal activity are compared with the long-term data set at a specific site to determine the next step in the disposal site management process (Germano et al. 1994). Focused DAMOS monitoring surveys may also feature additional types of data collection activities as deemed appropriate to achieve specific survey objectives, such as side-scan sonar, sub-bottom profiling, towed video, sediment coring, or grab sampling.

1.2 Introduction to the Massachusetts Bay Disposal Site

The MBDS is centrally located within Massachusetts Bay accessible from Boston Harbor as well as harbors along the northern and southern shorelines of the Bay (Figure 1-1). MBDS was officially designated an ocean dredged material disposal site by the U.S. Environmental Protection Agency (EPA) in 1992 (USEPA 1992; DeAngelo and Murray 1997). MBDS is situated approximately 22.2 km (11.9 nmi) southeast of Gales Point, Manchester, Massachusetts and receives sediments from dredging projects along coastal Massachusetts. The site is circular in shape and occupies a 10.75 km^2 (3.13 nmi^2) area on the seafloor (Figure 1-1). The site was relocated from the interim disposal site (Foul Area Disposal Site [FADS]), used for the disposal of dredged material from 1977 to 1993, to its current position centered at 42° 24.106' N, 70° 34.969' W (NAD 83) (Figure 1-2). The current location was also selected to avoid the northern part of the Industrial Waste Site (IWS), closed by EPA in 1977, where past disposal of debris and a wide range of industrial wastes (including containers of low-level radioactive wastes) had occurred (SAIC 1997a and 1997b).

Water depths at MBDS slope gradually from approximately 82 m (270 ft) along the southwestern boundary towards a shallow depression (approximately 92 m [300 ft] in depth) in the northeast quadrant of the site (Figure 1-3). North of the depression and outside of the MBDS boundary is a distinct topographic high (approximately 67 m [220 ft] in depth), thought to be a remnant glacial deposit (SAIC 1997a; Figures 1-2 and 1-3).

Since January 1994, the management strategy at MBDS has featured the controlled placement of small to moderate volumes of sediment to form individual disposal mounds arranged around the natural seafloor depression in the northeast quadrant of the site. The goal of this approach is to construct the boundary of a containment cell over time. Once complete, the containment cell may be used to limit the lateral spread of future dredged material or be used as part of confined aquatic disposal. By late 2007, seven dredged material disposal mounds had been constructed within MBDS (MBDS-A through MBDS-G; Figure 1-3). A brief description of the mounds and their origin is provided in Section 1.3 below.

In recent years, the USEPA Region 1 and USACE New England District have considered using sediments from the planned Boston Harbor deepening project to aid in the physical isolation of historical disposed sediments and barreled waste at the historic IWS (USACE and MassPort 2008). In order to test the feasibility of such a project, a capping demonstration project was performed at MBDS using sediment from another ongoing Boston Harbor dredging project. An area within the southern portion of MBDS was identified as a demonstration area, named the cap demonstration area (CDA), for evaluating a technique for potential future capping of the historical IWS (Figure 1-2). The capping demonstration project was performed from 2007-2008. The project demonstrated that standard split-hulled scow placement of dredged material allowed for development of a berm of consolidated dredged material that could minimize impact to/resuspension of historically placed material during the capping process (USACE 2013).

1.3 Historical Dredged Material Disposal Activity

Disposal of dredged material in the vicinity of MBDS dates back more than 60 years. The existing MBDS was officially designated as an ocean dredged material disposal site by the U.S. Environmental Protection Agency in 1993. Since that time the site has received over 10.5 million m^3 (13.7 million yd^3) of dredged material from Boston Harbor and other surrounding harbors. Seven distinct disposal mounds have been developed on the seafloor over that time period in the northern half of MBDS (MBDS-A through MBDS-G). Development of a seventh mound, MBDS-G, was confirmed during the most recent survey in 2007 (AECOM 2010, Figure 1-3).

The MBDS-A mound was formed from the disposal of fine-grained material, including consolidated clay, originating from the Third Harbor Tunnel Project between 1992 and 1994. The MBDS-B mound was formed from the disposal of sediment dredged from channels and harbors in the region from December 1994 through November 1998. The three subsequent disposal mounds (MBDS-C, MBDS-D, and MBDS-E) were constructed over a short period of time (1998-2000), consisting primarily of Boston Blue Clay dredged as part of the Boston Harbor Navigation Improvement Project. The MBDS-C mound is the largest of the disposal mounds, formed by the placement of nearly 1.4 million m^3 (1.8 million yd^3) of dredged material between November 1998 and August 1999. The MBDS-D mound is the smallest mound, formed by the disposal of approximately 386,000 m^3 (505,000 yd^3) of dredged material from Boston Harbor placed at the site over a 2.5-month period (August – October 1999). The fifth mound, MBDS-E, resulted from the disposal of over 750,000 m^3 (980,000 yd^3) of dredged material from

October 1999 through June 2000. A sixth mound, MBDS-F, was initiated in September 2000, and received just over 2.0 million m^3 (2.6 million yd^3) of dredged material between September 2000 and August 2007. A seventh mound, MBDS-G, received approximately 550,000 m^3 (720,000 yd^3) of dredged material deposited between September 2006 and August 2007 (Figure 1-3).

1.4 Previous MBDS Monitoring Events

Monitoring surveys have been conducted at or near the site that is currently known as MBDS since the early 1980's. Monitoring events that have occurred since MBDS was designated by EPA in 1992 are summarized in Table 1-1. Mounds at MBDS have been monitored individually to assess stability, thickness of dredged material, and benthic recolonization status relative to previous survey results and in comparison with nearby reference areas.

Previous DAMOS monitoring surveys at MBDS were conducted in 2007 (AECOM 2010), 2004 (ENSR 2005), 2000 (SAIC 2002), 1998/1999 (SAIC 2003), 1994 (SAIC 1997a) and 1993 (SAIC 1997b). The 1993 survey was the baseline survey for the reconfigured MBDS conducted to characterize the topography and sediment composition of the site for DAMOS management. Bathymetry, side-scan sonar, sediment acoustic characterization, and sediment-profile imaging surveys were performed in addition to sediment collection for grain size and chemical analyses. Results of the 1993 baseline survey indicated that the newly designated MBDS could be separated into two distinct areas: the southwestern area where no documented disposal had occurred and the northeastern portion where dredged material had been disposed and one dredged material disposal mound was already evident (MBDS-A).

The results of the surveys between 1992 and 2007 confirmed that dredged material placed at MBDS at designated buoys formed mounds on the seafloor that could be mapped and monitored in subsequent years. The targeted placement of dredged material has created a ring of mounds around a natural seafloor depression, with the goal of developing the boundaries of a containment cell for future placement of dredged material. The surveys identified that sediments on the surfaces of the mounds were rapidly colonized by mature, deposit-feeding communities that converged with the benthic conditions found at the three reference areas.

1.5 Recent Dredged Material Disposal Activity

From November 2007 to September 2012, approximately 1.5 million m^3 (~2 million yd^3) of dredged material—the majority of which (~1.3 million m^3 [~1.7 million yd^3]) originated from the construction of two confined aquatic disposal cells within

Boston's Inner Harbor—was placed at MBDS during 2008 (Table 1-2). The material from the confined aquatic disposal cell construction consisted primarily of consolidated Boston Blue Clay. Material from maintenance dredging within Boston and surrounding harbors consisting of fine sediment (typically somewhat organically enriched) was also placed at the site during this period (pers. comm. S. Wolf 2013). The pattern of individual disposal events for the November 2007 to September 2012 disposal period showed concentrations of large volume placement in the CDA to the southwest of MBDS-E and at MBDS-G mound (Figure 1-4). Substantially smaller volumes were placed at new locations within MBDS from 2009 to 2012 from a series a small harbor dredging projects (Figure 1-4 and Table 1-2).

1.6 2012 Survey Objectives

The 2012 confirmatory survey was designed to address the following two objectives:

- To characterize the seafloor topography and surficial features over a portion of MBDS including active and recently active target disposal locations by completing a high-resolution acoustic survey, and

- To use SPI/PV imaging to further define the physical characteristics of surficial sediment and to assess the benthic recolonization status (recovery of bottom-dwelling biological community) of disposal mounds at MBDS with recent placement activity.

Table 1-1.

Overview of Survey Activities at MBDS since 1992

Date	Purpose of Survey	Bathymetry Area (m × m) and type	# SPI Stations	Sediment Grabs (#) and Analyses	Additional Studies	DAMOS Contribution No.
9/1993	Baseline of reconfigured site	4000 × 4075 Single beam		Grain size, metals, PAHs, pesticides, PCBs, TOC (26)	Side-scan	115
8/1994	Periodic site monitoring		76			116
9/1998	Capping demonstration-baseline	800 × 800 Single beam	91	Grain size, color, consistency, other (13)	Side-scan	147
12/1998	Capping demonstration-single barge	800 × 800 Single beam	82		Side-scan	147
3/1999	Pre-capping demonstration	800 × 800 Single beam	30	Grain size, color, consistency, other (13)	Side-scan	147
9/2000	Post-capping demonstration	800 × 800 Single beam	33	Grain size, tracers	Side-scan, sediment cores (12)	147
8–10/ 2000	Periodic site monitoring	2400 × 2400 Single beam	39			134
9/2004	Periodic site monitoring	2400 × 2400 Multi-beam	45			162
8/2007	Periodic site monitoring	2100 × 3200 Multi-beam	63	Grain size, moisture content, and Atterberg limits	Box cores	181

Table 1-2.

Estimated Volume of Dredged Material Placed at MBDS from November 2007 through September 2012

Project	Disposal Dates	Volume (m^3)	Volume (yd^3)
Boston Harbor Rock Removal, Boston, MA	Nov 2007	573	750
Dorchester Bay, Boston, MA	Nov 2007–Jan 2008	5,046	6,600
Crane and Porter Rivers, Danvers, MA	Dec 2007–Feb 2008	58,282	76,226
Marina Basin, Old Colony Yacht Club, Dorchester, MA	Jan 2008–Dec 2008	5,123	6,700
Marina at Porter River, Riverview Marina, Danvers, MA	Feb 2008	1,376	1,800
Boston Inner Harbor Maintenance, Boston, MA	May 2008–Oct 2008	1,311,014	1,714,640
Green Harbor, Marshfield, MA	Nov 2009–Feb 2010	100,643	131,628
Victoria Marina, Danvers, MA	Nov 2009–Mar 2010	5,752	7,523
Hingham Harbor, Hingham, MA	Nov 2009–Mar 2010	56,771	74,250
Braintree Yacht Club, Braintree, MA	Nov 2010–Feb 2011	12,058	15,771
Plymouth Harbor, Plymouth, MA	Jan 2010	4,790	6,265
Danversport Yacht Club, Danvers, MA	Jan 2010–Jan 2011	7,557	9,884
Port Norfolk Yacht Club, Dorchester, MA	Jan 2011–Feb 2011	9,149	11,965
Mill Wharf Marina, Scituate, MA	Nov 2011–Dec 2011	1,529	2,000
Pilgrim Station, Plymouth, MA	Nov 2011–Dec 2011	9,558	12,500
Charles River and Boston Federal Navigation Project	Mar 2012–Apr 2012	3,058	4,000
Salem Wharf, Salem, MA	Aug 2012–Sept 2012	3,100	4,055
Total Volume		**1,595,379**	**2,086,557**

Reference: Data from Richard Loyd, USACE, May 2013.

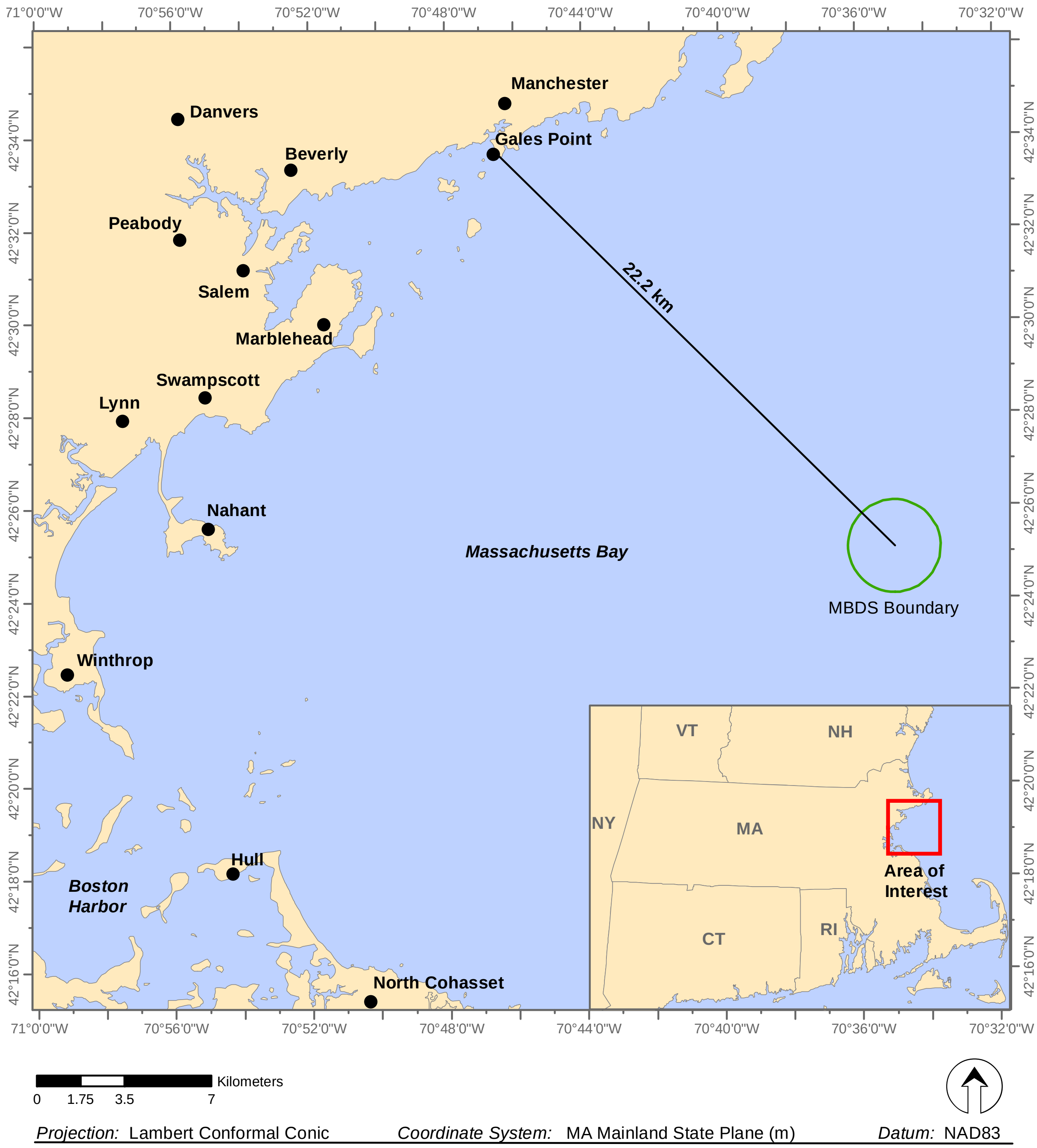

February 2013

Figure 1-1. Location of the Massachusetts Bay Disposal Site (MBDS)

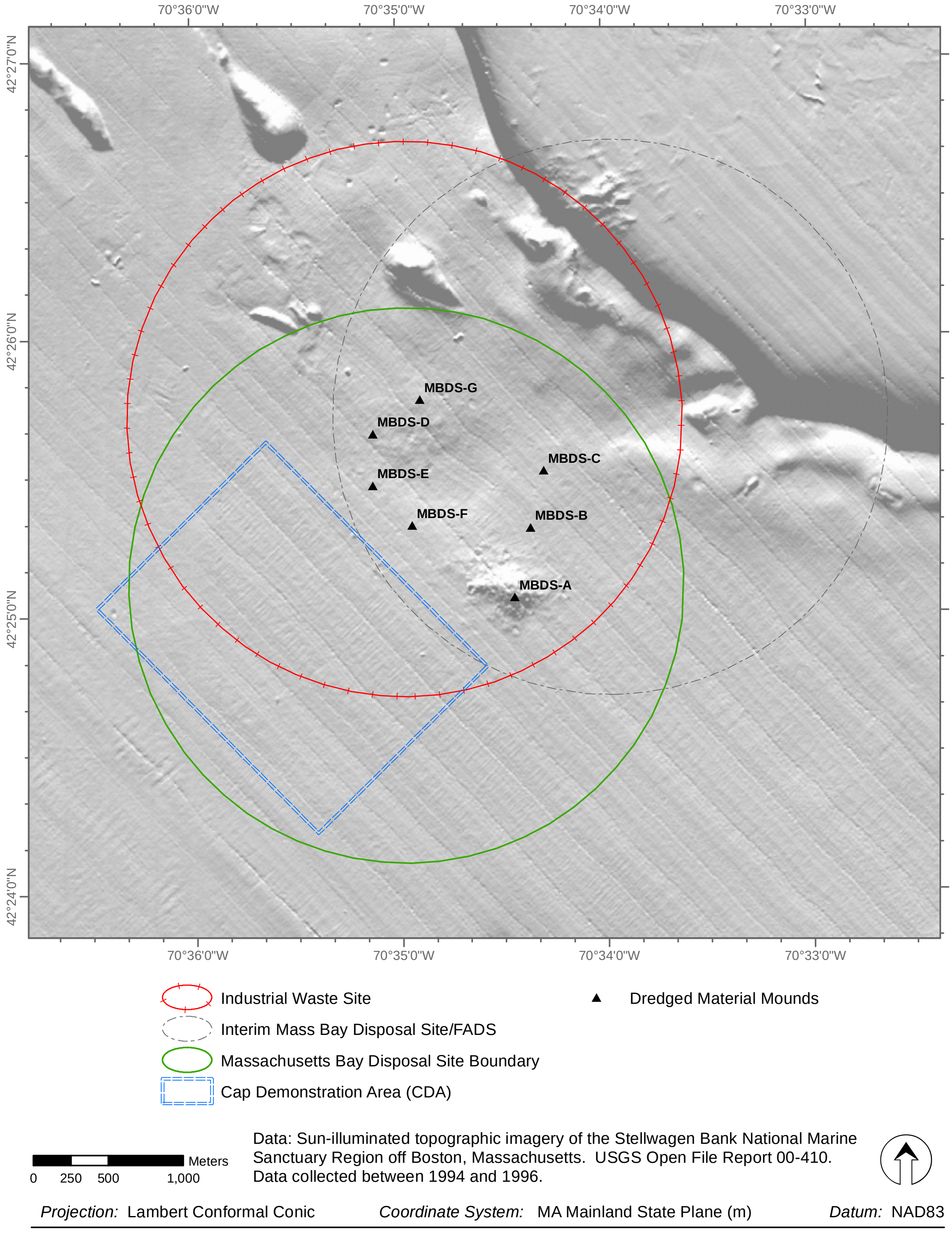

Figure 1-2. MBDS with historical site boundaries, dredged material mounds, and Cap Demonstration Area (CDA)

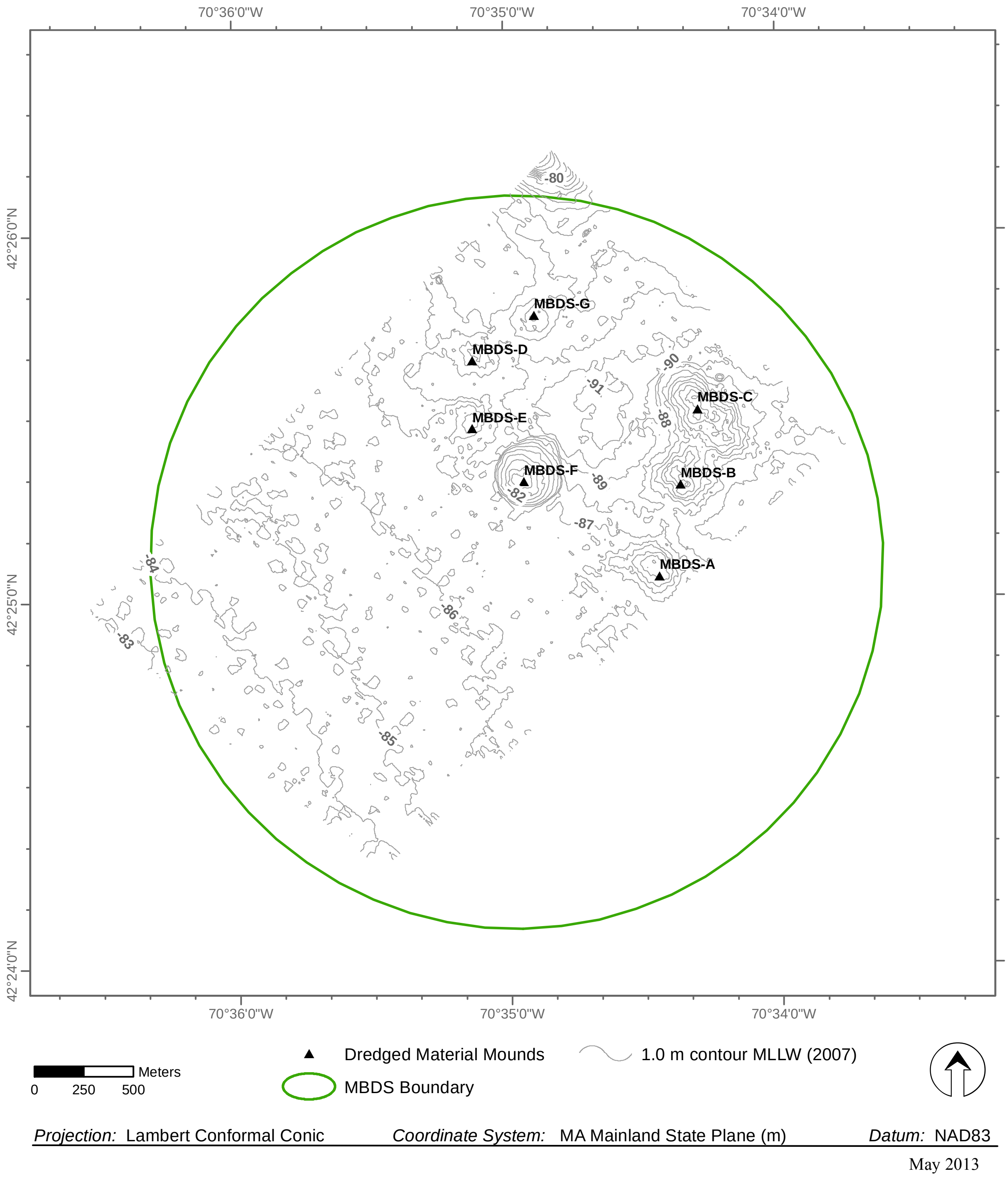

Figure 1-3. Bathymetric contour map of MBDS based on the 2007 survey (AECOM 2010)

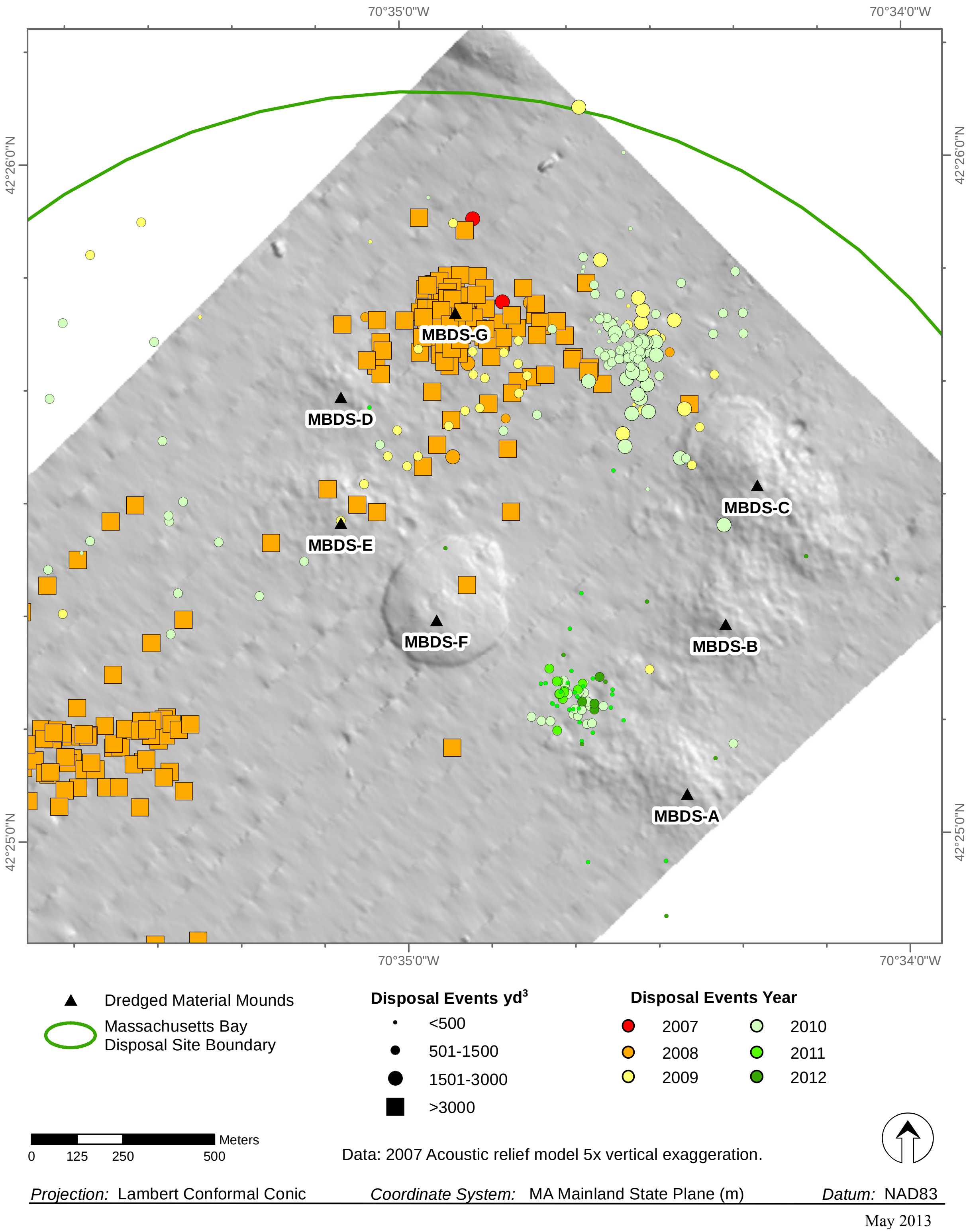

Figure 1-4. Location of disposal events at MBDS from November 2007 to September 2012

2.0 METHODS

The September/October 2012 survey at MBDS was conducted by a team of investigators from CR Environmental and Germano & Associates aboard the R/V *Jamie Hanna*. The acoustic survey was conducted on 25 and 27 September 2012 to assess dredged material distribution at MBDS. The SPI/PV survey was conducted on 18 October 2012 to assess benthic conditions at MBDS.

2.1 Survey Planning

In order to determine the position of the 2,000 × 3,000 m survey area, DAMOSVision hydrographers coordinated with NAE scientists, obtained the site coordinates, and expanded the survey area to provide complete coverage. These coordinates were imported to ArcView GIS software, and a proposed survey area encompassing the entire site was mapped and approved by NAE. In HYPACK® a series of survey lines spaced 150 m apart were designed for the survey area (Figure 2-1). Detailed Standard Operating Procedures (SOPs) for data collection and processing are available in Appendix A.

2.2 Navigation and On-Board Data Acquisition

Navigation for the surveys was accomplished using a Hemisphere 12-channel Differential Global Positioning System (DGPS) capable of receiving U.S. Coast Guard (USCG) Beacon corrections. Trimble DGPSs were available as backups. Both systems are capable of submeter horizontal position accuracy. The DGPS was interfaced to a laptop computer running HYPACK MAX® hydrographic survey software. HYPACK MAX® continually recorded vessel position and DGPS satellite quality and provided a steering display for the vessel captain to accurately maintain the position of the vessel along preestablished survey transects and targets.

Redundant vessel heading measurements were acquired using two compass systems, each capable of providing heading measurements accurate to within 0.05° up to 20 times per second. The primary heading device was an SG Brown Meridian Gyrocompass installed in the pilothouse to the port of the vessel's centerline. A dual-antenna Hemisphere VS-100 Crescent Digital compass and DGPS were installed above the pilot house as a backup for the gyrocompass. Both systems were interfaced to HYPACK® acquisition software.

The pulse-per-second (PPS) signals from DGPSs were hardware-interfaced to HYPACK MAX® using a translation circuit and provided microsecond-level accuracy of data stream time-tagging from each sensor.

2.3 Acoustic Survey

The acoustic survey in this study included bathymetric, backscatter, and side-scan sonar data collection and processing. The bathymetric data provided measurements of water depth that, when processed, were used to map the seafloor topography. The processed data was also compared with previous surveys to track changes in the size and location of seafloor features. This technique is the primary tool in the DAMOS Program for mapping the distribution of dredged material at disposal sites. Backscatter and side-scan sonar data provided images that supported characterization of surficial topography, sediment texture, and roughness. Backscatter data can be processed into a seamless image with corrections for topography while side-scan sonar data retains a higher resolution image without correction for topography. The comparison of synoptic acoustic data types has the greatest utility for assessment of dredged material placement.

2.3.1 Acoustic Data Collection

The 2012 multibeam bathymetric survey of MBDS was conducted on 25 and 27 September 2012. Data layers generated by the surveys included multibeam bathymetric, sediment acoustic backscatter (beam time-series data), and side-scan sonar data.

The acoustic survey of MBDS was conducted over a 2,000 × 3,000 m area that included most of the disposal site including the active mounds and capping demonstration area. Data were collected along survey lanes spaced 150 m apart with three cross-tie lines spaced at approximately 150 m apart and oriented north-south to assess data quality (Figure 2-1). Survey transect orientation was changed mid-survey on September 27, 2012 to address adverse and changing sea conditions. Deteriorating sea conditions and shifting winds forced a realignment of main scheme transects in the southwestern portion of the survey area. Real-time multibeam waterfall displays and coverage maps were monitored throughout data acquisition to assess data quality and overall coverage (Figure 2-1).

Bathymetric, acoustic backscatter, and side-scan sonar data were collected using a Reson 8101 Multibeam Echo Sounder (MBES). This 240-kHz system forms 101 1.5°-beams distributed equiangularly across a 150° swath. The MBES transducer was mounted amidships to the port rail of the survey vessel using a high-strength adjustable boom, and the primary DGPS antenna was attached to the top of the transducer boom.

The transducer depth below the water surface (draft) was checked and recorded at the beginning and end of data acquisition.

The MBES topside processor was equipped with components necessary to export depth solutions, backscatter, and side-scan sonar signals to the HYPACK MAX® acquisition computer via Ethernet communications. HYPACK MAX® also received and recorded navigation data from the DGPS, motion data from a serially interfaced TSS DMS 3-05 motion reference unit (MRU), and heading data from the Meridian and Hemisphere compass systems. Several patch tests were conducted during the survey to allow computation of angular offsets between the MBES system components. The system was calibrated for speed-of-sound in the local water body by performing conductivity-temperature-depth (CTD) casts at frequent intervals throughout the survey day with a Seabird SBE-19 Seacat CTD profiler. Additional confirmations of proper calibration, including static draft, were obtained using the "bar check" method, in which a metal plate was lowered beneath the MBES transducer to known depths (e.g., 2.0 and 5.0 m) below the water surface. Bar-check calibrations were accurate to within 0.05 m in tests conducted at the beginning and end of each day.

A data logging InSitu, Inc. LevelTroll tide gage was installed at the pier in Allerton Harbor, Hull prior to the survey. The gage was programmed to record a six-minute series of measurements.

2.3.2 Bathymetric Data Processing

Bathymetric data were processed using HYPACK HYSWEEP® software. Processing components are described below and included

- Adjustment of data for tide fluctuations
- Correction of ray bending associated with refraction in the water column
- Removal of spurious points associated with water column interference or system errors
- Development of a grid surface representing depth solutions
- Statistical estimation of sounding solution uncertainty
- Generation of data visualization products

Tidal adjustments were accomplished using a Tide Zoning Model (TZM) calculated by NOAA's Center for Operational Oceanographic Products and Services (CO-

OPS) specifically for this survey area. The model applied corrections of -6 minutes and height × 0.92 to the six-minute Mean Lower Low Water (MLLW) data series acquired at NOAA's Boston Tide Station (#8443970).

Correction of sounding depth and position (range and azimuth) associated with refraction due to water column stratification was conducted using a series of eleven sound-velocity profiles acquired by the survey team. Water column stratification was highly variable over the course of the survey (Figure 2-2). This variability is attributed to the well-documented presence of an internal wave in Massachusetts Bay which can result in vertical migration of the thermocline over tens of meters within short temporal and spatial scales. To minimize the effects of this variability on data quality, the upper two to three meters of each sound-velocity profile was adjusted as it was applied to each transect to minimize curvature over flat portions of the seabed. Data artifacts associated with refraction remain in the bathymetric surface model at a relatively fine scale (generally less than five to 10 cm) relative to the survey depth.

Data were filtered to accept only beams falling within an angular limit of 45° due to highly variable sound-velocity profiles associated with the Massachusetts Bay internal waves and resultant beam refraction. Spurious sounding solutions were flagged or rejected based on the careful examination of data on a sweep-specific basis.

The 240 kHz Reson 8101 MBES system has a published nadir beam width of 1.5° (across track) and 1.5° along track. Assuming an average slant range of 90 m per channel and a maximum beam angle of 45°, the average diameter of the beam footprint was calculated at approximately 3.3 × 4.7 m (15.7 m^2). Data were reduced to a cell (grid) size of 4.0 × 4.0 m, acknowledging the system's fine range resolution while accommodating beam position uncertainty. This data reduction was accomplished by calculating and exporting the average elevation for each cell in accordance with USACE recommendations (USACE 2002). A second data reduction process was conducted using HYPACK®'s implementation of CUBE (Combined Uncertainty and Bathymetry Estimator) software developed by scientists at University of New Hampshire/NOAA Center for Coastal and Ocean Mapping (UNH/NOAA CCOM). The CUBE-reduced data minimized the presence of random noise associated with severe sea conditions and refraction and was preferentially used to develop GIS layers. Both the average and CUBE-based data have been delivered digitally.

Within-cell standard deviations (1-sigma) ranged from 0 to 2.91 m (average 0.047). Ninety-nine percent of the cell-specific standard deviation values were less than 0.17 m. The average Root Mean Squared uncertainty at the 95^{th} percentile confidence interval (1.96 - sigma) was 0.09 m. Ninety-nine percent of these uncertainty values were less than 0.33 m. It is noteworthy that the most stringent National Ocean Service (NOS) and International Hydrographic Organization (IHO) standard for this project depth (Special Order 1A) would call for a 95th percentile confidence interval (95% CI) of 0.73 m at the maximum site depth (91.6 m) and 0.69 m at the average site depth (86.2 m).

Nadir data from the mainstay and cross-tie transects were compared to further refine the uncertainty assessment. Differences between co-located points occupied on perpendicular transects were tabulated and statistically analyzed to assess and report data quality relative to promulgated USACE performance standards (note that USACE Standards were developed for a maximum depth of 80 ft). The average difference between 31 co-located points at cross-tie intersections was -0.023 m, indicating that the TZM effectively minimized tide bias. The standard deviation of these comparisons was 0.191 m, indicating high repeatability. The 95th percentile accuracy estimate for cross-tide comparisons was calculated per USACE (2002) as 0.38 m, further demonstrating data compliance with the promulgated USACE performance standard of 0.61 m in depths greater than 40 ft (12.2 m).

Reduced data were exported in ASCII text format with fields for Easting, Northing, and MLLW elevation (meters). All data were projected to the Massachusetts State Plane (Mainland), NAD83 (metric). A variety of data visualizations were generated using a combination of IVS3D Fledermaus (V.7), ESRI ArcMap (V.10.1), and Golden Software Surfer (V. 10). Visualizations and data products included:

- ASCII databases of all processed soundings including MLLW depths and elevations
- Contours of seabed elevation (25-cm, 50-cm and 1.0-m intervals) in SHP format suitable for plotting using GIS and CAD software
- 3-dimensional surface maps of the seabed created using 5× vertical exaggeration and artificial illumination to highlight fine-scale features not visible on contour layers (delivered in grid and TIF formats), and
- An acoustic relief map of the survey area created using 5× vertical exaggeration, delivered in georeferenced TIF format.

2.3.3 Backscatter Data Processing

Backscatter data provided an estimation of surficial sediment texture based on sediment surface roughness and were extracted from cleaned files and converted to Generic Sensor Format (GSF). Mosaics of beam time-series (BTS) backscatter data were created using HYPACK®'s implementation of GeoCoder software developed by scientists at UNH/NOAA CCOM. Portions of backscatter data for five lines in the southeastern portion of the survey area were improperly recorded by HYPACK® during acquisition and contained a generic rather than sonar-specific dB offset. HYPACK® software engineers were unable to correct these files. CR Environmental calculated a survey-specific dB offset for affected portions of data by evaluating differences between these data and overlapping high quality backscatter data. Data were corrected, and a seamless mosaic of unfiltered BTS data was developed and exported in grayscale TIF format. BTS data were also exported in ASCII format with fields for Easting, Northing, and backscatter (dB). A Gaussian filter was applied to backscatter data to minimize nadir artifacts, and the filtered data were used to develop a grid of backscatter values using a 3-meter node interval. The grid was delivered in ESRI binary GRD format to facilitate comparison with other data layers.

2.3.4 Side-Scan Sonar Data Processing

The side-scan sonar data were processed using both Chesapeake Technology, Inc. SonarWiz software and HYPACK®'s implementation of GeoCoder software. Portions of side-scan sonar data for five lines in the southeastern portion of the survey area were improperly recorded by HYPACK® during acquisition and contained a generic rather than sonar-specific dB offset. HYPACK® software engineers were unable to correct these files. CR Environmental calculated a survey-specific dB offset for affected portions of data by evaluating differences between these data and overlapping high quality side-scan sonar data. Data were corrected, and a seamless mosaic of unfiltered side-scan sonar data was developed and exported in grayscale TIF format. Individual georeferenced TIF images of each sonar file and georeferenced mosaics with resolutions of 0.1–0.2 m/pixel were generated.

2.3.5 Acoustic Data Analysis

The processed bathymetric grids were converted to rasters, and bathymetric contour lines and acoustic relief models were generated and displayed using GIS. GIS was also used to calculate depth difference grids between the previous bathymetric survey and the 2012 bathymetric dataset. The previous bathymetric survey at MBDS was conducted in 2007. The depth difference grids were calculated by subtracting the 2007 survey depth estimates from the 2012 survey depth estimates at each point throughout the grid. The resulting depth differences were contoured and displayed using GIS. Backscatter and side-scan sonar mosaics and filtered backscatter grids were combined with acoustic relief models in GIS to facilitate visualization of relationships between acoustic datasets (images and color-coded grids are rendered with sufficient transparency to allow three-dimensional acoustic relief model to be visible underneath).

2.4 Sediment-Profile and Plan-View Imaging Survey

2.4.1 Sediment-Profile Imaging

Sediment-profile imaging (SPI) is a monitoring technique used to provide data on the physical characteristics of the seafloor as well as the status of the benthic biological community. The technique involves deploying an underwater camera system to photograph a cross section of the sediment-water interface. In the 2012 survey at MBDS, high-resolution SPI images were acquired using a Nikon® D7000 digital single-lens reflex camera mounted inside an Ocean Imaging® Model 3731 pressure housing system. The pressure housing sat atop a wedge-shaped prism with a front faceplate and a back mirror. The mirror was mounted at a 45° angle to reflect the profile of the sediment-water interface. As the prism penetrated the seafloor, a trigger activated a time-delay circuit that fired an internal strobe to obtain a cross-sectional image of the upper 15–20 cm of the sediment column (Figure 2-3).

The camera remained on the seafloor for approximately 20 seconds to ensure that a successful image had been obtained. Details of the camera settings for each digital image are available in the associated parameters file embedded in each electronic image file. For this survey, the ISO-equivalent was set at 640, shutter speed was 1/250, f-stop was f9, and storage was in compressed raw Nikon Electronic Format (NEF) files (approximately 9 MB each). Electronic files were converted to high-resolution JPEG (8-bit) format files (3300 × 4900 pixels) using Nikon Capture® NX2 software (Version 2.2.7).

Test exposures of the Kodak® Color Separation Guide (Publication No. Q-13) were made on deck at the beginning and end of the 2012 survey to verify that all internal electronic systems were working to design specifications and to provide a color standard against which final images could be checked for proper color balance. After deployment of the camera at each station, the frame counter was checked to ensure that the requisite number of replicates had been obtained. In addition, a prism penetration depth indicator on the camera frame was checked to verify that the optical prism had actually penetrated the bottom to a sufficient depth. If images were missed or the penetration depth was insufficient, the camera frame stop collars were adjusted and/or weights were added or removed, and additional replicate images were taken. Changes in prism weight amounts, the presence or absence of mud doors, and frame stop collar positions were recorded for each replicate image.

Each image was assigned a unique time stamp in the digital file attributes by the camera's data logger and cross-checked with the time stamp in the navigational system's computer data file. In addition, the field crew kept redundant written sample logs.

Images were downloaded periodically to verify successful sample acquisition and/or to assess what type of sediment/depositional layer was present at a particular station. Digital image files were renamed with the appropriate station names immediately after downloading as a further quality assurance step.

2.4.2 Plan-View Imaging

An Ocean Imaging® Model DSC16000 plan-view underwater camera (PV) system with two Ocean Imaging® Model 400-37 Deep Sea Scaling lasers mounted to the DSC16000 was attached to the sediment-profile camera frame and used to collect plan-view photographs of the seafloor surface; both SPI and PV images were collected during each "drop" of the system. The PV system consisted of a Nikon D-7000 encased in an aluminum housing, a 24 VDC autonomous power pack, a 500 W strobe, and a bounce trigger. A weight was attached to the bounce trigger with a stainless steel cable so that the weight hung below the camera frame; the scaling lasers projected two red dots that are separated by a constant distance (26 cm) regardless of the field-of-view of the PV system, which can be varied by increasing or decreasing the length of the trigger wire. As the camera apparatus was lowered to the seafloor, the weight attached to the bounce trigger contacted the seafloor prior to the camera frame hitting the bottom and triggered the PV camera (Figure 2-3). Details of the camera settings for each digital image are available in the associated parameters file embedded in each electronic image file; for this survey, the ISO-equivalent was set at 400. The additional camera settings used were as follows: shutter speed 1/20, f14, white balance set to flash, color mode set to Adobe RGB, sharpening set to none, noise reduction off, and storage in compressed raw NEF files (approximately 20 MB each). Electronic files were converted to high-resolution JPEG (8-bit) format files (3264 × 4928 pixels) using Nikon Capture® NX2 software.

Prior to field operations, the internal clock in the digital PV system was synchronized with the GPS navigation system and the SPI camera. Each PV image acquired was assigned a time stamp in the digital file and redundant notations in the field and navigation logs. Throughout the survey, PV images were downloaded at the same time as the SPI images after collection and evaluated for successful image acquisition and image clarity.

The ability of the PV system to collect usable images was dependent on the clarity of the water column. To minimize the effects of turbid bottom waters, the bounce trigger cable was shortened to 1 m in order to decrease the distance between the camera focal plane and the seafloor. By limiting the distance between the camera lens port and the intended subject, picture clarity was improved. One major drawback to the relatively short trigger cable length and close distance between the PV system and the seafloor was that the field-of-view of the PV system was decreased so that a smaller area of the seafloor was photographed.

2.4.3 SPI and PV Data Collection

Survey planning included review of 2007 SPI survey results (AECOM 2010) and preliminary September 2012 acoustic survey results. Recent dredged material was placed in three mound areas, MBDS-G, MBDS-H, and MBDS-I. At MBDS-G, dredged material was added to an existing mound, and a 300-meter diameter mound area was delineated. MBDS-H and MBDS-I are newly formed mounds and, a 250-meter diameter mound area was delineated for each mound (Figure 2-4). A random location generator was used to select 12 stations within MBDS-G. The preliminary analysis of bathymetric data indicated that mounds MBDS-H, and MBDS-I had little or no bathymetric expression and would need further placement of dredged material in the future. Mounds ‘H’ and ‘I’ were limited to four stations each, selected to characterize the backscatter patterns indicative of some dredged material placement. Three previously monitored reference areas (FG-23, MBD-REF, and SE-REF) were also surveyed, with 4 stations randomly selected within each reference area (Figure 2-5). SPI/PV station locations are provided in Table 2-1, and actual SPI/PV station replicate locations are provided in Table 2-2.

The SPI/PV survey was conducted at MBDS on 18 October 2012 aboard the R/V *Jamie Hanna*. At each station, the vessel was positioned at the target coordinates and the camera was deployed within a defined station tolerance of 10 m. Four replicate SPI and PV images were collected at each of the stations (Table 2-2). The three replicates with the best quality images from each station were chosen for analysis (Appendices B and C).

The DGPS described above was interfaced to HYPACK® software via laptop serial ports to provide a method to locate and record target sampling locations. Throughout the survey, the HYPACK® data acquisition system received DGPS data. The incoming data stream was digitally integrated and stored on the PC’s hard drive. Actual SPI/PV sampling locations were recorded as target files using this system.

2.4.4 SPI and PV Data Analysis

Computer-aided analysis of the resulting images provided a set of standard measurements to allow comparisons between different locations and different surveys. The DAMOS Program has successfully used this technique for over 30 years to map the distribution of disposed dredged material and to monitor benthic recolonization at disposal sites. For a detailed discussion of SPI methodology, see Appendix A and Germano et al. (2011).

Following completion of data collection, the digital images were analyzed using Adobe Photoshop® CS 5 Version 12.1. Images were first adjusted in Adobe Photoshop® to expand the available pixels to their maximum light and dark threshold range. Linear and areal measurements were recorded as number of pixels and converted to scientific units using the Kodak® Color Separation Guide for measurement calibration. Detailed results of all SPI image analyses are presented in Appendix B, and detailed results of all PV image analyses are presented in Appendix C.

2.4.4.1 SPI Data Analysis

Analysis of each SPI image was performed to provide measurement of the following standard set of parameters:

Sediment Type–The sediment grain size major mode and range were estimated visually from the images using a grain size comparator at a similar scale. Results were reported using the phi scale. Conversion to other grain size scales is provided in Appendix D. The presence and thickness of disposed dredged material were also assessed by inspection of the images.

Penetration Depth–The depth to which the camera penetrated into the seafloor was measured to provide an indication of the sediment density or bearing capacity. The penetration depth can range from a minimum of 0 cm (i.e., no penetration on hard substrates) to a maximum of 20 cm (full penetration on very soft substrates).

Surface Boundary Roughness–Surface boundary roughness is a measure of the vertical relief of features at the sediment-water interface in the sediment-profile image. Surface boundary roughness was determined by measuring the vertical distance between the highest and lowest points of the sediment-water interface. The surface boundary roughness (sediment surface relief) measured over the width of sediment-profile images typically ranges from 0 to 4 cm, and may be related to physical structures (e.g., ripples, rip-up structures, mud clasts) or biogenic features (e.g., burrow openings, fecal mounds, foraging depressions). Biogenic roughness typically changes seasonally and is related to the interaction of bottom turbulence and bioturbational activities.

Apparent Redox Potential Discontinuity (aRPD) Depth–The aRPD depth provides a measure of the integrated time history of the balance between near-surface oxygen conditions and biological reworking of sediments. Sediment particles exposed to oxygenated waters oxidize and lighten in color to brown or light gray. As the particles are buried or moved down by biological activity, they are exposed to reduced oxygen concentrations in subsurface pore waters and their oxic coating slowly reduces, changing color to dark gray or black. When biological activity is high, the aRPD depth increases;

when it is low or absent, the aRPD depth decreases. The aRPD depth was measured by assessing color and reflectance boundaries within the images.

Infaunal Successional Stage–Infaunal successional stage is a measure of the biological community inhabiting the seafloor. Current theory holds that organism-sediment interactions in fine-grained sediments follow a predictable sequence of development after a major disturbance (such as dredged material disposal), and this sequence has been divided subjectively into three stages (Rhoads and Germano 1982, 1986). Successional stage was assigned by assessing which types of species or organism-related activities were apparent in the images.

Additional components of the SPI analysis included calculation of means and ranges for the parameters listed above and mapping of means of replicate values from each station. Station means were calculated from three replicates from each station and used in statistical analysis.

2.4.4.2 PV Data Analysis

The PV images provided a much larger field-of-view than the SPI images and provided valuable information about the landscape ecology and sediment topography in the area where the pinpoint "optical core" of the sediment profile was taken. Unusual surface sediment layers, textures, or structures detected in any of the sediment-profile images can be interpreted in light of the larger context of surface sediment features; i.e., is a surface layer or topographic feature a regularly occurring feature and typical of the bottom in this general vicinity or just an isolated anomaly? The scale information provided by the underwater lasers allowed accurate density counts (number per square meter) of attached epifaunal colonies, sediment burrow openings, or larger macrofauna or fish which may have been missed in the sediment-profile cross section. Information on sediment transport dynamics and bedform wavelength were also available from PV image analysis. Analysts calculated the image size and field-of-view and noted sediment type; recorded the presence of bedforms, burrows, tubes, tracks, trails, epifauna, mud clasts, and debris; and included descriptive comments (Appendix C).

2.4.5 Statistical Methods

Statistical analysis was used to aid in the assessment of the benthic recolonization status of the recently formed mound relative to reference conditions. The two SPI parameters which are most indicative of recolonization status, and which also lend themselves to quantitative analysis, are the depth of the aRPD (an indirect measure of the degree of biological reworking of surface sediments) and the infaunal successional stage. For the statistical analysis, the mean value for aRPD (based on $n = 3$ replicate images) was utilized, while the maximum value among the three replicates was used as the successional stage rank for each station. The successional stage ranks had possible values between 0 (no fauna present) and 3 (Stage 3); half ranks were also possible for the "in-between" stages (e.g., Stage 1 going to 2 had a value of 1.5).

Traditionally, study objectives have been addressed using point null hypotheses of the form "There is no difference in benthic conditions between the reference area and the disposal mound." An approach using bioequivalence or interval testing is considered to be more informative than the point null hypothesis test of "no difference." In reality, there is always some small difference, and the statistical significance of this difference may or may not be ecologically meaningful. Without an associated power analysis, this type of point null hypothesis testing provides an incomplete picture of the results.

In this application of bioequivalence (interval) testing, the null hypothesis presumes the difference is great, i.e., an inequivalence hypothesis (e.g., McBride 1999). This is recognized as a 'proof of safety' approach because rejection of the inequivalence null hypothesis requires sufficient proof that the difference is actually small. The null and alternative hypotheses to be tested were:

$$H_0: \; d \leq -\delta \;\text{ or }\; d \geq \delta \text{ (presumes the difference is great)}$$

$$H_A: \; -\delta < d < \delta \text{ (requires proof that the difference is small)}$$

where d is the difference between the reference site and disposal mound means.

If the null hypothesis is rejected, it is concluded that the two means are equivalent to one another within ±δ units. The size of δ should be determined from historical data and/or best professional judgment to identify a maximum difference that is within background variability/noise and is therefore not ecologically meaningful. Based on historical DAMOS data, δ values of 1 for aRPD and 0.5 for successional stage rank (on the 0–3 scale) have been established.

The test of the interval hypothesis can be broken down into two one-sided tests (TOST) (McBride 1999 after Schuirmann 1987) which are based on the normal distribution, or, more typically, on Student's *t*-distribution when sample sizes are small and variances must be estimated from the data. The statistics used to test the interval hypotheses shown here are based on such statistical foundations as the Central Limit Theorem (CLT) and basic statistical properties of random variables. A simplification of the CLT states that the mean of any random variable is normally distributed. Linear combinations of normal random variables are also normal, so a linear function of means is also normally distributed. When a linear function of means is divided by its standard error the ratio follows a *t*-distribution with degrees of freedom associated with the variance estimate. Hence, the *t*-distribution can be used to construct a confidence interval around any linear function of means.

In the sampling design utilized in the 2012 SPI survey at MBDS, there were four distinct areas (three reference areas and the recent disposal mound MBDS-G), and the difference equation of interest was the linear contrast between the grand mean of the three reference means minus the mean on MBDS-G mound, or

$$[{}^{1}/_{3}\ (\mathrm{Mean}_{FG\text{-}23} + \mathrm{Mean}_{SE\text{-}REF} + \mathrm{Mean}_{MBD\text{-}REF}) - (\mathrm{Mean}_{MBDS\text{-}G})]$$

where Mean_{XXX} was the arithmetic mean for the stations within the specified area (each reference area or disposal MBDS-G mound).

The three reference areas collectively represented ambient conditions, but if there were mean differences among these three areas then pooling them into a single reference group would increase the variance beyond true background variability. The effect of keeping the three reference areas separate has little effect on the grand reference mean (if n is equal among these areas), but it maintains the variance as a true background variance for each individual population with its respective mean.

The difference equation, $\hat{d}$, for the comparison of interest was:

$$[{}^{1}/_{3}\ (\mathrm{Mean}_{FG\text{-}23} + \mathrm{Mean}_{SE\text{-}REF} + \mathrm{Mean}_{MBD\text{-}REF}) - (\mathrm{Mean}_{MBDS\text{-}G})] \qquad \text{[Eq. 1]}$$

and the standard error of each difference equation was calculated assuming that the variance of a sum is the sum of the variances for independent variables, or:

$$SE(\hat{d}) = \sqrt{\sum_{j} \left(S_j^2 c_j^2 / n_j\right)} \qquad \text{[Eq.2]}$$

where:

c_j = coefficients for the *j* means in the difference equation, $\hat{d}$ [Eq. 1] (i.e., for equation 1 shown above, the coefficients were 1/3 for each of the three reference areas, and -1 for the disposal mound).

S_j^2 = variance for the j^{th} area. If equal variances are assumed, a single pooled residual variance estimate can be substituted for each group, equal to the mean square error from an ANOVA based on all four groups.

n_j = number of replicate observations for the j^{th} area.

The inequivalence null hypothesis was rejected (and equivalence was concluded) if the confidence interval on the difference of means, $\hat{d}$, was fully contained within the interval [–δ , + δ]. Thus the decision rule was to reject H_0 if:

$$D_L = \hat{d} - t_{\alpha,\upsilon} se(\hat{d}) > -\delta \quad \text{and} \quad D_U = \hat{d} + t_{\alpha,\upsilon} se(\hat{d}) < \delta \qquad \text{[Eq. 3]}$$

where:

$\hat{d}$ = observed difference in means between the reference areas and mound

$t_{\alpha,\upsilon}$ = upper $(100-\alpha)^{th}$ percentile of a Student's *t*-distribution with υ degrees of freedom

$se(\hat{d})$ = standard error of the difference (Eq. 2)

υ = degrees of freedom for the standard error. If a pooled residual variance estimate was used, it was the residual degrees of freedom from an ANOVA on all groups (total number of stations minus the number of groups); if separate variance estimates were used, degrees of freedom were calculated based on the Brown and Forsythe estimation (Zar 1996).

Validity of the normality and equal variance assumptions were tested using Shapiro-Wilk's test for normality on the area residuals ($\alpha = 0.05$) and Levene's test for equality of variances among the four areas ($\alpha = 0.05$). If normality was not rejected but equality of variances was, then a parametric t-interval was used for the difference equation, and the variance for the difference equation was based on separate variances for each group. If systematic deviations from normality were identified, then a non-parametric bootstrapped interval was used.

Table 2-1.

MBDS 2012 Survey Target SPI/PV Station Locations

Target Station Locations			Target Station Locations		
Station	Latitude (N)	Longitude (W)	Station	Latitude (N)	Longitude (W)
1	42° 25.783'	70° 34.854'	19	42° 25.713'	70° 34.615'
2	42° 25.754'	70° 34.865'	20	42° 25.768'	70° 34.604'
3	42° 25.809'	70° 34.831'	21	42° 25.754'	70° 34.572'
4	42° 25.725'	70° 34.798'	22	42° 25.705'	70° 34.545'
5	42° 25.753'	70° 34.921'	23	42° 25.781'	70° 34.557'
6	42° 25.719'	70° 34.876'	24	42° 25.752'	70° 34.519'
7	42° 25.774'	70° 34.895'	25	42° 25.180'	70° 34.636'
8	42° 25.818'	70° 34.782'	26	42° 25.253'	70° 34.625'
9	42° 25.708'	70° 34.828'	27	42° 25.186'	70° 34.596'
10	42° 25.759'	70° 34.793'	28	42° 25.215'	70° 34.626'
11	42° 25.782'	70° 34.950'	29	42° 25.141'	70° 34.704'
12	42° 25.832'	70° 34.879'	30	42° 25.195'	70° 34.670'
13	42° 25.686'	70° 34.509'	31	42° 25.226'	70° 34.661'
14	42° 25.719'	70° 34.513'	32	42° 25.229'	70° 34.706'
15	42° 25.767'	70° 34.481'	33	42° 25.209'	70° 34.739'
16	42° 25.730'	70° 34.473'	34	42° 25.179'	70° 34.701'
17	42° 25.747'	70° 34.634'	35	42° 25.176'	70° 34.743'
18	42° 25.685'	70° 34.572'	36	42° 25.255'	70° 34.682'

Target Reference Station Locations		
Station	Latitude (N)	Longitude (W)
MBD-REF-37	42° 22.723'	70° 30.103'
MBD-REF-38	42° 22.754'	70° 30.264'
MBD-REF-39	42° 22.571'	70° 30.311'
MBD-REF-40	42° 22.791'	70° 30.149'
FG-23-41	42° 22.621'	70° 34.644'
FG-23-42	42° 22.689'	70° 34.679'
FG-23-43	42° 22.750'	70° 34.421'
FG-23-44	42° 22.705'	70° 34.561'
SE-REF-45	42° 20.084'	70° 27.898'
SE-REF-46	42° 20.017'	70° 27.870'
SE-REF-47	42° 19.944'	70° 27.963'
SE-REF-48	42° 20.042'	70° 27.791'

Note: Coordinate system NAD83

Table 2-2.

MBDS 2012 Survey Actual SPI/PV Replicate Locations

SPI/PV Replicate Locations					
Replicate	**Latitude (N)**	**Longitude (W)**	**Replicate**	**Latitude (N)**	**Longitude (W)**
MBDS-G-1A	42° 25.781'	70° 34.856'	MBDS-G-7A	42° 25.774'	70° 34.894'
MBDS-G-1B	42° 25.785'	70° 34.859'	MBDS-G-7B	42° 25.777'	70° 34.895'
MBDS-G-1C	42° 25.785'	70° 34.855'	MBDS-G-7C	42° 25.776'	70° 34.895'
MBDS-G-1D	42° 25.784'	70° 34.853'	MBDS-G-7D	42° 25.776'	70° 34.895'
MBDS-G-1E	42° 25.783'	70° 34.854'	MBDS-G-8A	42° 25.822'	70° 34.783'
MBDS-G-1F	42° 25.783'	70° 34.855'	MBDS-G-8B	42° 25.816'	70° 34.786'
MBDS-G-1G	42° 25.786'	70° 34.857'	MBDS-G-8C	42° 25.817'	70° 34.784'
MBDS-G-1H	42° 25.784'	70° 34.856'	MBDS-G-8D	42° 25.815'	70° 34.786'
MBDS-G-2A	42° 25.754'	70° 34.868'	MBDS-G-9A	42° 25.708'	70° 34.830'
MBDS-G-2B	42° 25.755'	70° 34.864'	MBDS-G-9B	42° 25.707'	70° 34.832'
MBDS-G-2C	42° 25.753'	70° 34.866'	MBDS-G-9C	42° 25.709'	70° 34.832'
MBDS-G-2D	42° 25.754'	70° 34.867'	MBDS-G-9D	42° 25.707'	70° 34.829'
MBDS-G-3A	42° 25.809'	70° 34.832'	MBDS-G-10A	42° 25.759'	70° 34.795'
MBDS-G-3B	42° 25.810'	70° 34.833'	MBDS-G-10B	42° 25.759'	70° 34.797'
MBDS-G-3C	42° 25.810'	70° 34.835'	MBDS-G-10C	42° 25.759'	70° 34.792'
MBDS-G-3D	42° 25.810'	70° 34.834'	MBDS-G-10D	42° 25.758'	70° 34.798'
MBDS-G-4A	42° 25.726'	70° 34.800'	MBDS-G-11A	42° 25.780'	70° 34.949'
MBDS-G-4B	42° 25.726'	70° 34.802'	MBDS-G-11B	42° 25.779'	70° 34.951'
MBDS-G-4C	42° 25.726'	70° 34.803'	MBDS-G-11C	42° 25.779'	70° 34.951'
MBDS-G-4D	42° 25.726'	70° 34.796'	MBDS-G-11D	42° 25.781'	70° 34.952'
MBDS-G-5A	42° 25.752'	70° 34.924'	MBDS-G-12A	42° 25.834'	70° 34.880'
MBDS-G-5B	42° 25.753'	70° 34.917'	MBDS-G-12B	42° 25.833'	70° 34.878'
MBDS-G-5C	42° 25.750'	70° 34.919'	MBDS-G-12C	42° 25.833'	70° 34.881'
MBDS-G-5D	42° 25.751'	70° 34.924'	MBDS-G-12D	42° 25.833'	70° 34.878'
MBDS-G-6A	42° 25.719'	70° 34.878'	MBDS-H-14A	42° 25.722'	70° 34.512'
MBDS-G-6B	42° 25.720'	70° 34.876'	MBDS-H-14B	42° 25.718'	70° 34.509'
MBDS-G-6C	42° 25.719'	70° 34.876'	MBDS-H-14C	42° 25.718'	70° 34.512'
MBDS-G-6D	42° 25.721'	70° 34.878'	MBDS-H-14D	42° 25.721'	70° 34.511'
MBDS-G-6E	42° 25.721'	70° 34.880'	MBDS-H-17A	42° 25.749'	70° 34.632'
MBDS-G-6F	42° 25.721'	70° 34.874'	MBDS-H-17B	42° 25.747'	70° 34.629'
MBDS-G-6G	42° 25.718'	70° 34.876'	MBDS-H-17C	42° 25.746'	70° 34.629'
MBDS-G-6H	42° 25.720'	70° 34.879'	MBDS-H-17D	42° 25.747'	70° 34.632'
MBDS-G-6I	42° 25.720'	70° 34.877'	MBDS-H-20A	42° 25.767'	70° 34.604'
MBDS-G-6J	42° 25.718'	70° 34.877'	MBDS-H-20B	42° 25.767'	70° 34.605'
MBDS-G-6K	42° 25.716'	70° 34.877'	MBDS-H-20C	42° 25.768'	70° 34.604'
MBDS-G-6L	42° 25.718'	70° 34.874'	MBDS-H-20D	42° 25.767'	70° 34.599'

Table 2-2., continued

SPI/PV Replicate Locations			Reference Replicate Locations		
Replicate	Latitude (N)	Longitude (W)	Replicate	Latitude (N)	Longitude (W)
MBDS-H-22A	42° 25.705'	70° 34.542'	MBD-REF-39D	42° 22.573'	70° 30.312'
MBDS-H-22B	42° 25.705'	70° 34.544'	MBD-REF-40A	42° 22.792'	70° 30.150'
MBDS-H-22C	42° 25.706'	70° 34.543'	MBD-REF-40B	42° 22.792'	70° 30.152'
MBDS-H-22D	42° 25.704'	70° 34.542'	MBD-REF-40C	42° 22.792'	70° 30.149'
MBDS-I-30A	42° 25.195'	70° 34.671'	MBD-REF-40D	42° 22.793'	70° 30.150'
MBDS-I-30B	42° 25.197'	70° 34.674'	FG-23-41A	42° 22.621'	70° 34.645'
MBDS-I-30C	42° 25.196'	70° 34.673'	FG-23-41B	42° 22.619'	70° 34.645'
MBDS-I-30D	42° 25.196'	70° 34.672'	FG-23-41C	42° 22.620'	70° 34.646'
MBDS-I-31A	42° 25.227'	70° 34.661'	FG-23-41D	42° 22.620'	70° 34.645'
MBDS-I-31B	42° 25.226'	70° 34.661'	FG-23-42A	42° 22.688'	70° 34.681'
MBDS-I-31C	42° 25.226'	70° 34.662'	FG-23-42B	42° 22.690'	70° 34.680'
MBDS-I-31d	42° 25.226'	70° 34.660'	FG-23-42C	42° 22.687'	70° 34.680'
MBDS-I-34A	42° 25.179'	70° 34.698'	FG-23-42D	42° 22.687'	70° 34.683'
MBDS-I-34B	42° 25.177'	70° 34.703'	FG-23-43A	42° 22.752'	70° 34.419'
MBDS-I-34C	42° 25.181'	70° 34.708'	FG-23-43B	42° 22.750'	70° 34.417'
MBDS-I-34D	42° 25.179'	70° 34.701'	FG-23-43C	42° 22.748'	70° 34.419'
MBDS-I-36A	42° 25.256'	70° 34.681'	FG-23-43D	42° 22.748'	70° 34.421'
MBDS-I-36B	42° 25.258'	70° 34.684'	FG-23-44A	42° 22.706'	70° 34.558'
MBDS-I-36C	42° 25.256'	70° 34.684'	FG-23-44B	42° 22.707'	70° 34.560'
MBDS-I-36D	42° 25.254'	70° 34.679'	FG-23-44C	42° 22.705'	70° 34.558'
Reference Replicate Locations			FG-23-44D	42° 22.705'	70° 34.563'
Replicate	Latitude (N)	Longitude (W)	SE-REF-45A	42° 20.081'	70° 27.899'
MBD-REF-37A	42° 22.724'	70° 30.109'	SE-REF-45B	42° 20.083'	70° 27.901'
MBD-REF-37A	42° 22.758'	70° 30.383'	SE-REF-45C	42° 20.084'	70° 27.897'
MBD-REF-37AA	42° 22.759'	70° 30.382'	SE-REF-45D	42° 20.086'	70° 27.900'
MBD-REF-37AB	42° 22.759'	70° 30.385'	SE-REF-46A	42° 20.015'	70° 27.875'
MBD-REF-37AC	42° 22.760'	70° 30.382'	SE-REF-46B	42° 20.016'	70° 27.871'
MBD-REF-37AD	42° 22.760'	70° 30.381'	SE-REF-46C	42° 20.016'	70° 27.874'
MBD-REF-37B	42° 22.725'	70° 30.108'	SE-REF-46D	42° 20.017'	70° 27.874'
MBD-REF-37C	42° 22.724'	70° 30.104'	SE-REF-47A	42° 19.943'	70° 27.963'
MBD-REF-37D	42° 22.724'	70° 30.100'	SE-REF-47B	42° 19.944'	70° 27.967'
MBD-REF-38A	42° 22.755'	70° 30.261'	SE-REF-47C	42° 19.945'	70° 27.963'
MBD-REF-38B	42° 22.755'	70° 30.266'	SE-REF-47D	42° 19.947'	70° 27.962'
MBD-REF-38C	42° 22.757'	70° 30.266'	SE-REF-48A	42° 20.040'	70° 27.796'
MBD-REF-38D	42° 22.758'	70° 30.262'	SE-REF-48B	42° 20.043'	70° 27.790'
MBD-REF-39A	42° 22.572'	70° 30.318'	SE-REF-48C	42° 20.045'	70° 27.793'
MBD-REF-39B	42° 22.572'	70° 30.311'	SE-REF-48D	42° 20.042'	70° 27.793'
MBD-REF-39C	42° 22.572'	70° 30.311'			

Notes: 1) Coordinate system NAD83

2) This table reflects all attempts to collect replicates at each target station. The three replicates with the best quality images were used for analysis.

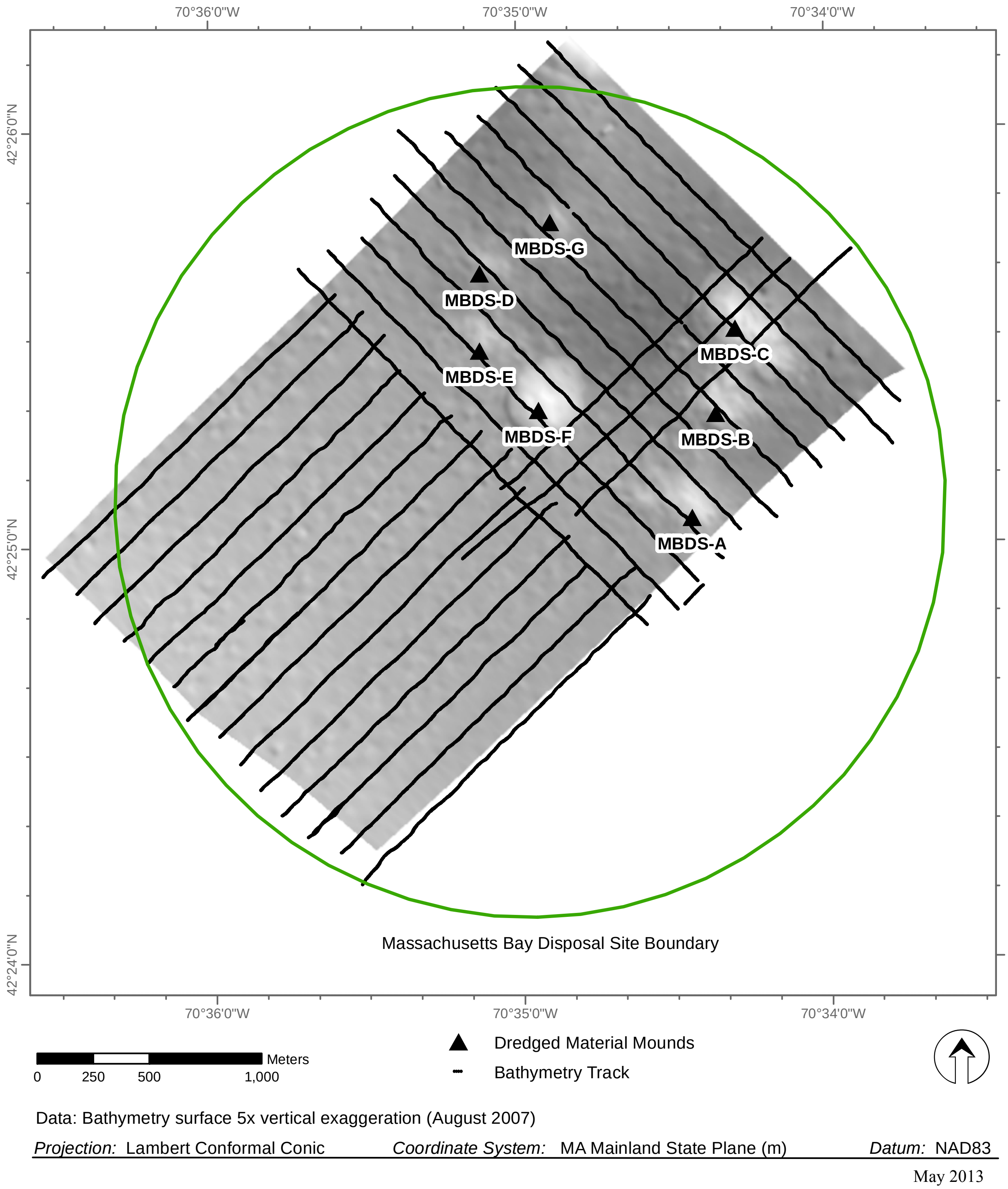

Figure 2-1. MBDS bathymetric survey boundary and tracklines

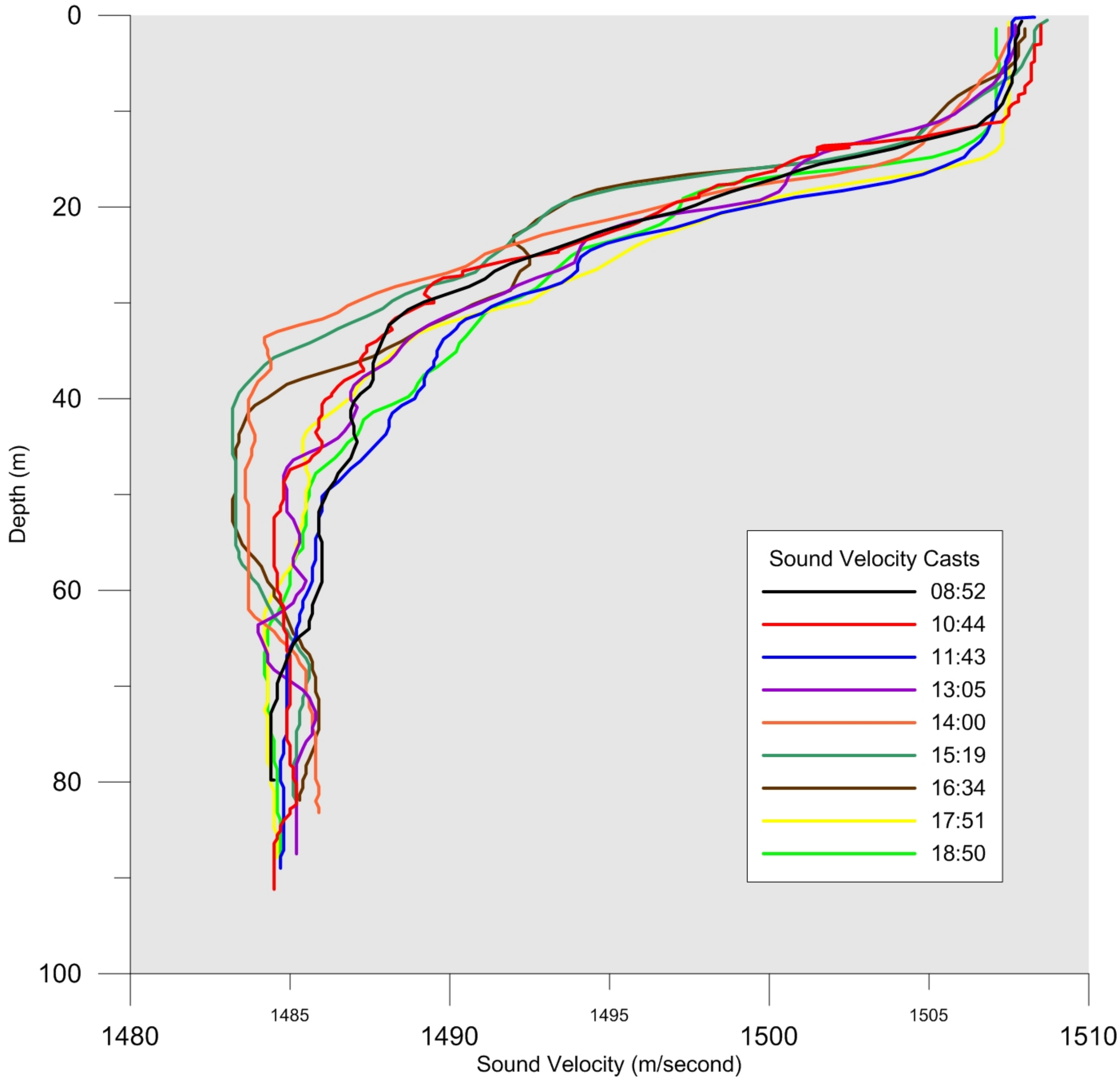

Figure 2-2. Sound-velocity profiles from September 27, 2012 at MBDS

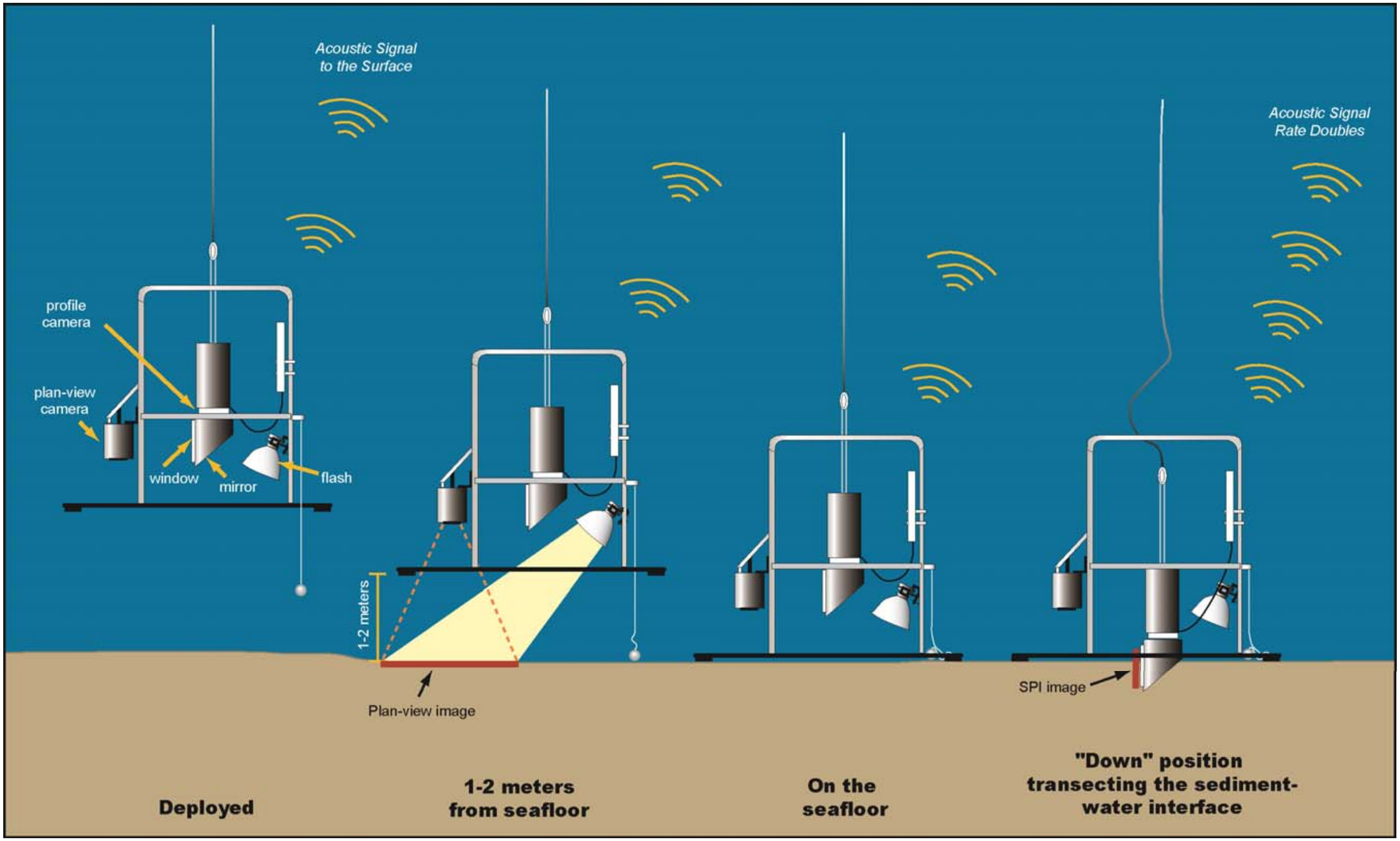

Figure 2-3. Schematic diagram of the SPI/PV camera deployment

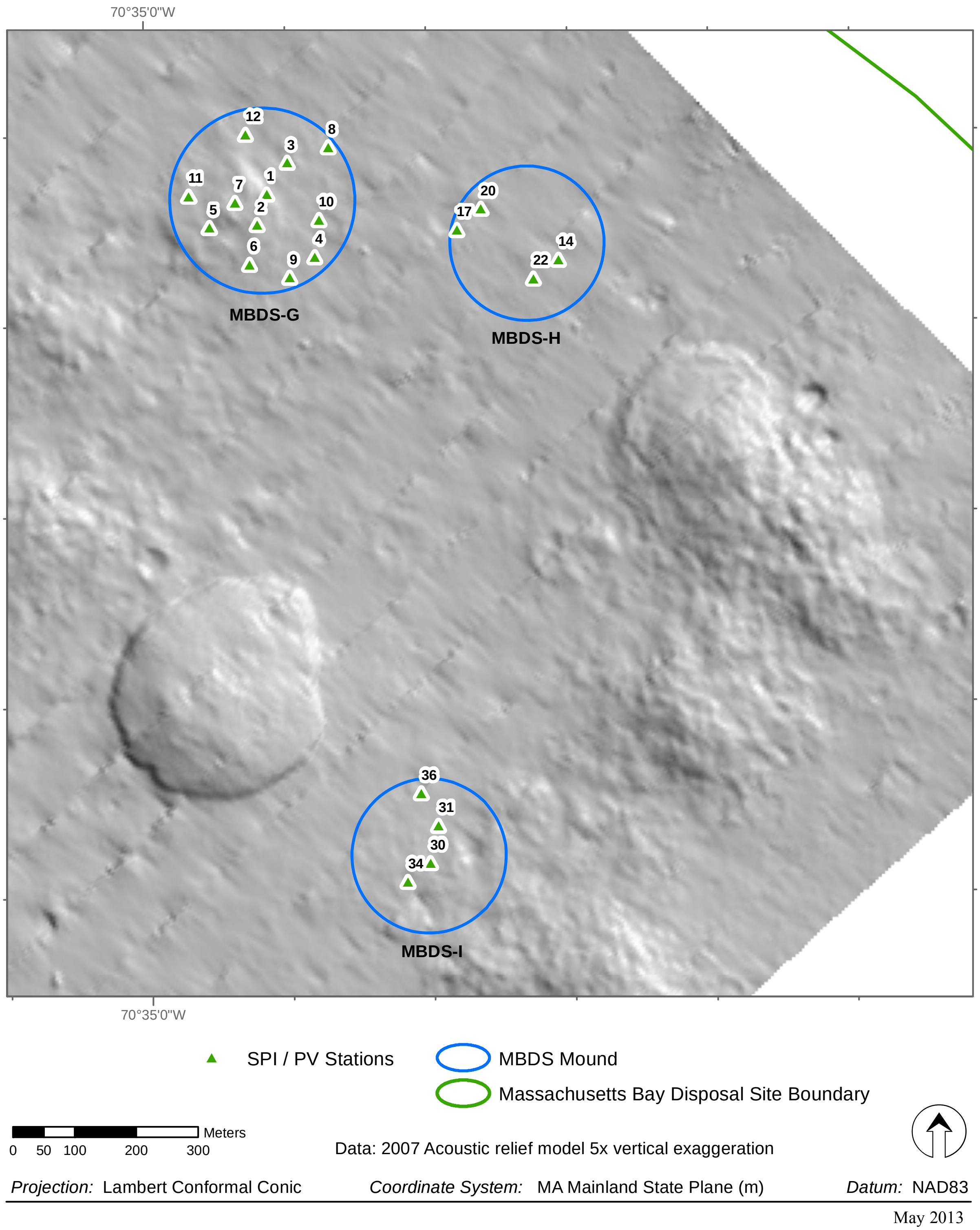

Figure 2-4. MBDS mounds G, H, and I with target SPI/PV stations indicated

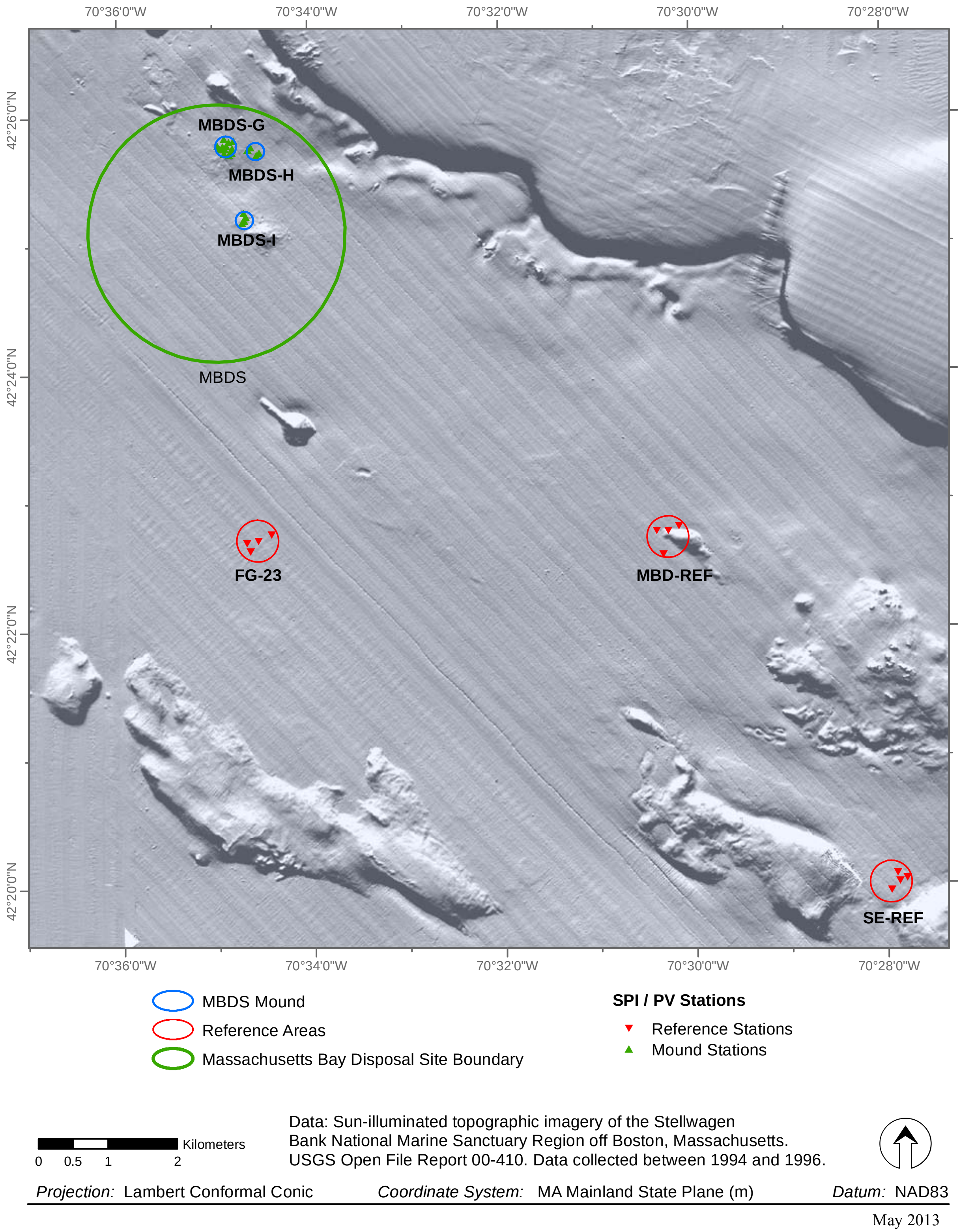

Figure 2-5. MBDS and reference areas with target sediment-profile image stations indicated

3.0 RESULTS

3.1 Acoustic Surveys

The acoustic survey results provided a complementary set of seafloor topographic measurements, backscatter measurements, and side-scan sonar imagery. The acoustic survey results for each data type are described below and integrated in the discussion (Section 4.0).

3.1.1 Existing Bathymetry

The overall site bathymetry surveyed in 2012 was consistent with that of the 2007 survey with water depths ranging from approximately 91 m in the depression in the northeast to 83 m in the southwest corner. The seafloor generally sloped uniformly downward from southwest to northeast to about the center of the disposal site (Figure 3-1). From the center of the site to the northeast, the seafloor formed an irregular basin surrounded by dredged material mounds. The irregular basin is an area with larger near-circular dredged material deposits in the northeast portion of the site and a complex area of smaller dredged material deposits to the southwest (Figure 3-1).

Multibeam bathymetric data rendered as a color scale by depth over an acoustic relief model (grayscale with hillshading) provided a more detailed representation of the surface of the mounds and site (Figure 3-2). The 2012 bathymetric survey confirmed the presence of seven disposal mounds (MBDS-A through MBDS-G) (Figure 3-2). All of these mounds had been previously identified; however, placement of approximately 1.5 million m^3 of material at three buoy locations since 2007 resulted in the enhancement of the MBDS-G mound and the formation of a two new placement areas, identified as MBDS-H and MBDS-I (Figure 3-2).

The six oldest existing mounds (MBDS-A through MBDS-F) have experienced minimal change in shape since the 2007 survey (Figure 3-2). The oldest and most southern mound, MBDS-A, was elongated in an east-west orientation, approximately 500 m in length and 5 m in height (Figure 3-2). The MBDS-B mound, located to the northeast of MBDS-A, had a diameter of approximately 350 m and a height of approximately 6 m. The MBDS-C mound was the largest, with an elongated shape oriented along a northwest-southeast axis that was approximately 600 m in length and rising to a peak height of approximately 8 m above the surrounding seafloor. The MBDS-C mound was partially conjoined with the MBDS-B mound to the south. To the west, the MBDS-D and MBDS-E mounds were much smaller, each with a diameter of approximately 250 m and height of approximately 3 m (Figure 3-2). The MBDS-F mound was located between the MBDS-E and MBDS-A mounds. MBDS-F is relatively large with a footprint of approximately 350 m and extending approximately 7 m above the seafloor (Figure 3-2).

The MBDS-G mound, which was first identified in the 2007 survey, was located directly north of MBDS-F and northeast of MBDS-D (Figure 3-2). The mound was cone-shaped with a circular footprint about 300 m in diameter and a height of approximately 8 m.

The deposits at MBDS-H were not discernible as a mound in the bathymetry (Figure 3-2) despite the location receiving over 100,000 m^3 of dredged material between November 2009 and March 2010 (Figure 1-4, Table 1-2). The deposits at MBDS-I were also not discernible in the bathymetry, but the location received less than 50,000 m^3 of dredged material between November 2010 and September 2012 (Figure 1-4, Table 1-2).

3.1.2 Acoustic Backscatter

Acoustic backscatter results provided a very clear representation of recent disposal activity throughout the survey area (Figure 3-3). The mosaic of backscatter intensity displayed dark areas (higher backscatter intensity) that corresponded to recent dredged material placement as well as areas that received dredged material prior to 2007 (compare Figures 1-4 and 3-3). The mosaic has clear evidence of isolated disposal impact features and curved trails of dredged material that have been observed at other disposal sites (Carey et al. 2012 and Valente et al. 2012). Filtered backscatter results were processed into a grid file and presented in a quantitative form where backscatter intensity values are assigned a color (Figure 3-4). In this filtered and gridded display, the finer-scale details were less visible, but the relative intensity of backscatter returns were easier to discern. The dredged material placed in the area of MBDS-I had a much stronger return (-18 to -11 dB) than other recently placed material (Figure 3-4). The material placed at MBDS-H produced a small area of elevated return but contrasted with MBDS-I this deposit had a very minor and spatially limited backscatter return. Older material placed on the CDA in 2008 also had relatively strong backscatter returns (Figure 3-4).

3.1.3 Side-scan Sonar

Side-scan sonar results also provided a clear representation of disposal activity, but with some distinct differences from the backscatter results (Figure 3-5). The side-scan sonar results have a higher resolution and are more responsive to minor surface textural features and slope than the backscatter. The placement area around MBDS-I had a very restricted area of stronger return compared to the large area in the backscatter (compare Figures 3-4 and 3-5). The disposal impact features and curved marks were clearer in the side-scan sonar data indicating that they retain some surface topographical/textural qualities.

3.1.4 Comparison with Previous Bathymetry

The 2012 bathymetry survey overlapped with the previous 2007 survey area, which allowed generation of a depth difference map, plotted at a 30 cm contour interval (Figure 3-6). The increased height of the MBDS-G mound was the most noticeable change, but the base of the mound remained similar to the 2007 footprint (AECOM 2010). Three additional areas of accumulation corresponded to locations that received dredged material after 2007, one within the CDA and two separate accumulations at MBDS-H and MBDS-I (Figure 3-6). Because of the substantial uncertainties in bathymetric depth measurement, due to water column stratification and speed of sound variation throughout the 2007 and 2012 surveys, the depth difference at MBDS was not used to quantitatively estimate volume placed at the site. The material on MBDS-F had an apparent consolidation of about 1 m which is consistent with results from other disposal site mounds within the first several years after placement (Valente et al. 2012). Other areas of apparent minor consolidation were identified over mounds B, C, and E.

3.2 Sediment-Profile and Plan-View Imaging

The objective of the SPI survey at MBDS was to assess benthic recolonization status and benthic habitat characteristics at three areas within the disposal site boundary that had received new deposits of dredged material since the last survey in 2007; the majority of the survey efforts were concentrated on MBDS-G mound (Stations 1–12), while four additional stations were sampled on each of two new mounds created since 2007: MBDS-H (Stations 14, 17, 20, 22) and MBDS-I (Stations 30, 31, 34, 36).

The data from the disposal site was compared with those collected at 12 stations spread among three different reference areas: FG-23 (Stations 41–44), MBD-REF (Stations 37A, 38–40), and SE-REF (Stations 45–48). At each of the stations, there were results for three replicate drops of the SPI/PV camera system. The three measurements for the majority of the SPI variables of interest (e.g., aRPD depth, prism penetration depth, boundary roughness) were averaged to get one value per station; the maximum among replicates was used as the successional stage rank for the station. A summary of the SPI and PV results for the disposal site and reference area stations is presented in Tables 3-1 and 3-2 as well as in Appendices B and C.

3.2.1 Reference Area Stations

Physical Sediment Characteristics: As had been found in previous surveys (AECOM 2010), the sediments at all three reference areas were a well-mixed, uniform light brown silt/clay (major mode ≥4 phi; Figures 3-7 and 3-8). Similar to reported results from the 2007 survey, there was one smaller region within MBD-REF that had mud-covered rocks present on top of the silt substratum (Figure 3-9). After sampling attempts at this location (Station 37) with no successful sediment-profile image obtained (Figure 3-10), the location was moved a short distance within the reference area where no rocks were present on the surface to prevent camera prism penetration (Station 37A).

Station-averaged prism penetration depths at the three reference areas ranged from 10.1 to 19.7 cm (Figure 3-11), with an overall mean reference station prism penetration depth of 17.0 cm (Table 3-1). The stop collar settings and weights were kept nearly constant (stop collar settings of 34 or 35.6 cm, and one or two weights per carriage; see Appendix C), so the variation in camera penetration depth was a good measure of relative sediment shear strength among locations within the reference areas. There was no evidence of organic enrichment or presence of subsurface methane gas in any of the profile images from the three reference areas.

Mean small-scale boundary roughness values at the reference stations ranged from 0.9 to 2.1 cm, with an overall mean value of 1.4 cm for the ambient seafloor (Figure 3-12); most of the small-scale topographic relief was due to roughness elements created by faunal activity (Figure 3-13; Appendix C).

Biological Conditions and Benthic Recolonization: The mean depth of the apparent RPD at the stations surveyed among the three reference areas ranged from 1.5 to 3.1 cm (Figure 3-14), with an overall mean depth of 2.4 cm (Table 3-1).

Images from every location at all three reference areas had evidence of mature, Stage 3 taxa present, consistent with findings from previous surveys (Figure 3-15). The mean depth of subsurface feeding voids (when present) was 9.1 cm (Table 3-1), with maximum feeding void depths ranging from 3.8 to 18.9 cm. Several stations in the reference area showed evidence of biogenic re-working to depths exceeding the prism penetration depth (Figure 3-16).

3.2.2 Disposal Site Stations

Physical Sediment Characteristics: Many of the images from MBDS-G mound (to which additional dredged material was added in the past five years) showed the classic cross-section mosaic of chaotic sedimentary fabric with high-albedo inclusions of consolidated clay (Figure 3-17). All of the stations on this mound had a sediment grain size major mode of ≥4 phi (silt/clay sediment, Figure 3-18). Many of the consolidated clay clumps were still visible on the sediment surface in the associated plan-view images (Figure 3-19) on MBDS-G mound from the recent disposal activities, while distinct depositional layers of sediment from multiple disposal events were evident in some of the sediment-profile images from this mound (Figure 3-20).

While sediments at MBDS-H mound were of similar grain size major mode and range as those of MBDS-G mound (Table 3-2), the material disposed at MBDS-I mound had a much higher sand component (Figure 3-18) in the cross-sectional images, even though evidence of some consolidated clay clumps were visible on the sediment surface (Figure 3-21).

Mean camera prism penetration depth ranged from 5.2 to 19.8 cm (Figure 3-22) with an overall disposal site penetration depth of 13.6 cm (Table 3-2). The range of sediment particle sizes and sorting had a large effect on sediment shear strength; as a result, stop collar settings and weights were adjusted during the course of the survey. Areas within the site that had a higher sand component (like MBDS-I mound) had much lower prism penetration values, despite being actively bioturbated (Figure 3-23). While some of the dredged material disposed within the past five years definitely had a higher organic content than native sediments (Figure 3-24), none of the locations showed any evidence of subsurface methane gas presence or the occurrence of low oxygen conditions in the overlying water at the sediment surface.

Mean small-scale surface boundary roughness within the disposal site boundaries ranged from 0.7 to 5.8 cm, with an overall mean of 1.9 cm (Table 3-2). The small-scale topographic relief was primarily biogenic in nature, except for locations sampled on MBDS-I mound, where the largest boundary roughness values were measured; the topographic roughness measured in this location was mainly due to consolidated clumps of clay from dredged material disposal which had not yet broken down (Figure 3-25).

Biological Conditions and Benthic Recolonization: The mean depth of the apparent RPD ranged from 0.8 to 4.7 cm (Table 3-2, Figure 3-26), with an overall mean aRPD depth of 2.5 cm for locations within the MBDS boundary (Table 3-2). Evidence of Stage 3 taxa was found at all locations sampled (Figure 3-27). The thickness of dredged material deposits exceeded the prism penetration depth and was visually obvious (Figure 3-25), but the disposed material had been thoroughly recolonized by mature successional assemblage deposit-feeding taxa (Figure 3-28). Many of the clay clumps found on the surface had been intact long enough to become colonized by epifaunal fouling organisms typically found on rocky surfaces, e.g., hydroids, bryozoans, etc. (Figure 3-29).

The mean depth of subsurface feeding voids ranged from 5.3 to 17.1 cm (Table 3-2); all the sediments surveyed within the disposal site showed evidence of active bioturbation as well as surface foraging activity (Figure 3-30).

3.3 Statistical Comparisons

3.3.1 Mean aRPD Depths

The three reference areas were fairly similar, although SE-REF had slightly higher mean and smaller variance for the aRPD depth values (Table 3-3, Figure 3-31). Results for the normality test indicate that the area residuals (i.e., each observation minus the area mean) were normally distributed (Shapiro-Wilk's test p-value = 0.90). The assumption of equal variances was rejected by Levene's test (p = 0.023) so a separate variance estimate and associated degrees of freedom were used to compute the variance for the difference equation shown in Table 3-4.

The difference between MBDS-G mound and the mean of the reference locations was less than 0.1 cm. The two 95% confidence bounds for the inequivalence test on this difference were [-0.51, 0.61]. These bounds are fully contained within the interval [-1.0, +1.0], which are the limits of what is considered to be ecologically equivalent. Hence, it is concluded that MBDS-G mound is statistically equivalent to the mean reference area conditions for the aRPD depth endpoint.

3.3.2 Successional Stage Ranks

All disposal site stations and reference areas indicated successional stages at Stage 3 or equivalent. With identical means and zero variance, no statistics were needed for comparisons between reference and mounds in order to conclude statistical equivalence.

Table 3-1.

Summary of MBDS Reference Station SPI Results, October 2012

Location	Station	Station Grain Size Major Mode (phi)	Station Mean Penetration (cm)	Station Mean Boundary Roughness (cm)	Station Mean aRPD Depth (cm)	Methane Present?	Station Maximum Void Depth (cm)	Highest Successional Stage Present
MBD-REF	37A	>4	16.9	1.5	3.0	no	13.1	1 on 3
MBD-REF	38	>4	10.1	2.1	1.5	no	6.4	1 on 3
MBD-REF	39	>4	17.8	1.5	1.9	no	-	1 on 3
MBD-REF	40	>4	17.4	1.2	2.1	no	-	1 on 3
FG-23	41	>4	16.6	1.3	3.1	no	-	1 on 3
FG-23	42	>4	17.9	1.7	2.1	no	9.6	1 on 3
FG-23	43	>4	16.5	0.9	2.4	no	3.8	1 on 3
FG-23	44	>4	16.7	0.9	1.9	no	16.4	1 on 3
SE-REF	45	>4	18.0	2.1	2.2	no	5.1	1 on 3
SE-REF	46	>4	17.9	1.2	2.8	no	17.2	1 on 3
SE-REF	47	>4	19.7	1.1	2.5	no	18.7	1 on 3
SE-REF	48	>4	18.7	1.6	2.8	no	18.9	1 on 3
	Min	NA	10.1	0.9	1.5	NA	3.8	NA
	Max	NA	19.7	2.1	3.1	NA	18.9	NA
	Mean	NA	17.0	1.4	2.4	NA	12.1	NA

Table 3-2.

Summary of MBDS SPI Results, October 2012

Location	Station	Station Grain Size Major Mode (phi)	Station Mean Penetration (cm)	Station Mean Boundary Roughness (cm)	Station Mean aRPD Depth (cm)	Methane Present?	Station Maximum Void Depth (cm)	Highest Successional Stage Present
MBDS-G	01	>4	10.0	3.3	1.3	no	9.7	2 on 3
MBDS-G	02	>4	12.1	1.8	1.6	no	13.0	1 on 3
MBDS-G	03	>4	13.5	1.4	2.2	no	12.5	1 on 3
MBDS-G	04	>4	13.6	0.9	3.5	no	17.1	1 on 3
MBDS-G	05	>4	16.1	0.9	2.6	no	13.9	1 on 3
MBDS-G	06	>4	15.4	1.3	2.9	no	5.8	1 on 3
MBDS-G	07	>4	11.1	2.8	1.1	no	12.5	1 on 3
MBDS-G	08	>4	17.6	0.7	3.6	no	13.0	1 on 3
MBDS-G	09	>4	18.7	2.2	3.3	no	15.3	1 on 3
MBDS-G	10	>4	19.8	2.4	3.0	no	8.8	1 on 3
MBDS-G	11	>4	7.9	3.2	0.8	no	7.7	1 on 3
MBDS-G	12	>4	11.4	1.3	1.7	no	7.4	1 on 3
MBDS-H	14	>4	19.3	1.6	4.7	no	16.0	1 on 3
MBDS-H	17	>4	16.6	1.8	2.6	no	8.1	1 on 3
MBDS-H	20	>4	18.7	1.4	3.5	no	15.4	1 on 3
MBDS-H	22	>4	19.3	1.2	3.1	no	16.0	1 on 3
MBDS-I	30	4-3/>4	12.6	5.8	2.8	no	13.0	1 on 3
MBDS-I	31	4-3	5.2	1.7	1.3	no	6.7	1 on 3
MBDS-I	34	4-3	6.0	1.8	1.8	no	6.0	1 on 3
MBDS-I	36	4-3	6.3	1.4	2.9	no	5.3	1 on 3
	Min	NA	5.2	0.7	0.8	NA	5.3	NA
	Max	NA	19.8	5.8	4.7	NA	17.1	NA
	Mean	NA	13.6	1.9	2.5	NA	11.2	NA

Table 3-3.

Summary of Station Means by Sampling Location

Area	N	Mean aRPD Depth (cm) Mean	Standard Deviation
Reference Locations			
MBD-REF	4	2.1	0.65
SE-REF	4	2.5	0.29
FG-23	4	2.4	0.53
Mean:		2.3	
Disposal Mound			
MBDS-G	12	2.3	0.99

Table 3-4.

Summary Statistics and Results of Bioequivalence Testing for aRPD Depth Values

Difference Equation	Observed Difference ($\hat{d}$)	SE($\hat{d}$)	df for SE ($\hat{d}$)	95% Lower Confidence Bound	95% Upper Confidence Bound
Mean REF – Mean MBDS-G Mound	0.052	0.32	15.9	-0.51	0.61

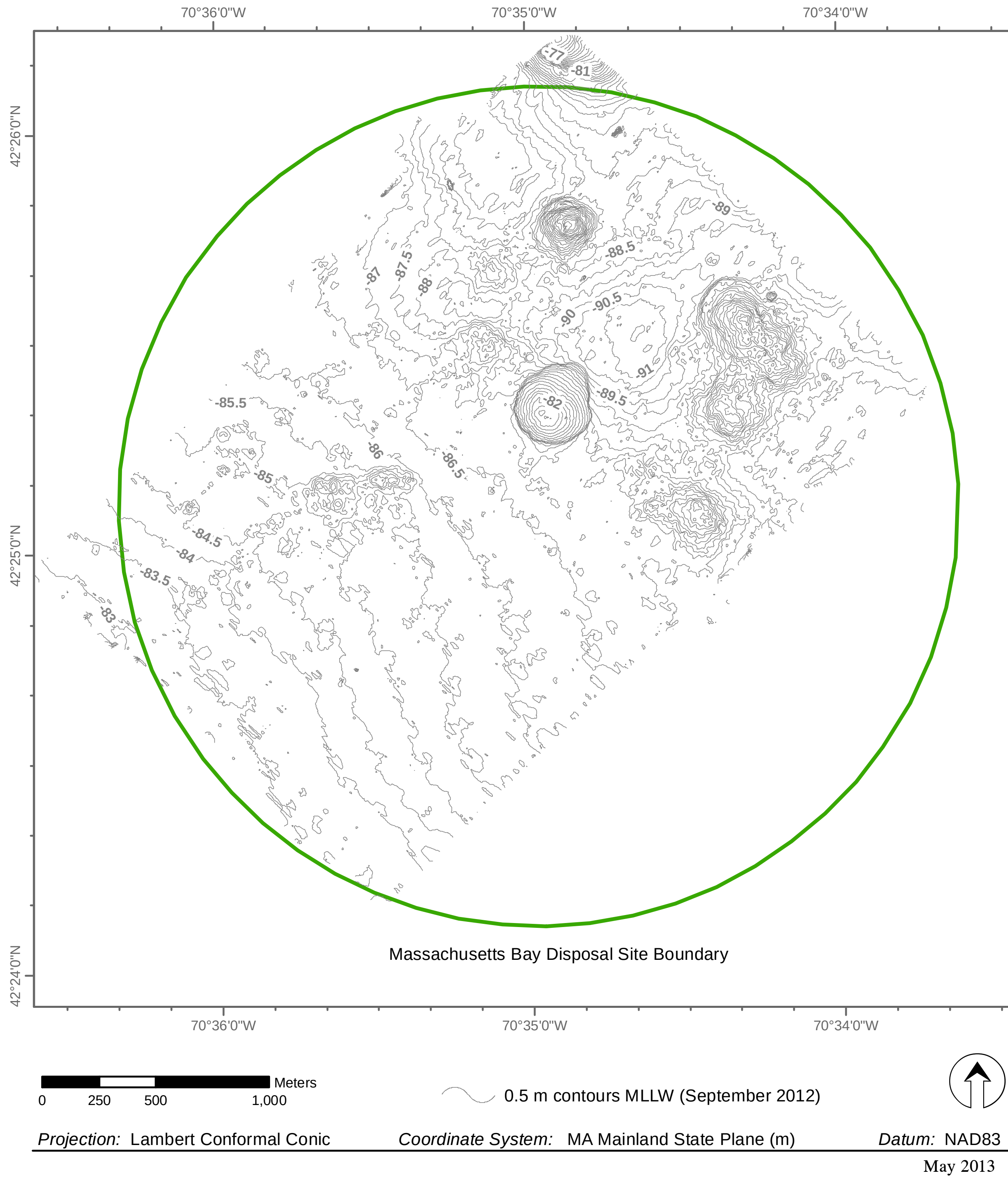

Figure 3-1. Bathymetric contour map of MBDS – September 2012

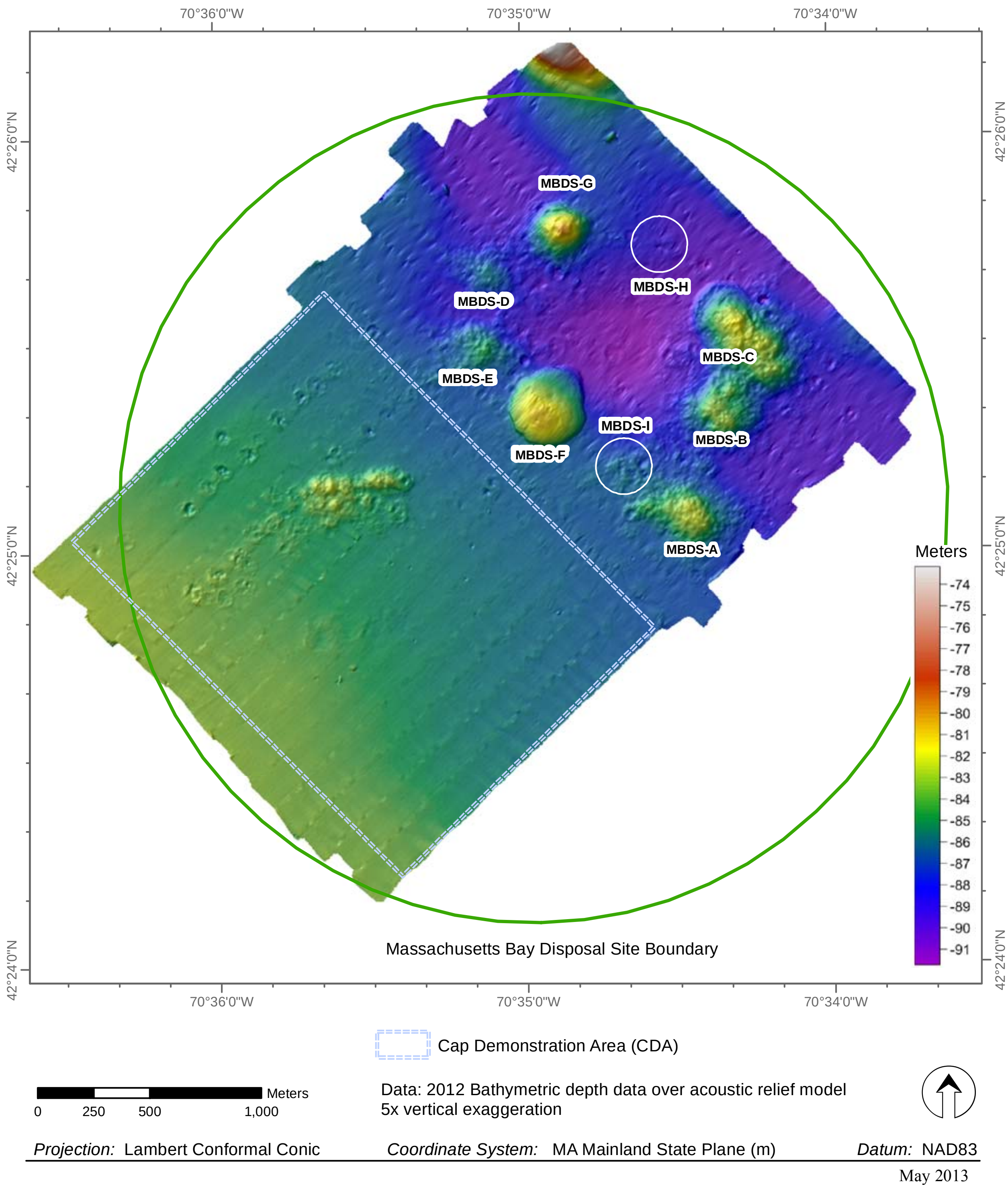

Figure 3-2. Bathymetric depth data over acoustic relief model of MBDS – September 2012

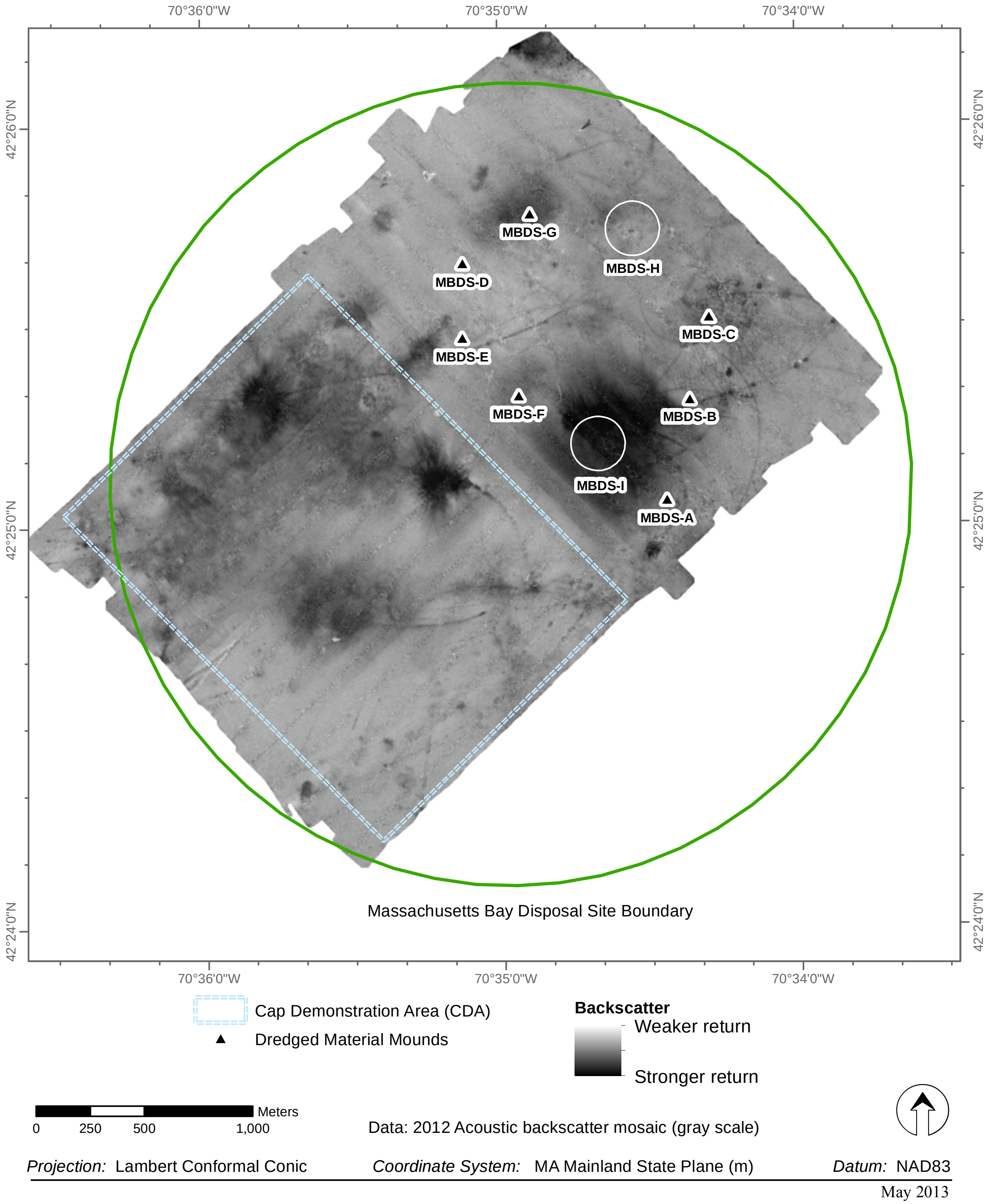

Figure 3-3. Mosaic of unfiltered backscatter data of MBDS – September 2012

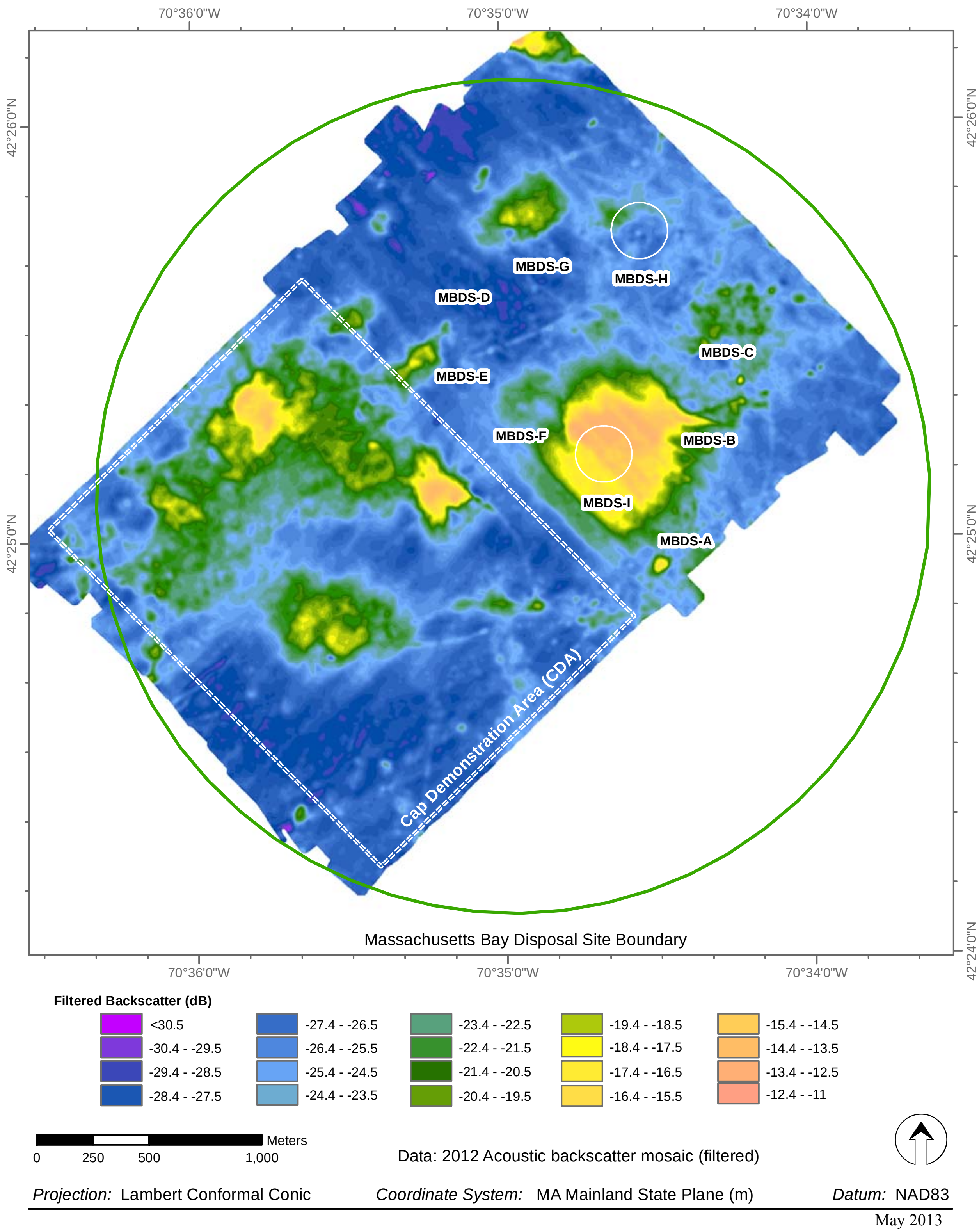

Figure 3-4. Filtered backscatter of MBDS – September 2012

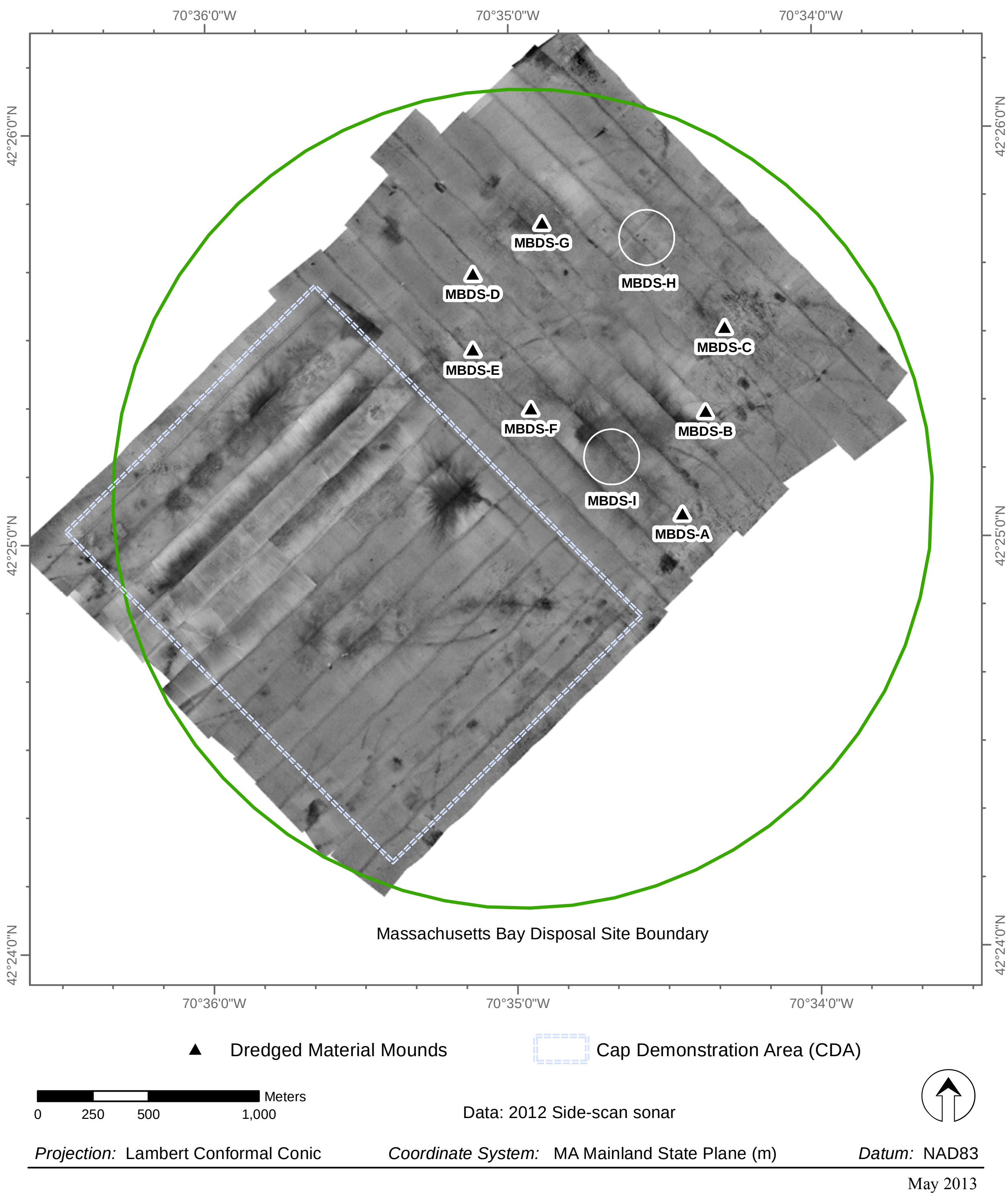

Figure 3-5. Side-scan mosaic of MBDS – September 2012

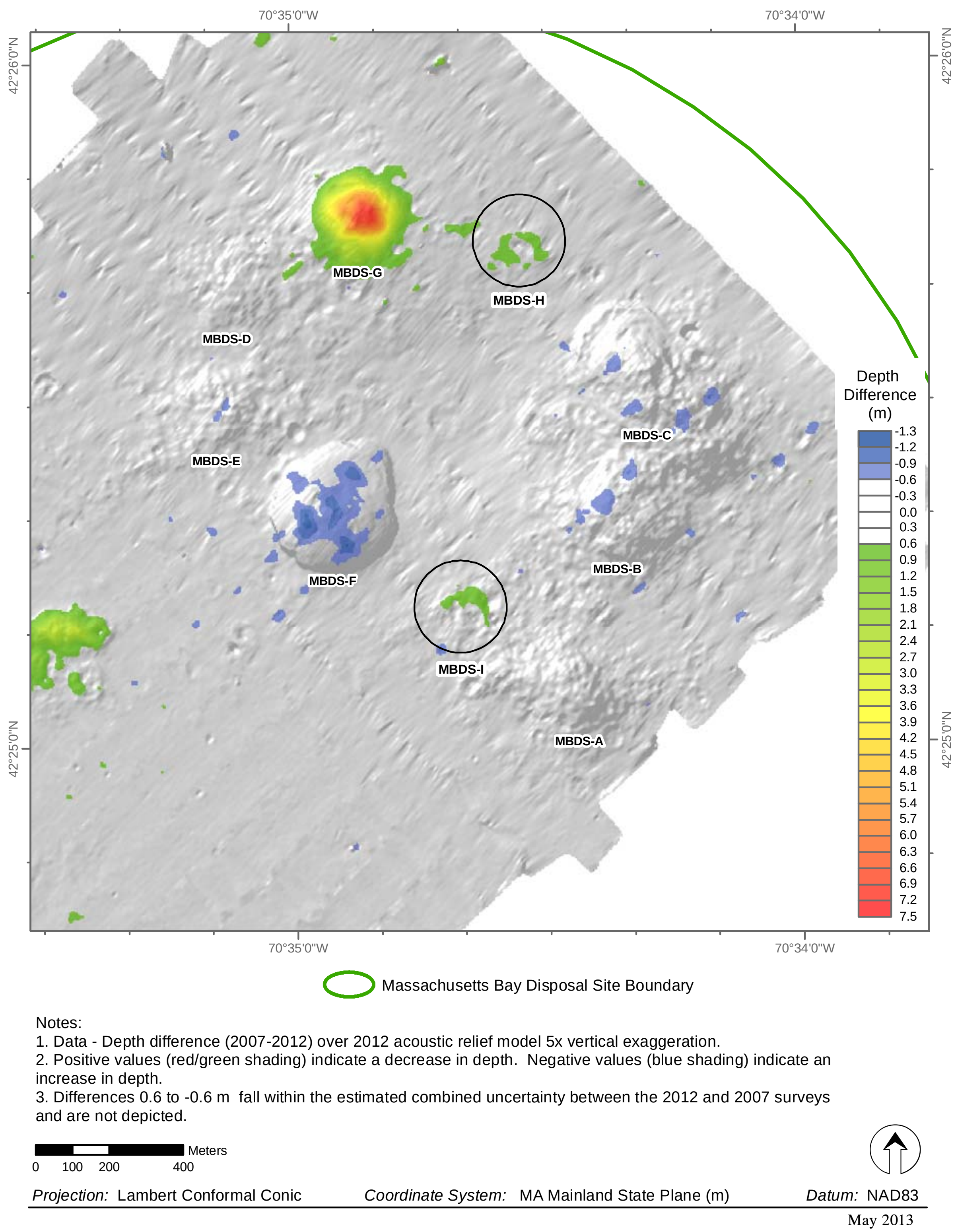

Figure 3-6. MBDS depth difference: 2012 vs. 2007

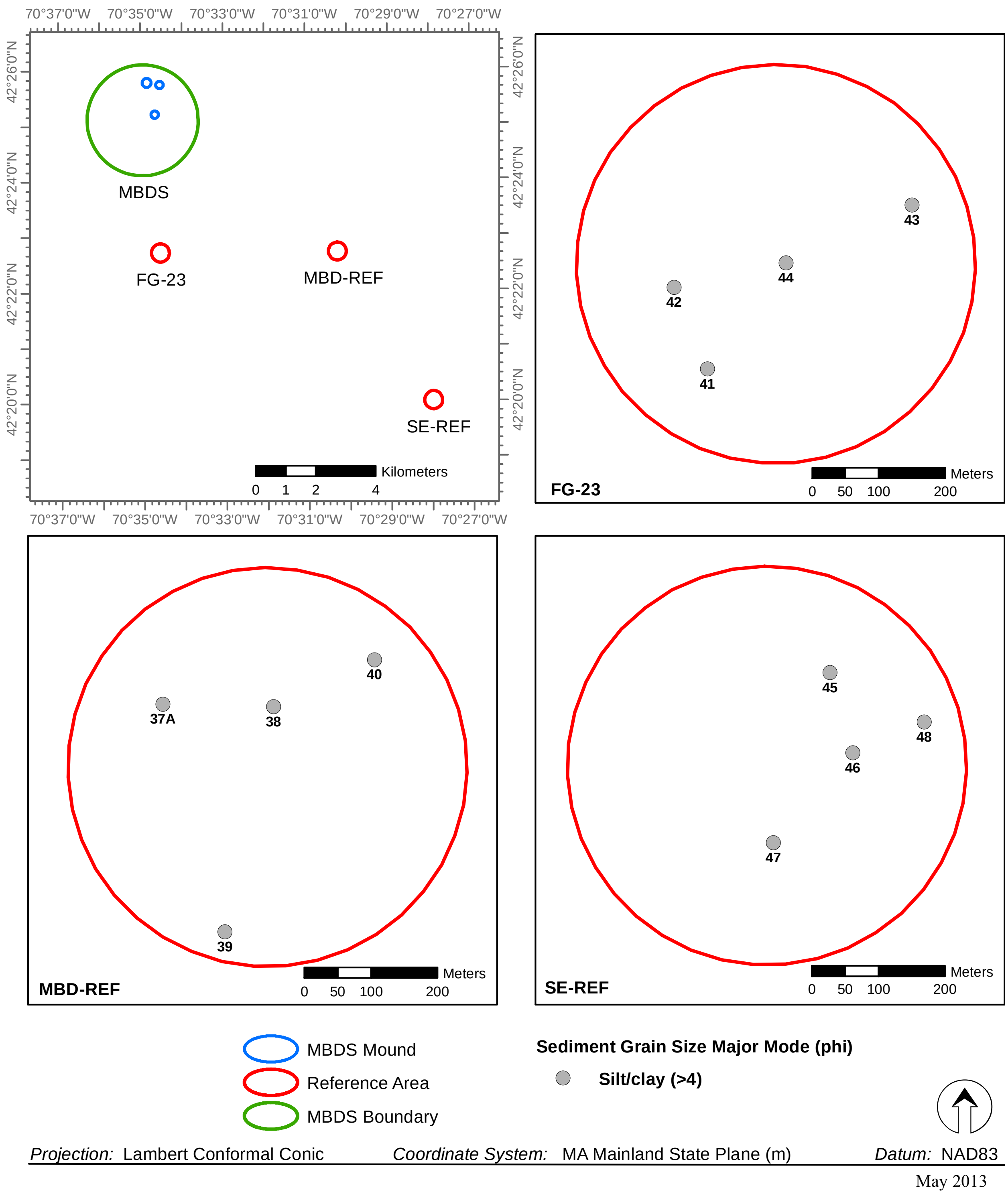

Figure 3-7. Sediment grain size major mode (phi units) at the MBDS reference areas

Figure 3-8. Sediment-profile image from MBDS-REF Station 37A showed well-sorted, silt/clay sediments that are typical for locations at the three MBDS reference areas

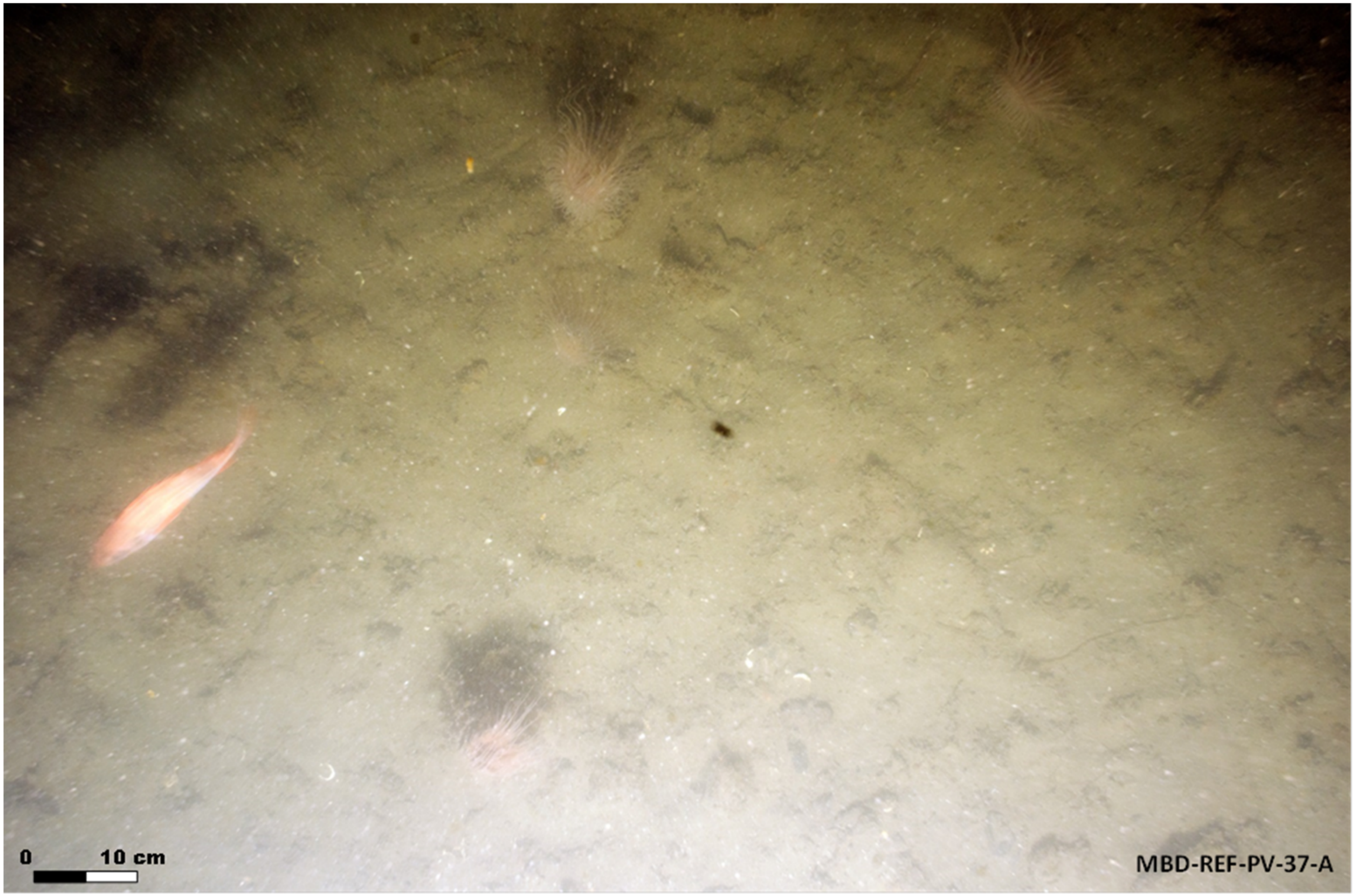

Figure 3-9. Plan-view image from MBD-REF Station 37 showed some *Cerianthid* anemones among the rocks on the sediment surface

Figure 3-10. Sediment-profile image from MBD-REF Station 37 showed minimal prism penetration because of the rocks on the sediment surface

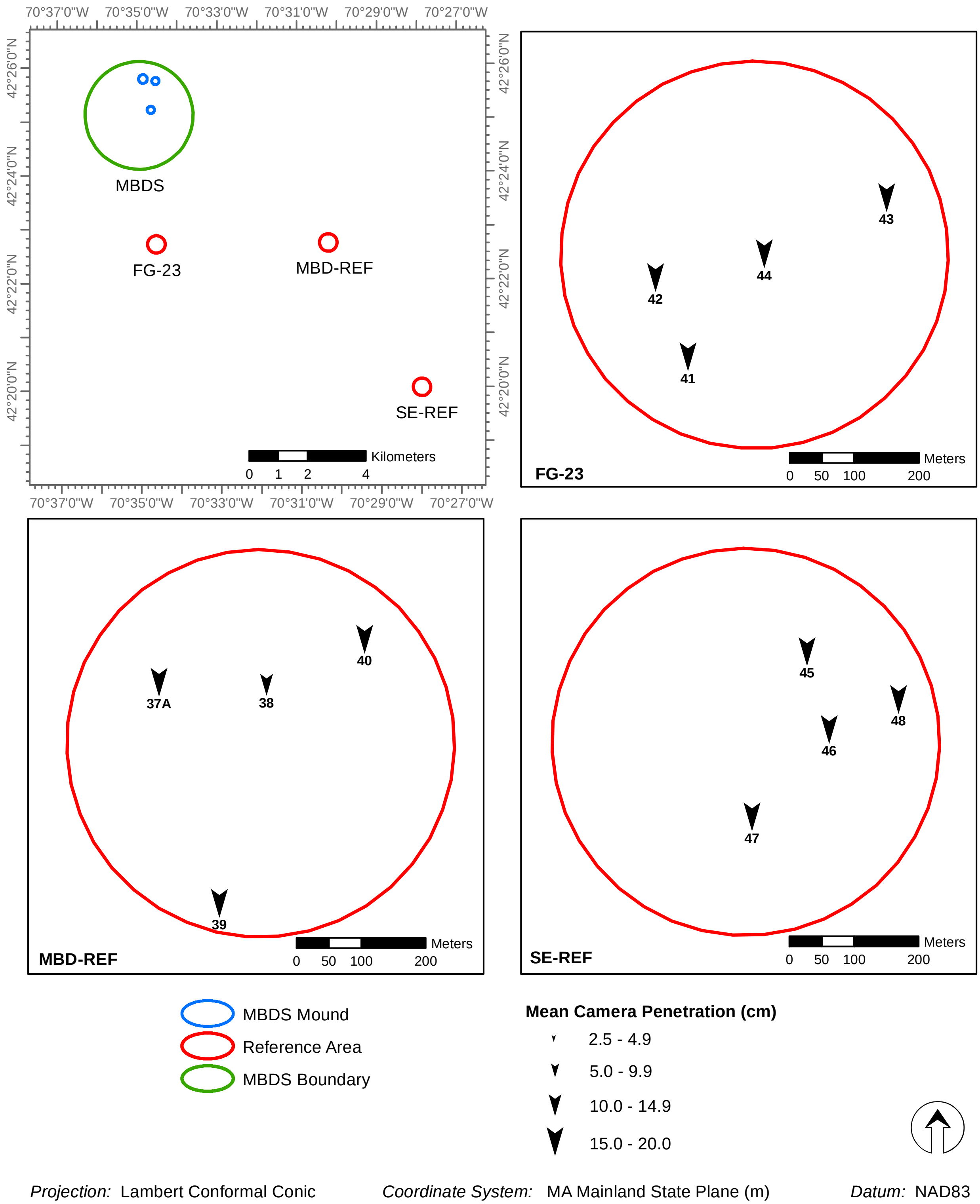

May 2013

Figure 3-11. Mean station camera prism penetration depths (cm) at the MBDS reference areas

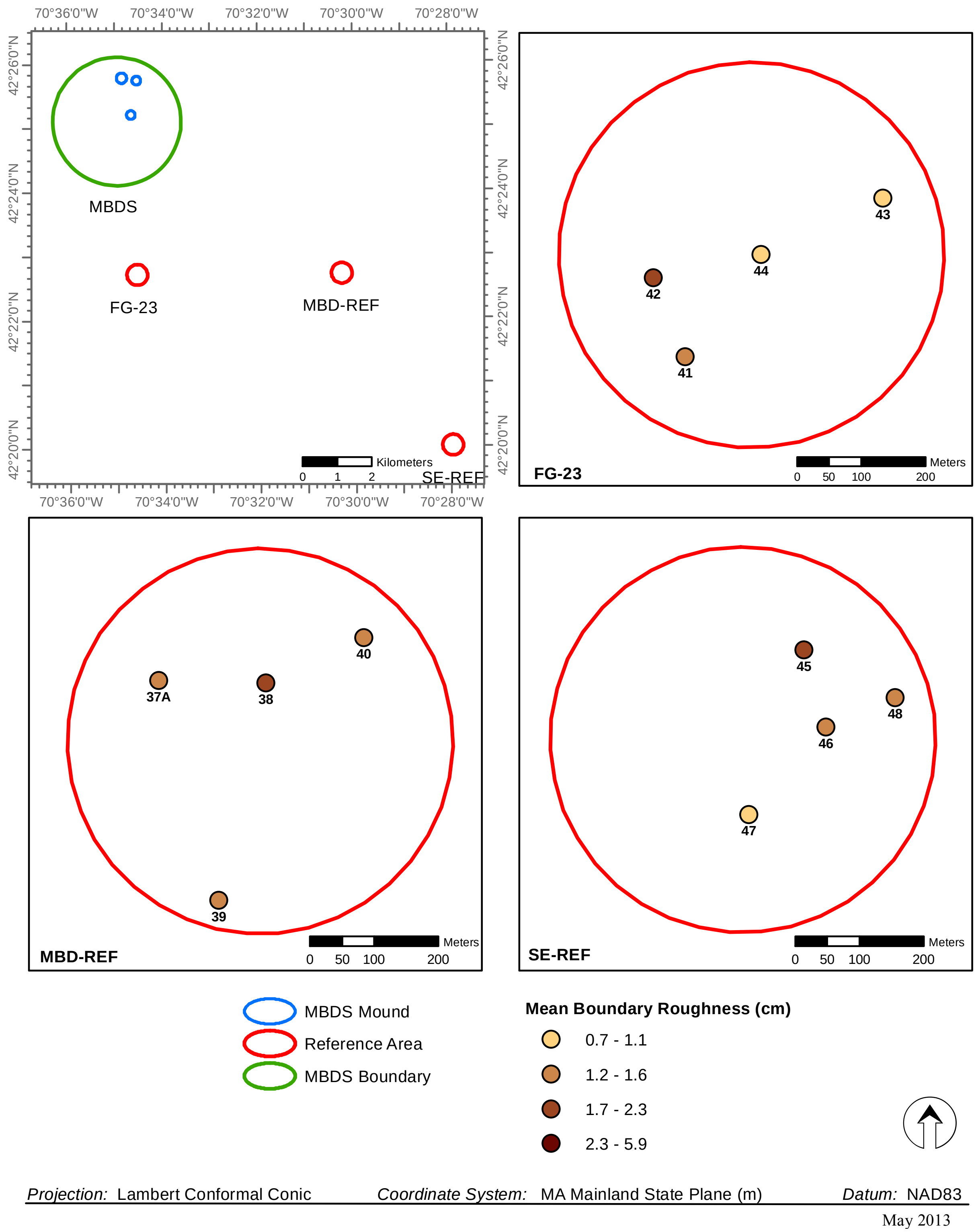

Figure 3-12. Mean station small-scale boundary roughness values (cm) at the MBDS reference areas

Figure 3-13. Sediment-profile image from Station 43 in FG-23 showed the small-scale surface relief caused by infaunal burrowing activities

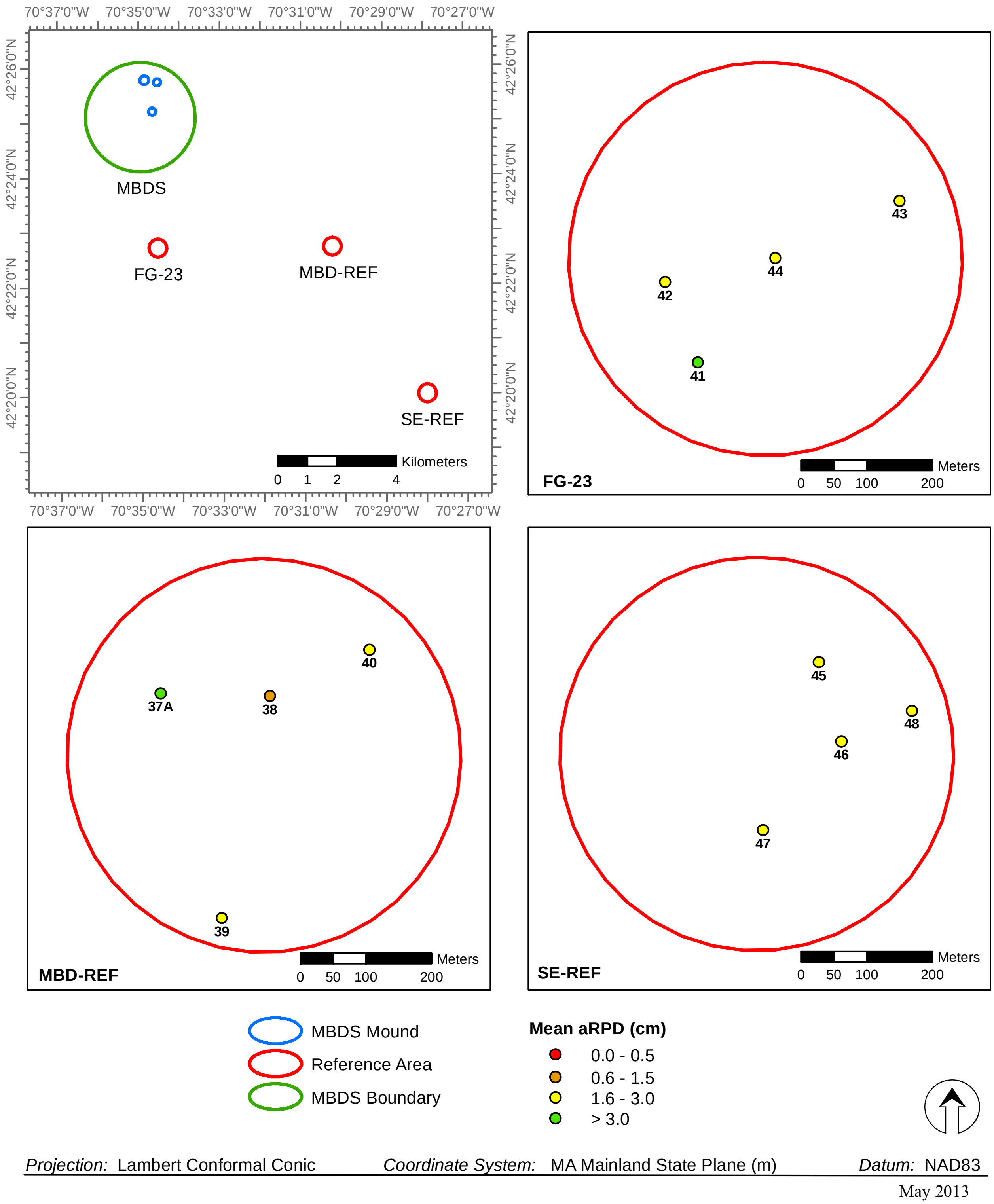

Figure 3-14. Mean station aRPD depth (cm) at the MBDS reference areas

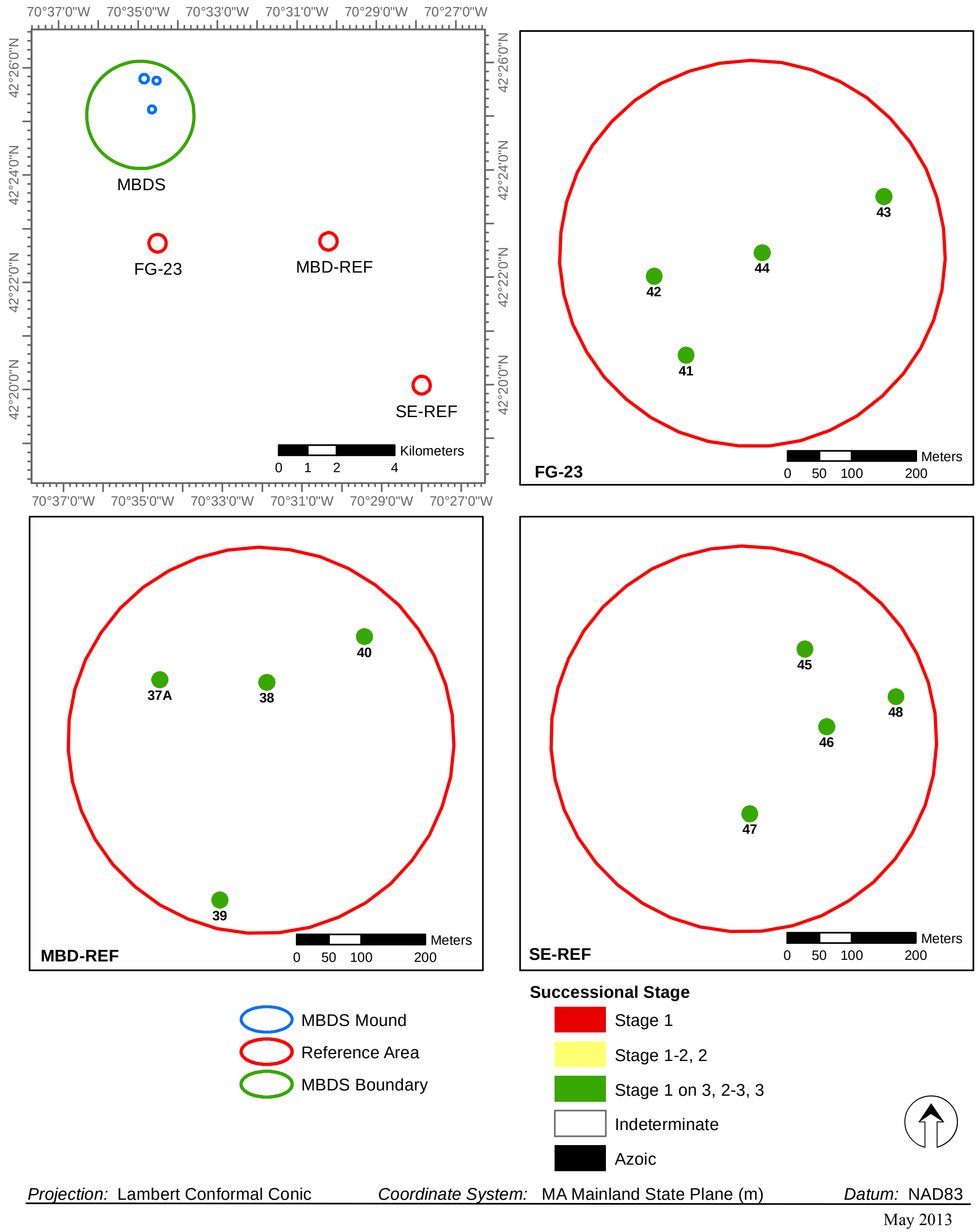

Figure 3-15. Infaunal successional stages found at locations sampled in the three MBDS reference areas

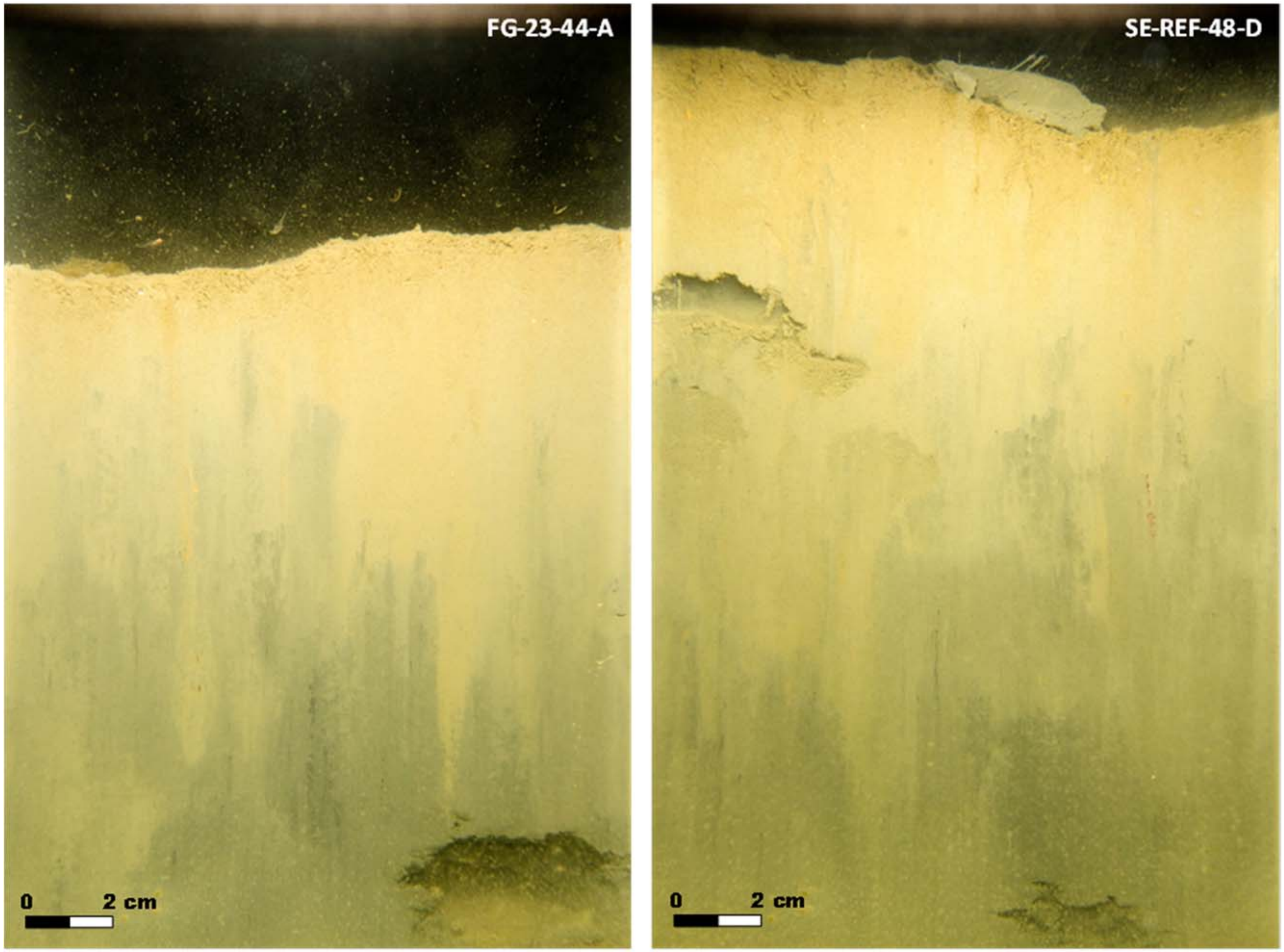

Figure 3-16. Sediment-profile images from Station 44 (left) in FG-23 and Station 48 (right) in SE-REF showed evidence of biogenic burrowing and feeding activities that extended beyond the depth of the prism penetration

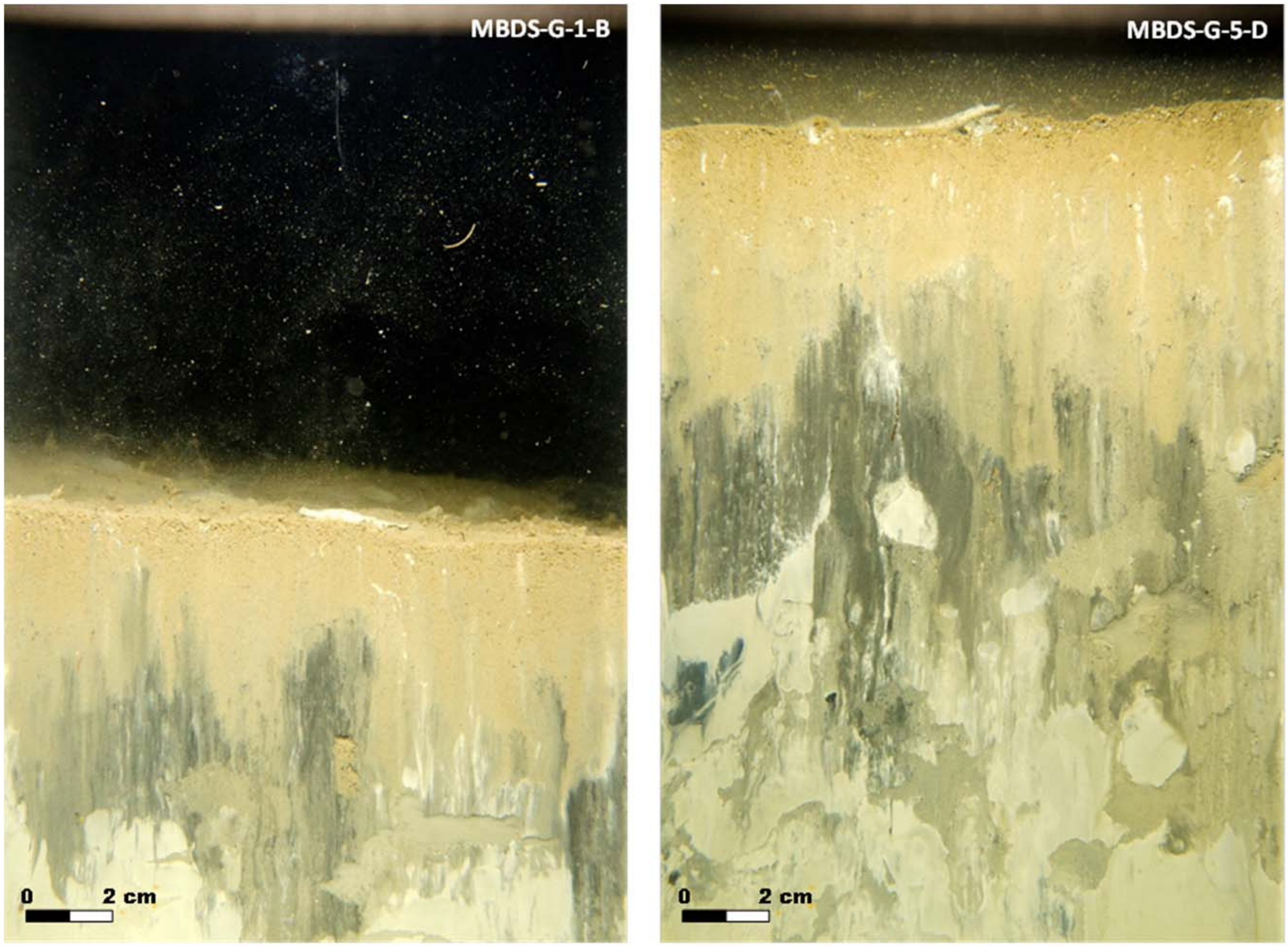

Figure 3-17. Sediment-profile images from MBDS-G Station 1 (left) and Station 5 (right) showed consolidated clay inclusions among the organically enriched subsurface silt/clay sediments

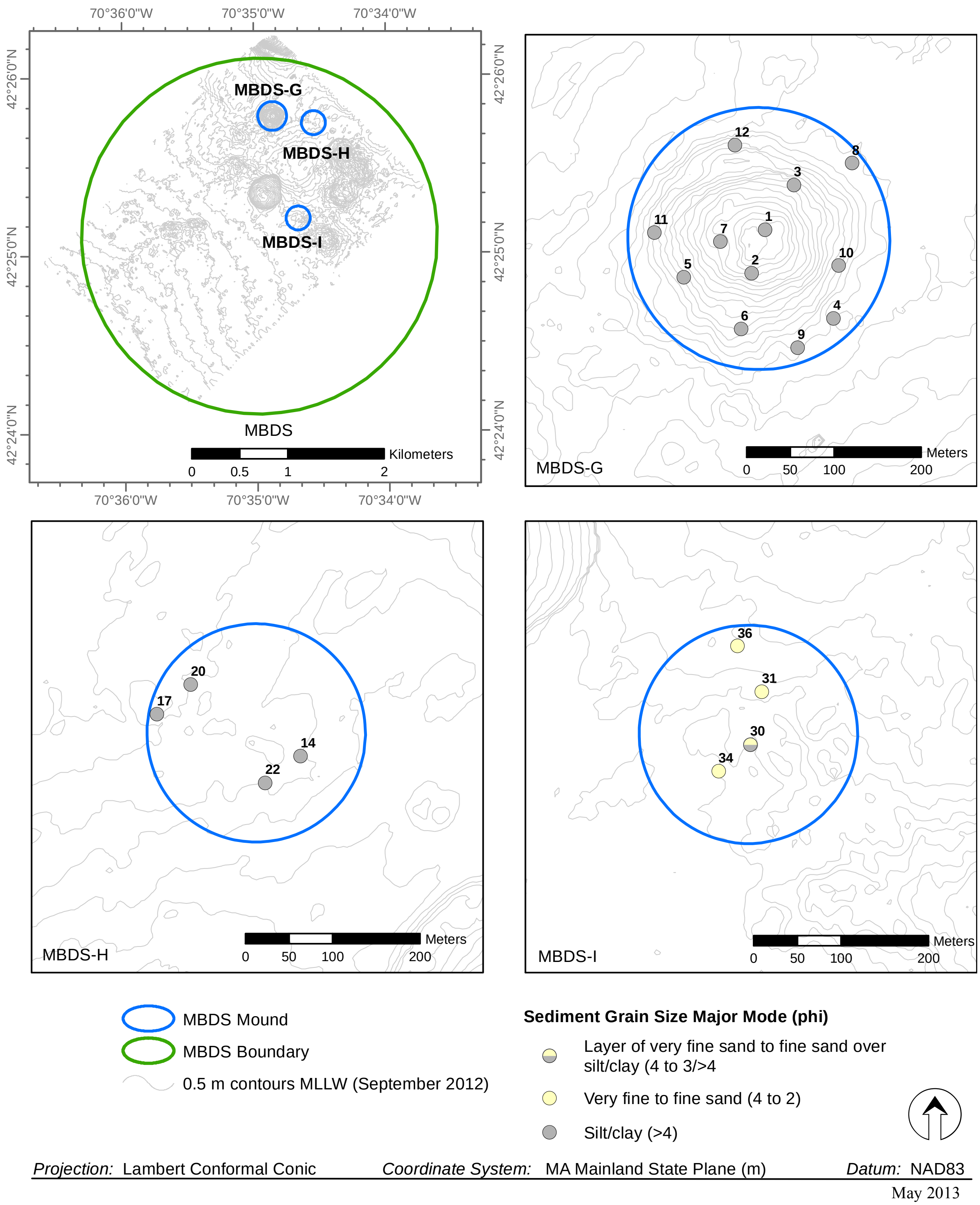

Figure 3-18. Sediment grain size major mode (phi units) at stations sampled within the MBDS boundary

Figure 3-19. Plan-view images from MBDS-G Stations 1 (top), 2 (center) and 11 (bottom) showed consolidated clay clumps from recent disposal activities which will disintegrate over time

Figure 3-20. Sediment-profile image from MBDS-G Station 4 showed evidence of the old sediment-water interface (lighter colored horizon) at depth, while the more recent deposit had already been colonized and reworked by infauna

Figure 3-21. Plan-view images from Station 30 (top) and Station 34 (bottom) on MBDS-I mound showed clay clumps that provided some surface relief that will attract fish and larger epifaunal foragers

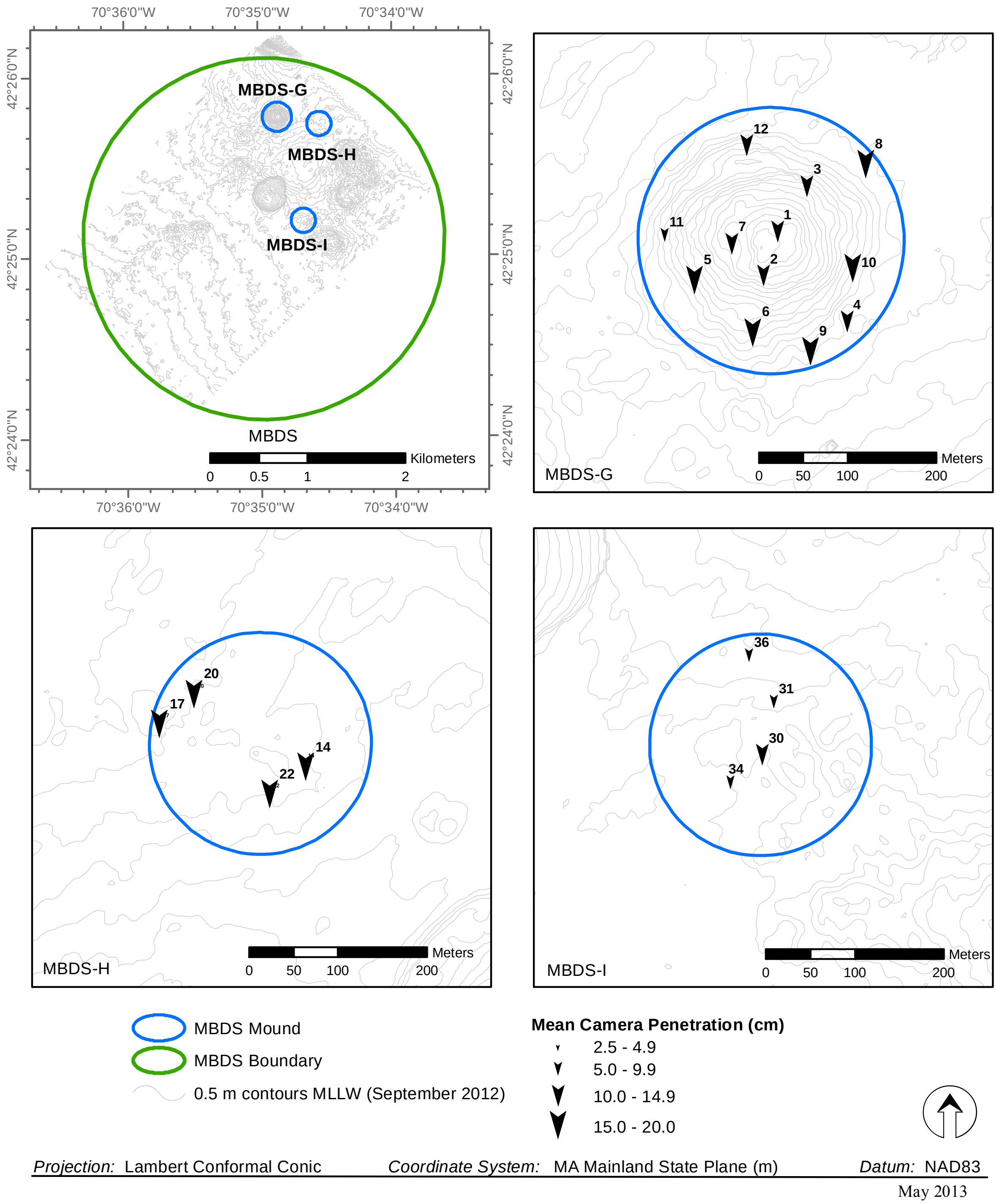

Figure 3-22. Mean station camera prism penetration depths (cm) at the MBDS disposal mounds

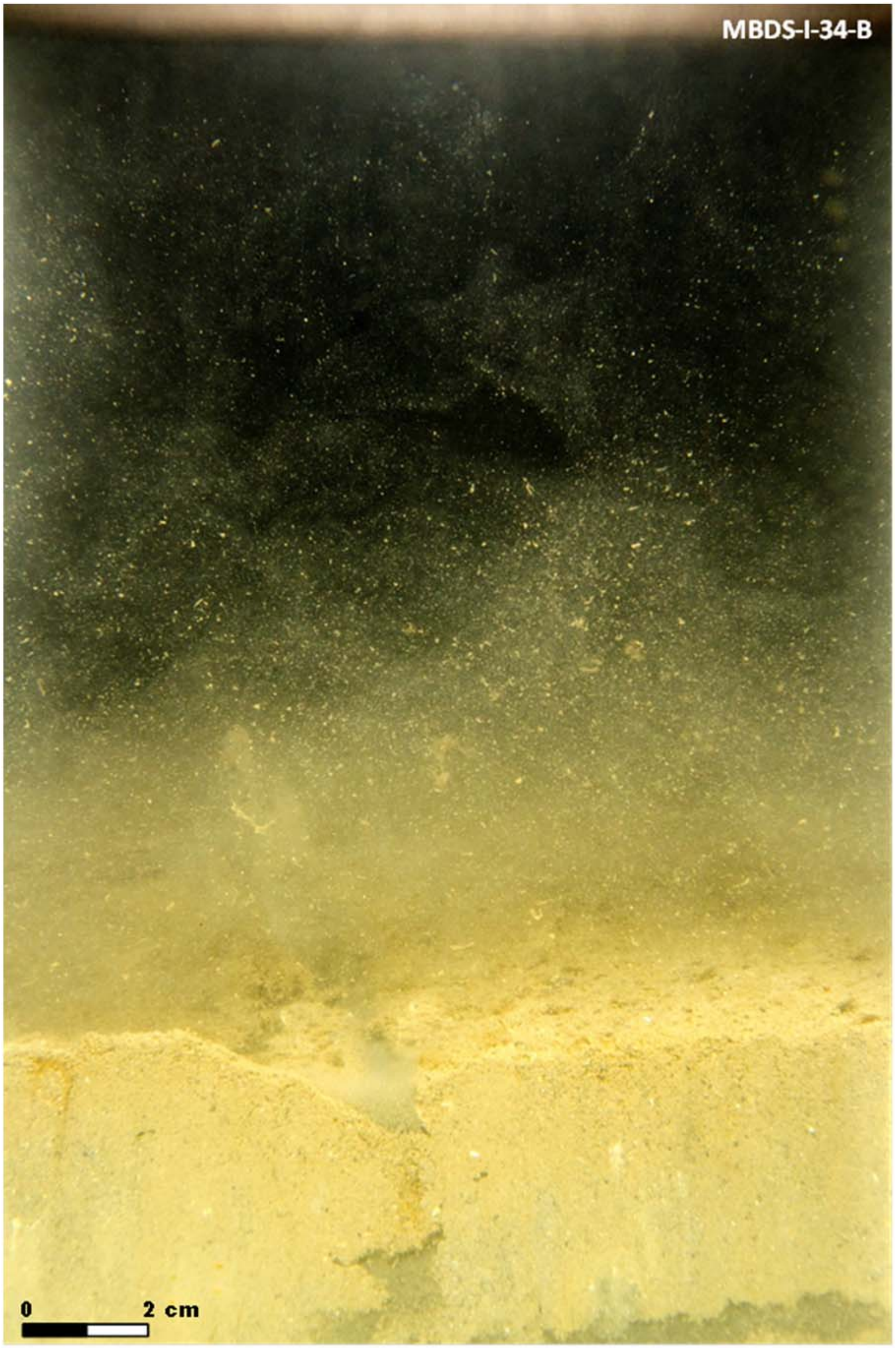

Figure 3-23. Sediment-profile image from Station 34 (MBDS-I mound) showed evidence of extensive biological reworking yet still had relatively high shear strength because of the high proportion of sand-sized particles in the disposed material.

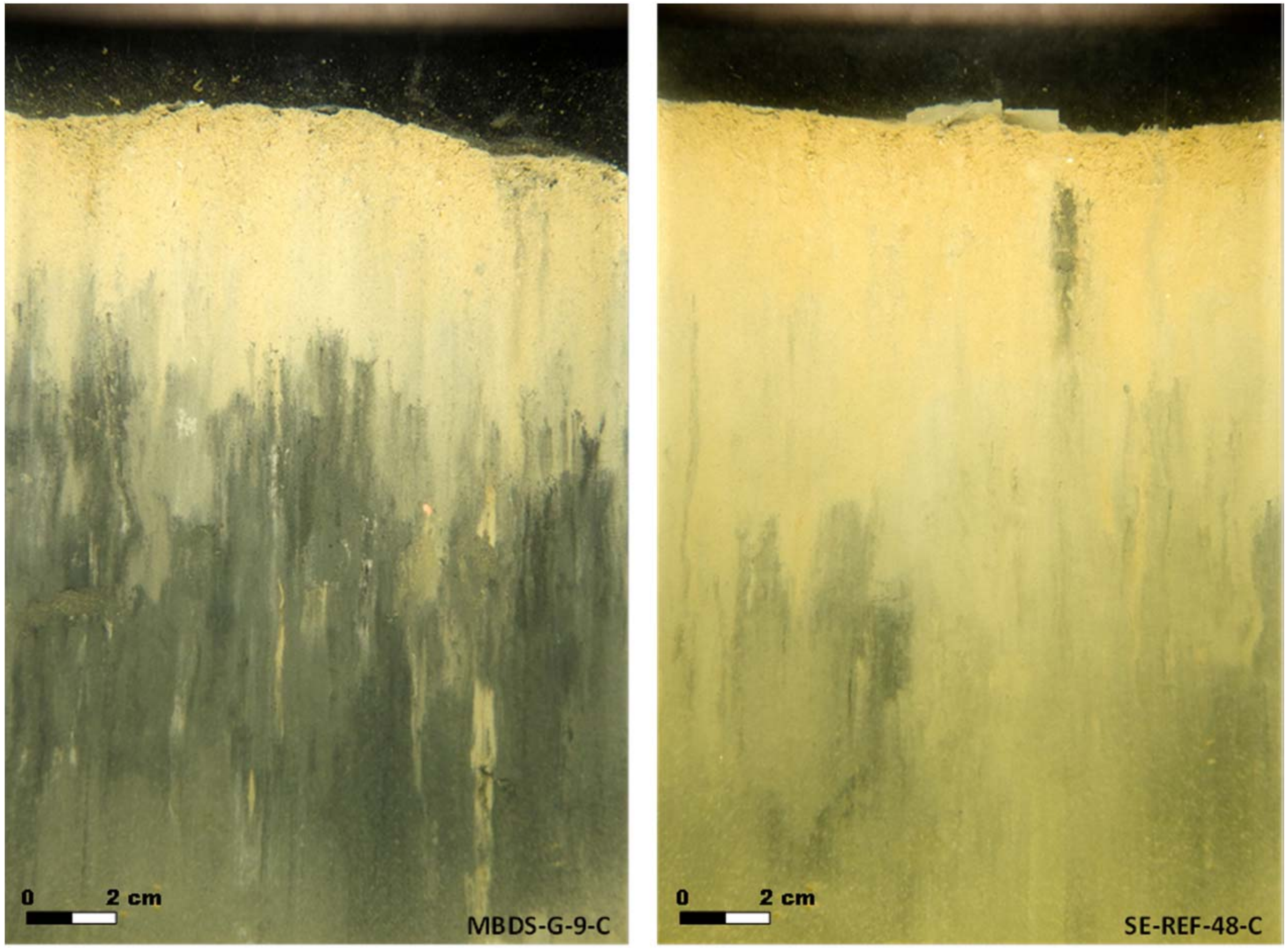

Figure 3-24. Sediment-profile image from MBDS-G Station 9 (left) showed low reflectance of subsurface organically-enriched sediments at the disposal site as compared with reference area image from SE-REF Station 48 (right) which showed higher reflectance of subsurface sediments from the ambient seafloor with lower organic content

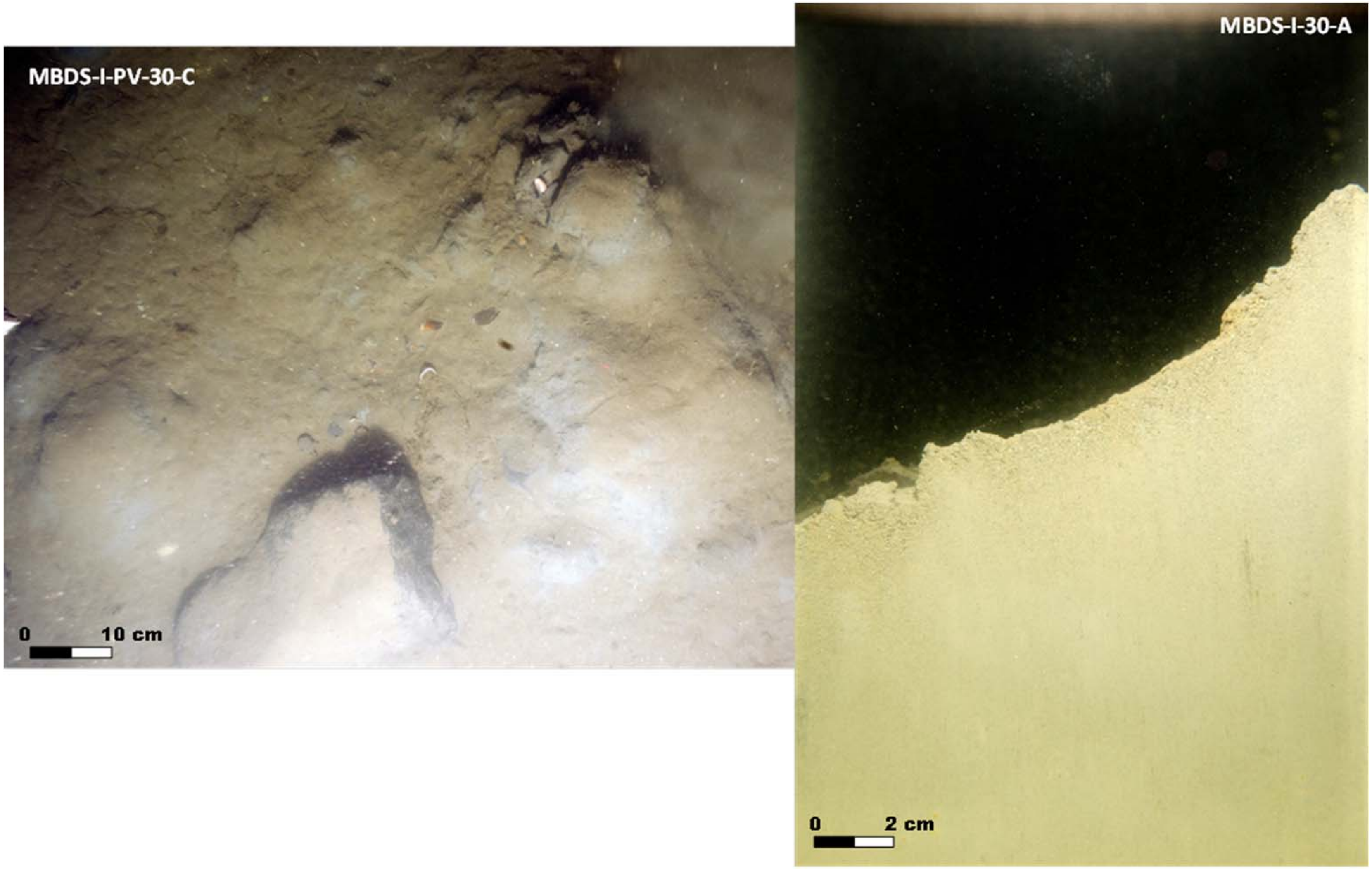

Figure 3-25. Plan-view and sediment-profile images from Station 30 showed the physical clay clump structures responsible for the high surface boundary roughness values measured at MBDS-I mound

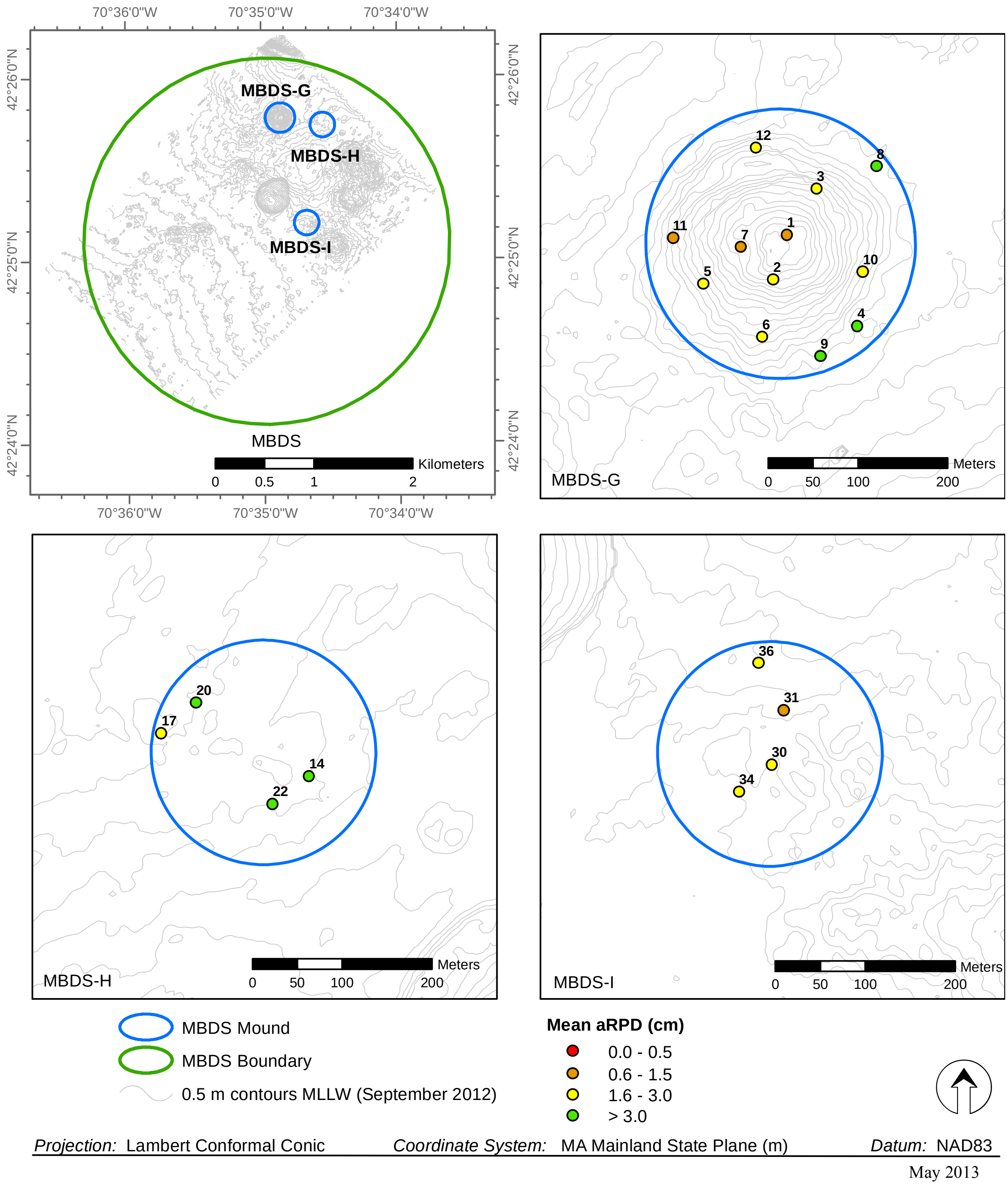

Figure 3-26. Mean station depth of the apparent RPD (cm) at locations within the MBDS designated boundary

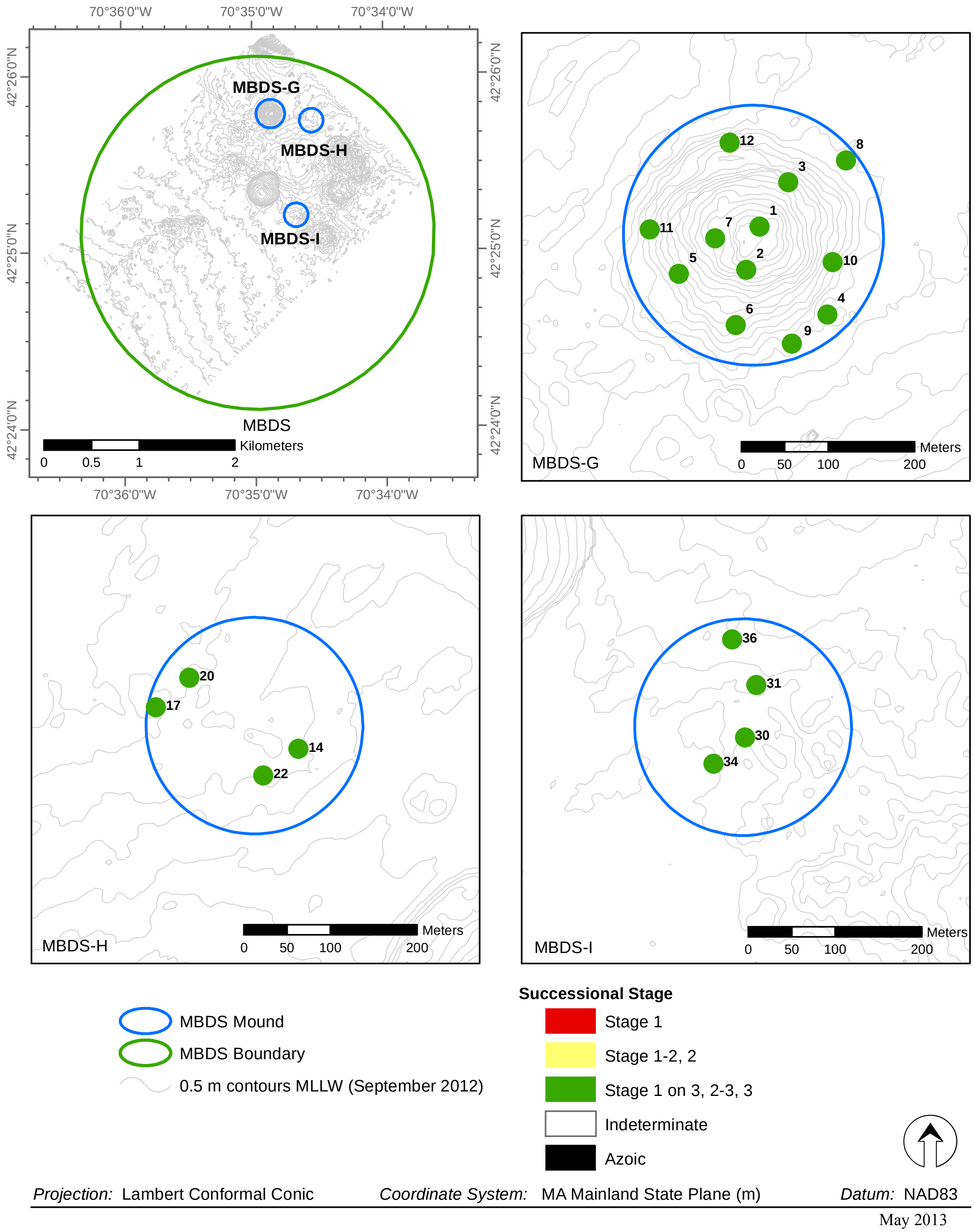

Figure 3-27. Infaunal successional stages at locations sampled within the MBDS boundary

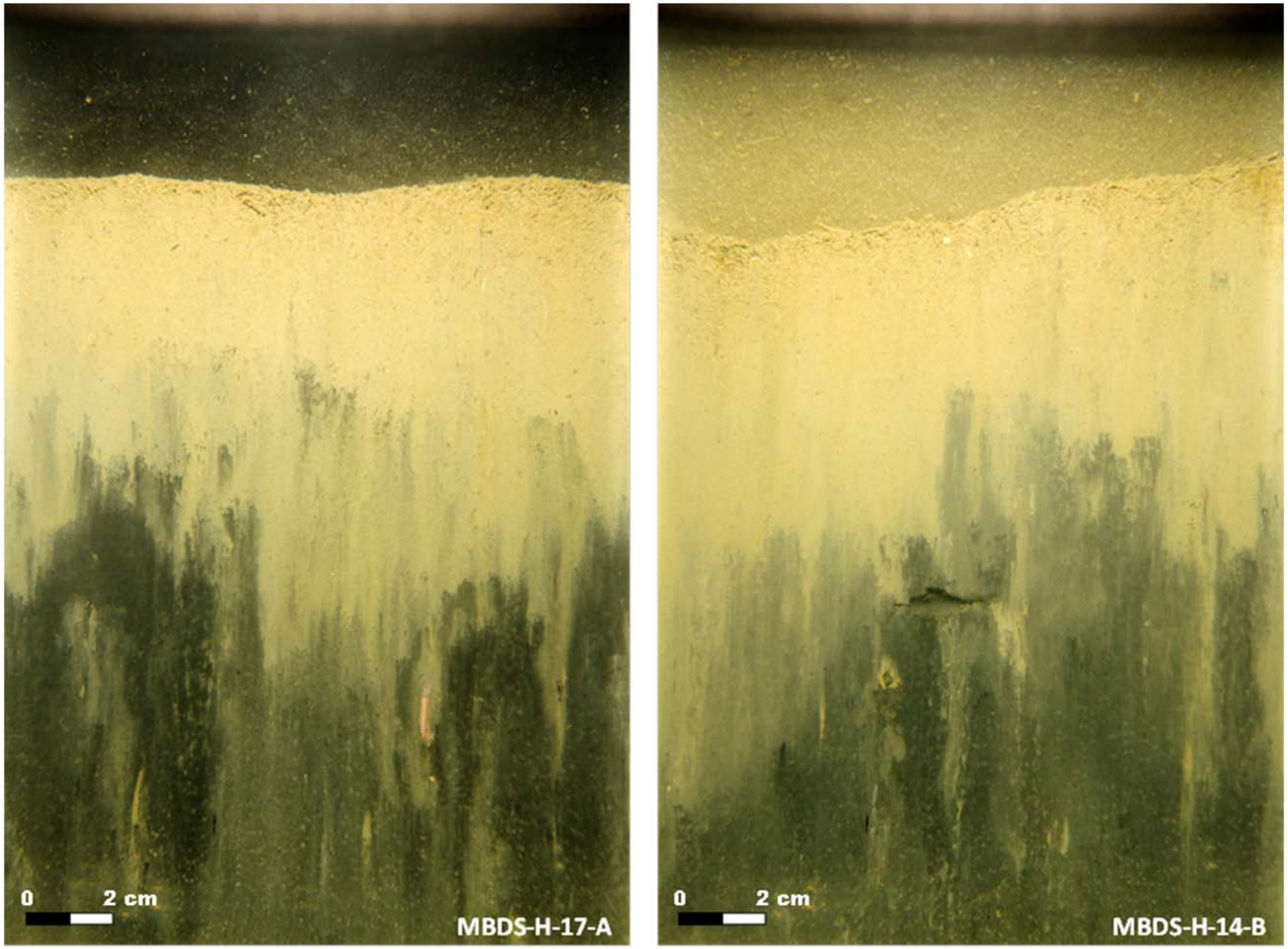

Figure 3-28. Sediment-profile images from MBDS-H Station 17 (left) and Station 14 (right) still had obvious visual evidence of their dredged material origin, yet the presence of Stage 3 taxa was readily apparent

Figure 3-29. Plan-view image from MBDS-G Station 1 showed clay clumps from disposal operations that have been intact long enough to serve as a colonizing surface for suspension-feeding colonial invertebrates

Figure 3-30. Plan-view image from MBDS-G Station 6 showed burrow openings of infaunal deposit feeders as well as shrimp on the sediment surface along with surface tracks from recent crab foraging

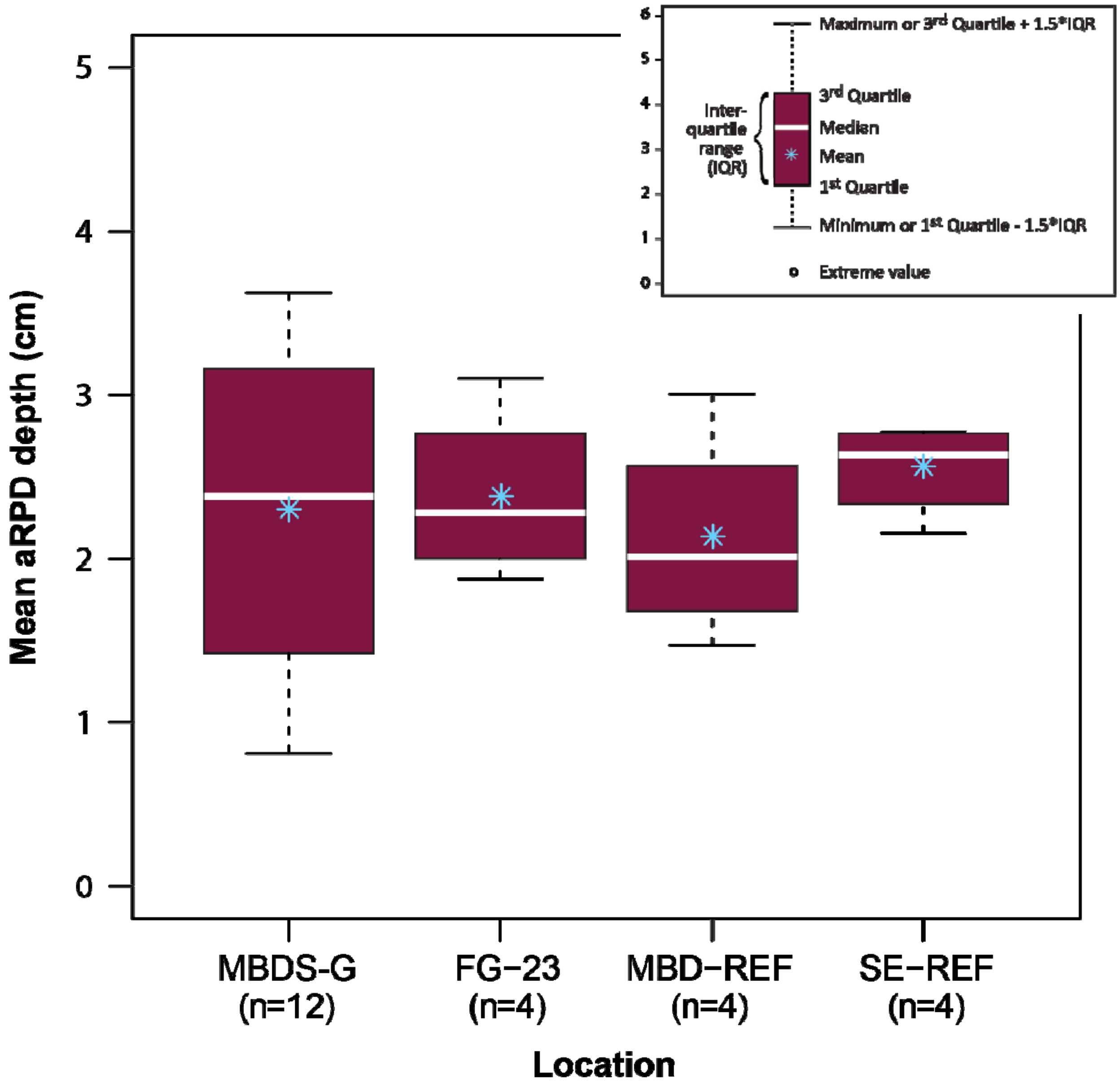

Figure 3-31. Boxplot of distribution of aRPD depth values at MBDS reference areas and disposal site. Boxplots use ranges and quartiles to display relative differences in medians, dispersion and skewness among areas. These are graphical aids for visualizing the results of statistical tests on normality (contraindicated by lack of symmetry in the box and "whiskers"), and equality of variances (contraindicated by widely disparate ranges between boxplots for different areas).

4.0 DISCUSSION

The objectives of the August 2012 survey efforts at MBDS were to first characterize the seafloor topography and surficial features of a portion of MBDS, including active and recently active target disposal locations, by completing a high-resolution acoustic survey. Using the results of the acoustic survey as a guide, SPI/PV imaging was performed to further define the physical characteristics of surficial sediment and to assess the benthic recolonization status (recovery of bottom-dwelling animals) of disposal mounds at MBDS with recent placement activity.

4.1 Seafloor Topography

The high resolution acoustic survey revealed a group of mounds rising from 1 to 8 m above the surrounding seafloor (Figure 4-1). This observation is consistent with expectations resulting from placement of a large amount of dredged material (over 1.5 million m^3) since the previous survey targeting a variety of release locations (Figure 1-4). The topographic changes included increased height of the MBDS-G mound (from 3 m in 2007 to over 8 m in 2012), less than 1 m of accumulation at MBDS-H and MBDS-I mounds, and about 1 m of consolidation at the MBDS-F mound which had not received any additional material (Figure 3-6).

The overall size of the MBDS-G mound was proportional to the volume of material disposed at this location (nearly 1.5 million m^3). The consolidation at the MBDS-F mound was well within the ranges associated with self-weight consolidation of dredged material after placement; MBDS-F mound received over 1.5 million m^3 of dredged material between 2004 and 2007, but no additional material had been placed since then. The lack of a significant measureable elevation change at MBDS-H and MBDS-I mounds was consistent with the low volume placed there as well as the likely high water content of maintenance material placed there (Table 1-2).

Because MBDS-H and MBDS-I mounds have very little relief, it is expected that they will receive more dredged material prior to the next monitoring survey in order to begin to complete the rings of mounds surrounding the depression at MBDS.

The small-scale topography of each of the mounds at MBDS (Figure 4-1) provided some indication of the nature of placement activities (volume, geotechnical properties of the dredged material). The MBDS-F mound was very smooth in profile with a distinct edge and had almost no texture on the surface. In contrast the MBDS-A, -B, -C, -D and -E mounds all had clear evidence of placement impact features characteristic of dredged material placement activities (Carey et al. 2012, Valente et al. 2012). The MBDS-G mound retained some placement impact features but resembled a more sharply defined version of the MBDS-F mound than it did the other mounds at the site (Figure 4-1). Both MBDS-F and MBDS-G mounds received large volumes of consolidated clay material dredged from the construction of Boston Harbor confined aquatic disposal cells as well as maintenance material at MBDS-G between 2007 and 2009 (Table 1-2 and AECOM 2010). Mound F received material between September 2004 and May 2006; Mound G after September 2006 (AECOM 2010). The presence of the consolidated clay observed on the surface in SPI and PV images and the small-scale topography of the mounds was consistent with construction of mounds that retained a smooth coherent form and absorbed placement activities with relatively little disturbance of the surface (Figure 4-1).

4.2 Distribution of Dredged Material

The history of placement of dredged material at MBDS is complex, but has been managed carefully since the site was designated an ocean dredged material disposal site by the U.S. Environmental Protection Agency (EPA) in 1992 (USEPA 1992; DeAngelo and Murray 1997). The distribution of dredged material in eight placement locations can be evaluated by examining backscatter results and side-sonar results in relation to the seafloor topography (Figure 4-2).

The mosaic of backscatter intensity provided clear evidence that the dredged material placement at the MBDS-G, MBDS-H and MBDS-I mounds resulted in very different patterns on the seafloor (Figure 3-3). There was an oval-shaped pattern of higher intensity backscatter over the MBDS-G mound and a very small circular pattern at the location of the MBDS-H mound (Figure 4-2). At the MBDS-I mound, the pattern of higher intensity backscatter was extensive, approximately 1000 m along a north-south axis and 750 m east-west. This distribution pattern appeared to be affected by the margins of the MBDS-F and MBDS-B mounds, such that the higher intensity backscatter was constrained by the slope of these mounds (Figure 4-2). The widespread distribution of higher backscatter was interpreted as placement of high water content dredged material that spread laterally over the seafloor. This pattern was defined more clearly in the filtered backscatter presented as a grid of values (Figure 4-3). The filtered and gridded backscatter removed some of the details but allowed a comparison of relative intensity distinct from the grayscale representation of seafloor topography. The area at the MBDS-I mound had the highest intensity of backscatter and overlapped the MBDS-A mound, but did not extend onto the MBDS-F or MBDS-B mounds (Figure 4-3).

Side-scan sonar results contrasted somewhat with the backscatter results at the MBDS-I mound (Figure 4-4). The side-scan sonar mosaic had only a small circular pattern of higher returns about 125 m in diameter at the MBDS-I placement location but did not have the larger area of intensity seen in the backscatter results (compare Figures 4-2, 4-3 and 4-4). The side-scan sonar results collected in 2007 (prior to the initiation of placement at MBDS-H and MBDS-I mounds) had many of the same tracks from dredged material placement, but did not have the pattern seen at MBDS-I in 2012 (Figure 4-5). Side-scan sonar is more responsive to surface texture and slope effects than backscatter collected from snippets. The interpretation of the difference in results was that the side-scan sonar detected a pattern of sand and fine scale clay clumps seen in the SPI and PV (Figures 3-18 and 3-21). The backscatter results detected the thin layer of high water content of dredged material that spread from the placement locations.

4.3 Benthic Recolonization

The results of the SPI/PV survey confirmed recolonization results similar to past surveys at MBDS (SAIC 1997a, 2002; ENSR 2005; AECOM 2010) when dredged material deposits are given sufficient time for recovery (Rhoads et al. 1978); mature successional assemblages were found throughout the disposal site as well as at the reference areas. Even though the physical evidence of dredged material disposal was still very apparent (Figures 3-25 and 3-29), Stage 3 taxa were present at all locations sampled; both the aRPD depth and infaunal successional status within the disposal site were equivalent to conditions found on the ambient seafloor. Given the lack of any additional observed anthropogenic disturbance factors, e.g., bottom trawling, it is not surprising that the soft-bottom infaunal community has had sufficient time for complete recovery.

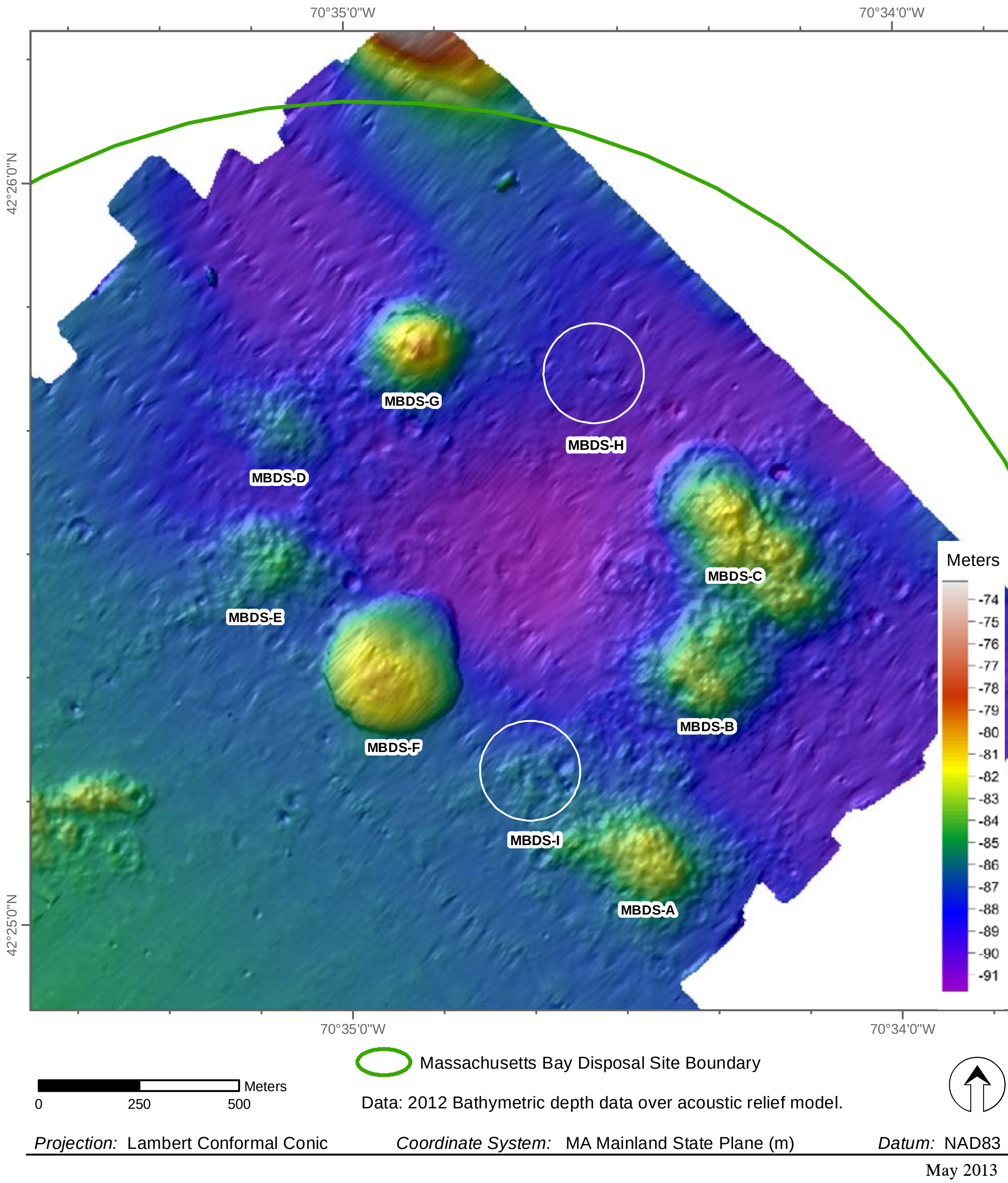

Figure 4-1. Acoustic relief model zoomed to extent of all mounds at MBDS

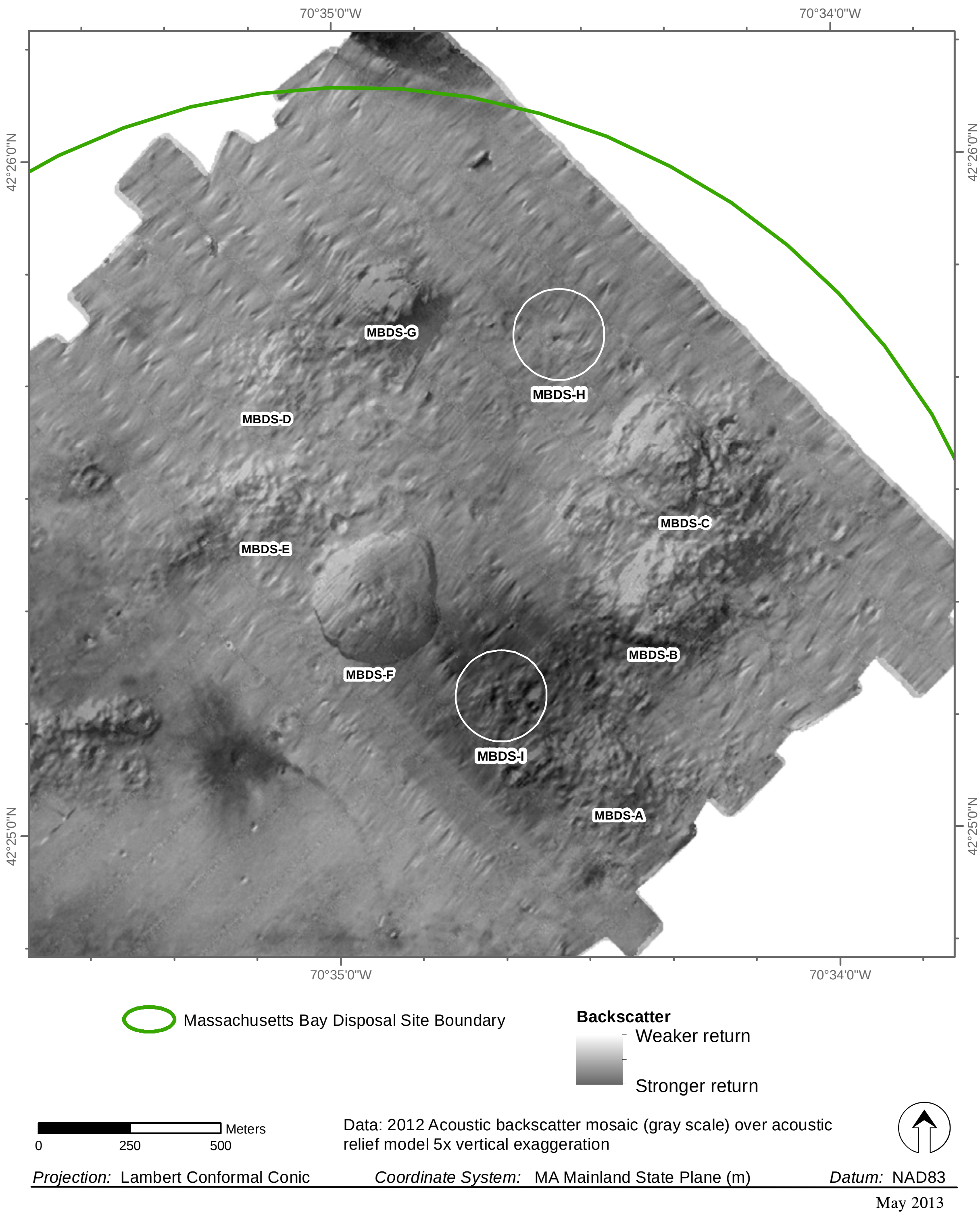

Figure 4-2. Backscatter mosaic over acoustic relief model zoomed to extent of all mounds at MBDS

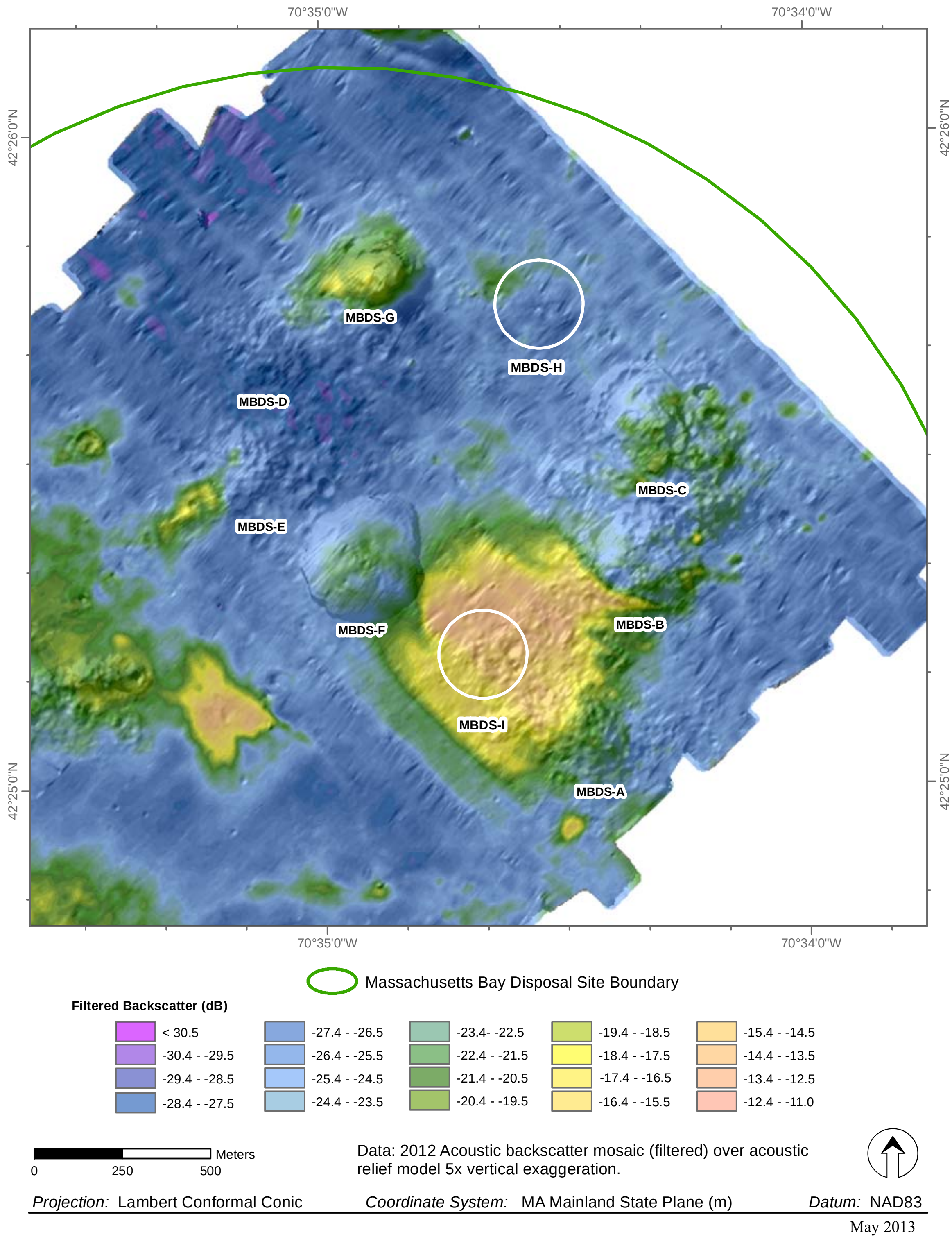

Figure 4-3. Filtered backscatter (quantitative) over acoustic relief model zoomed to extent of all mounds at MBDS

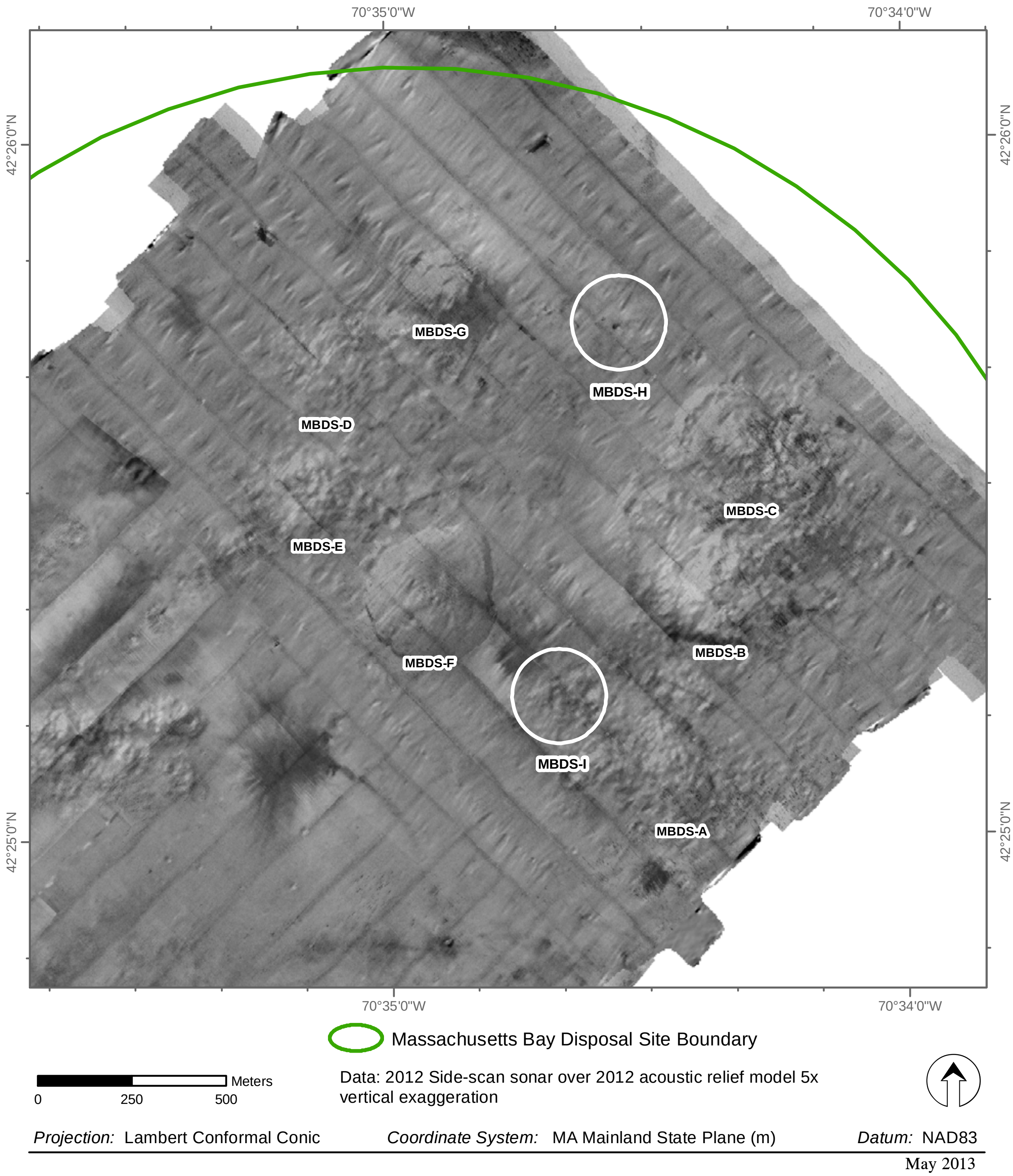

Figure 4-4. Side-scan sonar mosaic over acoustic relief model zoomed to extent of all mounds at MBDS - 2012

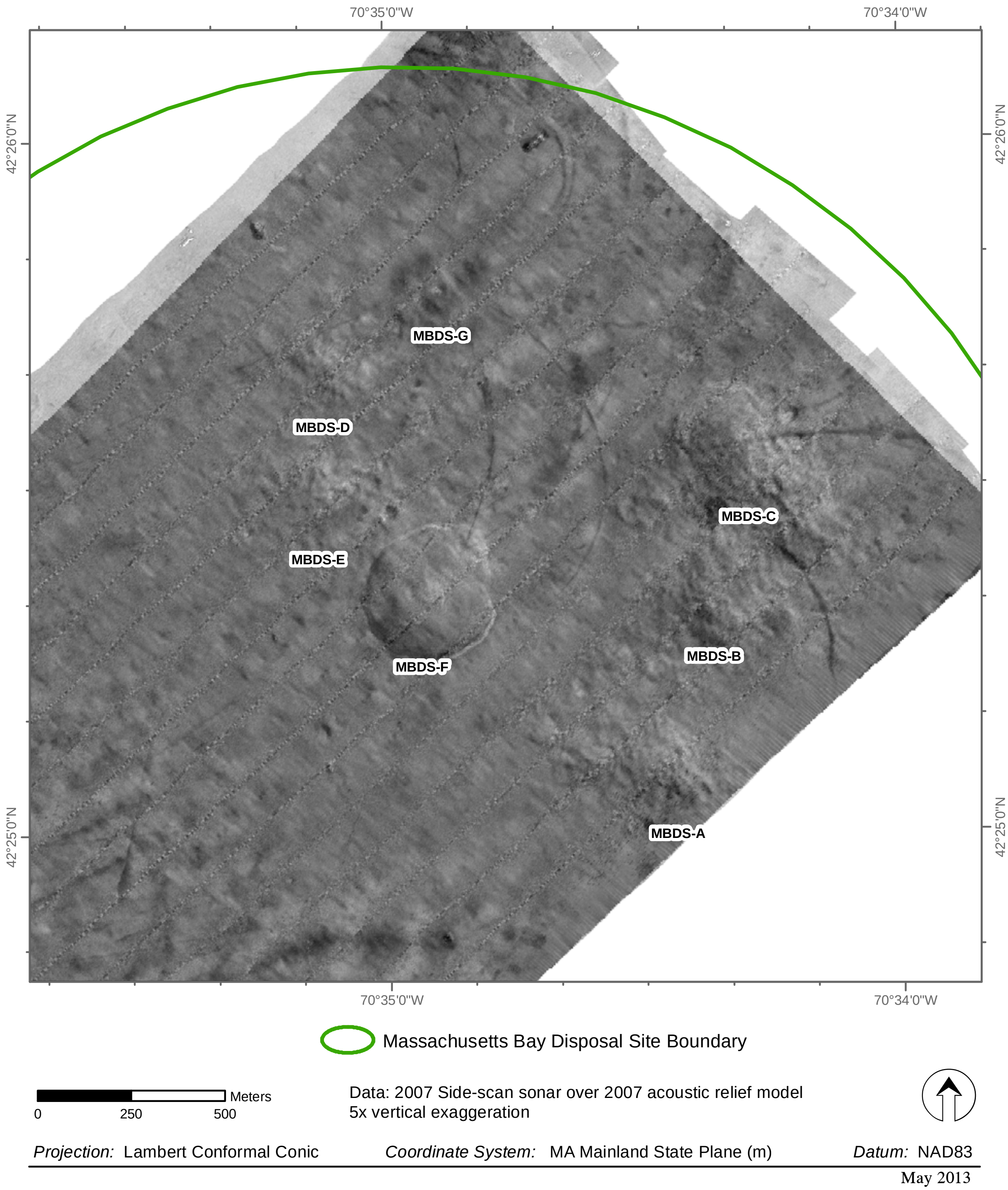

Figure 4-5. Side-scan sonar mosaic over acoustic relief model zoomed to extent of all mounds at MBDS - 2007

5.0 CONCLUSIONS AND RECOMMENDATIONS

The combined acoustic and SPI/PV surveys performed at MBDS in September and October 2012 provided the following findings:

- The dredged material placed at MBDS between 2007 and 2012 resulted in three features on the seafloor: the MBDS-G mound increased in height from 3 m to 8 m but retained a similar footprint to that seen in 2007; the MBDS-H mound accumulated less than 1 m in height and had a small footprint detectable in backscatter (ca. 125 m in diameter); the MBDS-I mound accumulated less than 1 m in height but had a large footprint detectable in backscatter (ca. 1000 × 750 m). The size and extent of the MBDS-G mound was similar to that expected from placement of nearly 1.5 million m^3 of dredged material in 90-m water depths. The limited height of the MBDS-H and MBDS-I mounds were attributed to placement of small volumes (ca. 100,000 m^3 and 50,000 m^3 respectively) of dredged material with high water content that formed thin layers surrounding the placement locations.

- The sediments on the surface of the MBDS-G dredged material mound showed evidence of complete recovery of the benthic community characteristics typical of the surrounding seafloor (Stage 3 successional community assemblage).

- The surface sediments on the MBDS-G mound had aRPD depths equivalent to reference area values. Given the presence of a healthy equilibrium deposit-feeding assemblage, it is expected that the aRPD depths on the mound will continue to be comparable to reference area values.

- The disposal site and reference areas displayed a robust benthic community assemblage with relatively uniform sediment characteristics that made mapping and characterizing dredged material distribution and seafloor condition straightforward.

- Given the complete recovery of the benthic infaunal community, it is predicted that the effects from any future disposal operations at MBDS would be transient, and the infaunal community would quickly re-establish itself in a time frame of 12-18 months following completion of disposal operations.

Based on the findings of the 2012 MBDS survey, the following recommendations are proposed:

R1) Future dredged material placement should be directed to the MBDS-H and MBDS-I mounds to increase their height and continue formation of the ring of mounds.

R2) High resolution acoustic surveys should be conducted if future dredged material placement activities are performed at the site to monitor the morphology and stability of the existing dredged material mounds as well as the formation of additional deposits. Surveys should be optimized to reduce internal wave effects in the water column during months with reduced stratification or well-mixed conditions (Spring or Fall).

R3) Benthic recolonization should be monitored with SPI/PV surveys at any future mounds formed as a result of placement activity.

6.0 REFERENCES

AECOM. 2010. Monitoring Survey at the Massachusetts Bay Disposal Site, August 2007. DAMOS Contribution No. 181. U.S. Army Corps of Engineers, New England District, Concord, MA, 88 pp.

Carey, D. A.; Hickey, K.; Myre, P. L.; Read, L. B.; Esten, M. E. 2012. Monitoring Surveys at the Historical Brenton Reef Disposal Site 2007 & 2009. DAMOS Contribution No. 187. U.S. Army Corps of Engineers, New England District, Concord, MA, 130 pp.

DeAngelo, E. C.; Murray, P. M. 1997. Baseline Survey of the Reconfigured Massachusetts Bay Disposal Site, 14 September 1993. DAMOS Contribution No. 115. U.S. Army Corps of Engineers, New England District, Concord, MA.

ENSR. 2005. Monitoring Survey at the Massachusetts Bay Disposal Site, September 2004. DAMOS Contribution No. 162. U.S. Army Corps of Engineers, New England District, Concord, MA, 64 pp.

Fredette, T. J.; French, G. T. 2004. Understanding the physical and environmental consequences of dredged material disposal: history in New England and current perspectives. Mar. Pollut. Bull. 49:93–102.

Germano, J. D.; Rhoads, D. C.; Lunz, J. D. 1994. An Integrated, Tiered Approach to Monitoring and Management of Dredged Material Disposal Sites in the New England Regions. DAMOS Contribution No. 87. U.S. Army Corps of Engineers, New England Division, Waltham, MA, 67 pp.

Germano, J. D.; Rhoads, D. C.; Valente, R. M.; Carey, D. A.; Solan, M. 2011. The use of sediment-profile imaging (SPI) for environmental impact assessments and monitoring studies: lessons learned from the past four decades. Oceanogr. Mar. Biol. Ann. Rev. 49:235–285.

McBride, G. B. 1999. Equivalence tests can enhance environmental science and management. Aust. New Zeal. J. Stat. 41(1):19–29.

Murray, P. M. 1994. Chemical analysis of sediment sampling at the Massachusetts Bay Disposal Site: 5–7 June 1989. SAIC Report No. C98. Submitted to the U.S. Army Corps of Engineers, New England Division, Concord, MA.

Rhoads, D. C.; Germano, J. D. 1982. Characterization of organism-sediment relations using sediment-profile imaging: an efficient method of remote ecological monitoring of the seafloor (REMOTS System). Mar. Ecol. Prog. Ser. 8:115–128.

Rhoads, D. C.; Germano, J. D. 1986. Interpreting long-term changes in benthic community structure: a new protocol. Hydrobiologia 142:291–308.

Rhoads, D. C.; McCall, P. L.; Yingst, J. Y. 1978. Disturbance and production on the estuarine seafloor. American Scientist 66: 577-586.

SAIC. 1997a. Monitoring Cruise at the Massachusetts Bay Disposal Site, August 1994. DAMOS Contribution No. 116 (SAIC Report No. 330). U.S. Army Corps of Engineers, New England Division, Concord, MA.

SAIC. 1997b. Baseline Survey of the Reconfigured Massachusetts Bay Disposal Site, 14 September 1993. DAMOS Contribution No. 115 (SAIC Report No. 317). U.S. Army Corps of Engineers, New England Division, Concord, MA.

SAIC. 2002. Monitoring Cruise at the Massachusetts Bay Disposal Site, Fall 2000. DAMOS Contribution No. 134 (SAIC Report No. 545). US Army Corps of Engineers, New England Division, Concord, MA.

SAIC. 2003. Massachusetts Bay Disposal Site Capping Demonstration Project, 1998-2000. DAMOS Contribution No. 147 (SAIC Report No. 551). US Army Corps of Engineers, New England Division, Concord, MA.

Schuirmann, D. J. 1987. A comparison of the two one-sided tests procedure and the power approach for assessing the equivalence of average bioavailability. J. Pharmacokinet. Biopharm. 15:657–680.

USACE. 2002. Engineering and Design Hydrographic Surveying. EM1110-2-1003.

USACE. 2013. "Mystic River Navigation Project." U.S. Army Corps of Engineers, New England District. http://www.nae.usace.army.mil/Missions/CivilWorks/Navigation/Massachusetts/Mystic.aspx (15 May 2013).

USACE and MassPort. 2008 Draft Feasibility Report and Supplemental Environmental Impact Statement/ (Massachusetts Environmental Impact Report) for Deep Draft Navigation Improvement (EOEEA #12958) Boston Harbor. Boston, Chelsea and Revere, Massachusetts.

USEPA. 1992. Designation of an ocean dredged material disposal site in Massachusetts Bay: Final Environmental Impact Statement, July 1992. U.S. Environmental Protection Agency, Region I, Boston, MA.

Valente, R. M.; Carey, D. A.; Read, L. B.; Esten, M. E. 2012. Monitoring Survey at the Central Long Island Sound Disposal Site October 2009. DAMOS Contribution No. 184. U.S. Army Corps of Engineers, New England District, Concord, MA, 90 pp.

Zar, J. H. 1996. Biostatistical analysis. Third edition. New Jersey: Prentice Hall.

INDEX

APPENDIX A

STANDARD OPERATING PROCEDURES

STANDARD OPERATING PROCEDURE

For Marine Operations Associated with the DAMOS Program

Prepared for US Army Corps of Engineers – NE District
Contract Number: W912WJ-12-D-0004

September 2012, Revision 1

Prepared by: DAMOSVision
Newport, RI
401-849-9236
September 2012

STANDARD OPERATING PROCEDURE

For Marine Operations Associated with the DAMOS Program

Prepared for US Army Corps of Engineers – NE District
Contract Number: W912WJ-12-D-0004

September 2012, Revision 1

Drew A. Carey **September 20, 2012**

Reviewed by Drew Carey, PhD, Managing Partner Date

Table of Contents

1.0 INTRODUCTION

DAMOSVision will lead the DAMOS Program field effort. Specifically, CR Environmental, Inc. will be responsible for acoustic surveys and navigation and Germano & Associates will be responsible for sediment-profile imaging (SPI) and plan-view underwater camera (PV) surveys. For each site surveyed, a pre-survey letter work plan will be submitted providing a schedule and summary of field activities. The pre-survey letter work plan will provide a map of the survey area, including the disposal site and reference area boundaries, and bathymetric sampling locations. An addendum to the letter work plan will be provided after the acoustic survey and prior to the SPI/PV survey and will provide SPI/PV sampling locations in map and tabular format.

This draft document describes the methods that will be used and standard operating procedures (SOPs) that will be followed when collecting and analyzing data as part of the 2012 DAMOS Program field effort. This document is submitted to Battelle Memorial Institute to support their management oversight, quality, and safety roles on this DAMOS Program task order. This document is organized to provide methods and SOPs as follows:

- Section 2 – Acoustic survey methods;
- Section 3 – SPI and PV survey methods;
- Section 4 – Acoustic survey specifications and SOPs
- Section 5 – SPI and PV survey specifications and SOPs

2.0 NAVIGATION AND ACOUSTIC SURVEY METHODS

Acoustic surveys include bathymetric, backscatter, and side-scan sonar data collection and processing. The bathymetric data provide measurements of water depth that, when processed, can be used to map the seafloor topography. The processed data can also be compared with previous surveys to track changes in the size and location of seafloor features. This technique is the primary tool in the DAMOS Program for mapping the distribution of dredged material at disposal sites. Backscatter and side-scan sonar data provided images that supported characterization of surficial topography, sediment texture, and roughness. Backscatter data can be processed into a seamless image with corrections for topography while side-scan sonar data retains a higher resolution image without correction for topography. The comparison of synoptic acoustic data types has the greatest utility for assessment of dredged material placement. Typical methods applied for navigation, on-board data acquisition, and acoustic data collection, processing and analysis are described below. Implementation of these methods may be modified based on site-specific conditions, such as sea-state, water depth, and proximity to GPS and tide gage stations.

2.1 Navigation and On-Board Data Acquisition

Navigation for the surveys will be accomplished using a Hemisphere 12-channel Differential Global Positioning System (DGPS) capable of receiving U.S. Coast Guard (USCG) Beacon corrections. Trimble DGPSs are available as backups. Both systems are capable of submeter horizontal position accuracy. The DGPS is interfaced to a laptop computer running HYPACK MAX® hydrographic survey software. HYPACK MAX® continually record vessel position and DGPS satellite quality and provide a steering display for the vessel captain to accurately maintain the position of the vessel along preestablished survey transects and targets.

Redundant vessel heading measurements are acquired using two compass systems, each capable of providing heading measurements accurate to within 0.05° up to 20 times per second. The primary heading device is an SG Brown Meridian Gyrocompass installed in the pilothouse to the port of the vessel’s centerline. A dual-antenna Hemisphere VS-100 Crescent Digital compass and DGPS are installed above the pilot house as a backup for the gyrocompass. Both systems are interfaced to HYPACK® acquisition software.

The pulse-per-second (PPS) signals from DGPSs are hardware-interfaced to HYPACK MAX® using a translation circuit and provided microsecond-level accuracy of data stream time-tagging from each sensor.

2.2 Acoustic Survey Methods

Acoustic surveys include bathymetric, backscatter, and side-scan sonar data collection and processing. The bathymetric data provide measurements of water depth that, when processed, are used to map the seafloor topography. The processed data is also compared with previous surveys to track changes in the size and location of seafloor features. This technique is the primary tool in the DAMOS Program for mapping the distribution of dredged material at disposal sites. Backscatter and side-scan sonar data provide images that supported characterization of surficial topography, sediment texture, and roughness. Backscatter data can be processed into a seamless image with corrections for topography while side-scan sonar data retains a higher resolution image without correction for topography. The comparison of synoptic acoustic data types has the greatest utility for assessment of dredged material placement.

2.2.1 Acoustic Data Collection

The pre-survey letter work plan will specify the acoustic survey grid, the planned lane orientation, the lane spacing, and other survey information. Data layers generated by the surveys typically include multibeam bathymetry, sediment acoustic backscatter (beam time-series data), and side-scan sonar data.

Bathymetric, acoustic backscatter and side-scan sonar data will be collected using a Reson 8101 Multibeam Echo Sounder (MBES) or comparable equipment. This 240-kHz system forms 101 1.5°-beams distributed equiangularly across a 150° swath. The MBES transducer is typically mounted amidships to the port rail of the survey vessel using a high strength adjustable boom, and the DGPS antenna will be attached to the top of the transducer boom. The transducer depth below the water surface (draft) will be checked and recorded at the beginning and end of data acquisition.

The MBES topside processor is equipped with components necessary to export depth solutions, backscatter, and side scan sonar signals to the HYPACK MAX® acquisition computer via Ethernet communications. HYPACK MAX® also receives and records navigation data from the DGPS, motion data from a serially interfaced TSS DMS 3-05 motion reference unit (MRU), and heading data from the Meridian and Hemisphere compass systems. Several patch tests will be conducted during the surveys to allow computation of angular offsets between the MBES system components. The system will be calibrated for local water mass speed of sound by performing conductivity-temperature-depth (CTD) casts at frequent intervals throughout each survey day with a Seabird SBE-19 Seacat CTD profiler. Additional confirmations of proper calibration, including static draft, will be obtained using the "bar check" method, in which a metal plate will be lowered beneath the MBES transducer to known depths (e.g., 2.0 and 5.0 m) below the water surface.

Water depths over the survey area will be recorded in meters and referenced to mean lower low water (MLLW) based on water levels recorded at the nearest NOAA station or comparable tide gage. Every reasonable effort will also be made to establish a backup tide gage to support the survey. HYPACK MAX® software will be used to manage data acquisition and storage of data from the echosounder and the navigation system. HYPACK MAX® also records depth, vessel heave, heading, position, and time along each survey transect line.

2.2.2 Bathymetric Data Processing

MBES bathymetric data will be processed using HYSWEEP® software. Data for outer beams greater than 60-degrees offset from nadir (vertical) will be excluded from processing to minimize the impact of refraction and vessel motion on data quality. Preliminary steps of data processing include: application of tide corrections; adjustment of beam orientation using the results of patch test calibrations; correction of soundings for minor variations in water column sound velocity; and removal of outlying sounding solutions associated with water column interference (e.g. marine mammals, fish, or suspended debris).

The cleaned and adjusted data will be further processed to calculate seafloor elevations based on evaluation of overlapping swath data and will be exported in delimited ASCII text format for mapping in ArcGIS®10.0 (GIS). The vertical uncertainty of soundings within each of these cells will also be calculated and exported in ASCII format to aid statistical assessment of data quality.

Processed bathymetric data will be converted to a regularly spaced binary grid representing the seafloor elevation using Golden Software's Surfer V11.0. This grid will be used to create bathymetric contours at statistically defensible intervals. The grid will also be used to create an interactive three-dimensional model of the survey area using IVS3D Fledermaus software.

2.2.3 Backscatter Data Processing

MBES backscatter data will be processed using HYPACK®'s implementation of GeoCoder software developed by NOAA's Center for Coastal and Ocean Mapping Joint Hydrographic Center (CCOM/JHC). GeoCoder will be used to create a mosaic best suited for substratum characterization through the use of innovative beam-angle correction algorithms.

Snippets backscatter data (beam-specific ping time-series records) will be extracted from cleaned files and will be converted to Generic Sensor Format (GSF) files. Mosaics of beam time-series (BTS) backscatter data will be created from GSF data using GeoCoder, and will be exported in grayscale TIF raster format. BTS data will also be exported in ASCII format with fields for Easting, Northing, and backscatter (dB). These data will be gridded using kriging algorithms and filtered with a mild low-pass Gaussian filter to minimize nadir artifacts. The filtered grids will used to develop maps of backscatter values using 2.0 m (6.6 ft) (horizontal resolution) node intervals.

2.2.4 Side-Scan Sonar Data Processing

The side-scan sonar data will be processed using both Chesapeake Technology, Inc. SonarWiz software and HYPACK®'s implementation of GeoCoder software. Individual georeferenced TIF images of each sonar file and georeferenced mosaics with acoustically relevant resolutions will be generated. The mosaic of side-scan sonar data will be merged with bathymetric data and formatted for 3D display using Fledermaus® software.

2.2.5 Acoustic Data Analysis

The processed bathymetric grids will be converted to rasters and bathymetric contour lines will be generated and displayed using GIS. GIS or Fledermaus will also be used to calculate depth difference grids between previous surveys and the current bathymetric dataset. The most recent bathymetric surveys at each site will be reviewed and the most recent high-quality bathymetric survey data will be utilized to support depth differencing. The resulting depth differences will be contoured and displayed using GIS.

2.3 Sediment-Profile and Plan-view Imaging Methods

Sediment-profile imaging (SPI) and plan-view underwater camera (PV) imaging are monitoring techniques used to provide data on the physical characteristics of the seafloor as well as the status of the benthic biological community. The pre-survey letter work plan will specify the SPI and PV survey design and sampling locations. In some cases, sampling locations may be modified during the survey due to site-specific conditions.

2.3.1 Sediment-Profile Imaging Data Collection

The sediment-profile imaging technique involves deploying an underwater camera system to photograph a cross section of the sediment-water interface. Acquisition of high-resolution sediment-profile images is accomplished using a Nikon D7000 digital single-lens reflex camera with a 16.2 megapixel image sensor mounted inside an Ocean Imaging Model 3731 pressure housing system. The pressure housing sits atop a wedge-shaped prism with a front faceplate and back mirror. The mirror is mounted at a 45º angle to reflect the profile of the sediment-water interface. As the prism penetrated the seafloor, a trigger activates a time-delay circuit that fires an internal strobe to obtain a cross-sectional image of the upper 15–20 cm of the sediment column (Figure 1). The camera remains on the seafloor for approximately 20 seconds to ensure that a successful image has been obtained. Details of the camera settings for each digital image are available in the associated parameters file embedded in each electronic image file. For the 2012 surveys, the ISO-equivalent will likely be set at 640, shutter speed was 1/250, f8, and storage in compressed raw Nikon Electronic Format (NEF) files (approximately 18 MB each). Electronic files will be converted to high-resolution jpeg (8-bit) format files (3264 × 4928 pixels) using Nikon Capture® NX2 software (Version 2.3.1).

Test exposures of the Kodak® Color Separation Guide (Publication No. Q-13) will be made on deck at the beginning of each survey to verify that all internal electronic systems are working to design specifications, the camera is in proper focus, and to provide color and measurement scales for subsequent image analysis. After deployment of the camera at each station, the frame counter is checked to ensure that the requisite number of replicate images has been obtained. In addition, a prism-penetration depth indicator on the camera frame is checked to verify that the optical prism has actually penetrated the bottom to a sufficient depth. If images are missed or the penetration depth is insufficient, the camera frame stop collars are adjusted and/or weights are added or removed, and additional replicate images are taken. Changes in prism weight amounts, the presence or absence of mud doors (to limit over-penetration in soft sediments), and frame stop collar positions are recorded for each replicate image.

Each image is assigned a unique time stamp in the digital file attributes by the camera's data logger and cross-checked with the time stamp in the navigational system's computer data file. In addition, the field crews keep redundant written sample logs. Images are downloaded periodically to verify successful sample acquisition and/or to assess what type of sediment/depositional layer are present at a particular station. Digital image files are re-named with the appropriate station name immediately after downloading as a further quality assurance step.

2.3.2 Plan-view Underwater Camera (PV) Imaging Data Collection

An Ocean Imaging Model DSC16000 plan-view underwater camera (PV) system with two Ocean Imaging Model 400-37 Deep Sea Scaling lasers mounted to the DSC16000 are attached to the sediment profile camera frame and used to collect plan-view photographs of the seafloor surface; both SPI and PV images are collected during each "drop" of the system. The PV system consisted of Nikon D-7000 encased in an underwater housing, a 24 VDC autonomous power pack, a 500 W strobe, and a bounce trigger. A weight will be attached to the bounce trigger with a stainless steel cable so that the weight hung below the camera frame; the scaling lasers project 2 red dots that are separated by a constant distance (26 cm) regardless of the field-of-view of the PV, which can be varied by increasing or decreasing the length of the trigger wire. As the camera apparatus is lowered to the seafloor, the weight attached to the bounce trigger contacts the seafloor prior to the camera frame hitting the bottom and triggers the PV (Figure 1). Details of the camera settings for each digital image are available in the associated parameters file embedded in each electronic image file; for the 2012 survey, the ISO-equivalent will likely be set at 400. Electronic files will be converted to high-resolution jpeg (8-bit) format files (3264 × 4928 pixels) using Nikon Capture NX2 software.

Prior to field operations, the internal clock in the digital PV camera is synchronized with the GPS navigation system and the SPI camera. Each PV image acquired is assigned a time stamp in the digital file and redundant notations in the field and navigation logs. Throughout the survey, PV images are downloaded at the same time as the sediment profile images after collection and evaluated for successful image acquisition and image clarity.

The ability of the PV camera to collect usable images is dependent on the clarity of the water column. To minimize the effects of turbid bottom waters, the bounce trigger cable may be shortened in order to decrease the distance between the camera focal plane and the seafloor. By limiting the distance between the camera lens port and the intended subject, picture clarity may be improved. One major drawback to the short trigger cable length and close distance between the PV camera and the seafloor is that the field-of-view of the PV system is decreased so that a smaller area of the seafloor is photographed. Even with the short trigger cable, many PV images were not usable due to the highly turbid bottom waters. The length of the trigger cable and associated distance above the seafloor of the PV image will be adjusted for each survey depending on site specific conditions.

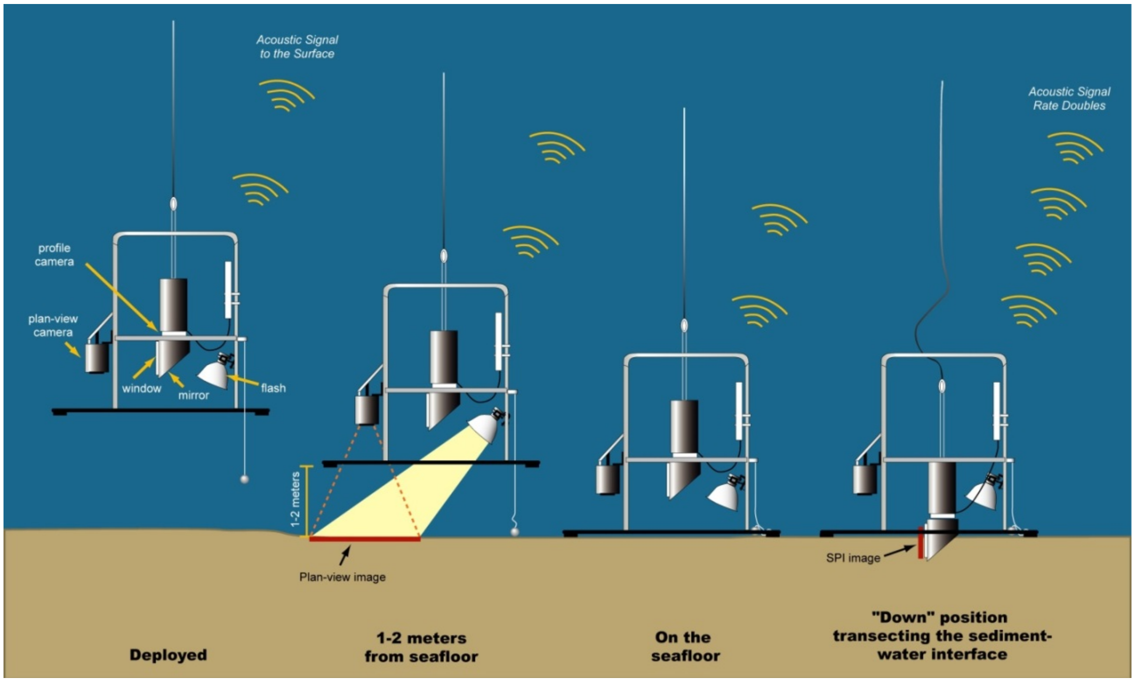

Figure 1. Schematic diagram of SPI/PV deployment

2.3.3 SPI and PV Data Analysis

Computer-aided analysis of the resulting images provides a set of standard measurements that enables comparison between different locations and different surveys. The DAMOS Program has successfully used this technique for over 30 years to map the distribution of disposed dredged material and to monitor benthic recolonization at disposal sites. Following completion of data collection, the digital images will be analyzed using Adobe Photoshop CS 5 Version 12.1 or comparable analysis software. Images are first be adjusted to expand the available pixels to their maximum light and dark threshold range. Linear and areal measurements are recorded as number of pixels and converted to scientific units using the Kodak® Color Separation Guide for measurement calibration.

Analysis of each SPI image is performed to provide measurement of the following standard set of parameters:

Sediment Type–The sediment grain size major mode and range are estimated visually from the images using a grain-size comparator at a similar scale. Results are reported using the phi scale and are converted to other grain-size scales. The presence and thickness of disposed dredged material is also assessed by inspection of the images.

Penetration Depth–The depth to which the camera penetrated into the seafloor is measured to provide an indication of the sediment density or bearing capacity. The penetration depth can range from a minimum of 0 cm (i.e., no penetration on hard substrates) to a maximum of 20 cm (full penetration on very soft substrates).

Surface Boundary Roughness–Surface boundary roughness is a measure of the vertical relief of features at the sediment-water interface in the sediment-profile image. Surface boundary roughness is determined by measuring the vertical distance between the highest and lowest points of the sediment-water interface. The surface boundary roughness (sediment surface relief) measured over the width of sediment-profile images typically ranges from 0 to 4 cm, and may be related to physical structures (e.g., ripples, rip-up structures, mud clasts) or biogenic features (e.g., burrow openings, fecal mounds, foraging depressions). Biogenic roughness typically changes seasonally and is related to the interaction of bottom turbulence and bioturbational activities.

Apparent Redox Potential Discontinuity (aRPD) Depth–aRPD depth provides a measure of the integrated time history of the balance between near-surface oxygen conditions and biological reworking of sediments. Sediment particles exposed to oxygenated waters oxidize and lighten in color to brown or light gray. As the particles are buried or moved down by biological activity, they are exposed to reduced oxygen concentrations in subsurface pore waters and their oxic coating slowly reduces, changing color to dark gray or black. When biological activity is high, the aRPD depth increases; when it is low or absent, the aRPD depth decreases. The aRPD depth is measured by assessing color and reflectance boundaries within the images.

Infaunal Successional Stage–Infaunal successional stage is a measure of the biological community inhabiting the seafloor. Current theory holds that organism-sediment interactions in fine-grained sediments follow a predictable sequence of development after a major disturbance (such as dredged material disposal), and this sequence has been divided subjectively into three stages (Rhoads and Germano 1982, 1986). Successional stage is assigned by assessing which types of species or organism-related activities are apparent in the images.

Additional components of the SPI analysis include calculation of means and ranges for the parameters listed above and mapping of means of replicate values from each station.

3.0 MULTIBEAM SONAR SURVEY SPECIFICATIONS AND STANDARD OPERATING PROCEDURES

The specifications and standard operating procedures (SOPs) described below were adapted from National Ocean Service (NOS) 2011 Hydrographic Survey Specifications, US Army Corps of Engineers (USACE) 2004 Hydrographic Surveying guidance, and CR Environmental's DAMOS and offshore project experience.

3.1 Training

The users of this SOP should have the minimum training as specified by USACE, 2004 Section 11-4(h), as follows:

"h. Training requirements. Multibeam system operators require considerable expertise in both surveying and on CADD workstations. Prior to using multibeam systems on USACE surveys, system operators should have completed specialized training. Presently, the Corps PROSPECT course on Hydrographic Surveying Techniques is not considered sufficient for multibeam training. Comprehensive training courses are available from: (1) the University of New Brunswick, (2) Coastal Oceanographics, Inc., (3) Triton Elics International, (4) Odom Hydrographic Systems, Inc., (5) University of New Hampshire-NOAA Joint Hydrographic Center, or (6) The Hydrographic Society of America seminars. Multibeam manufacturers may also offer specialized training sessions. In addition, the operator should have completed a manufacturer or Corps PROSPECT course associated with the differential GPS system, inertial compensating system, and CADD processing/editing system employed. For contracted multibeam survey services, the Architect-Engineer (A-E) contract solicitations should require that proposals identify the experience and training of system operators in Block 7 of the SF 255."

3.2 Equipment and Survey Vessel Specifications

1. The Multibeam Echo Sounder (MBES) system frequency should be approximately 200 kHz if backscatter data will be acquired. Frequencies >300-kHz are not currently supported and are severely constrained by wavelength.

2. The MBES System should be capable of recording both backscatter ("Snippets") and side scan, unless otherwise directed.

3. The motion sensor should provide a 20-Hz stream of dynamic roll and pitch measurements with an accuracy of 0.05 degrees or better.

4. The heading sensor should be accurate to at least 0.1-degrees RMS (root mean square).

5. Heave corrections should be accurate to 0.2 feet or 5% of heave amplitude, whichever is greater.

6. The navigation system should be capable of real-time sub-meter horizontal accuracy. As many DAMOS sites are distant from shore, real-time kinematic (RTK) DGPS is often impossible or unnecessary due to acoustic limitations.

7. The vessel should be surveyed by a Registered Land Surveyor. Reference points should be documented and archived.

8. A squat/settlement calibration of the survey vessel should be performed annually using either NOS or USACE methods.

9. PPS (pulse per second) timing or equivalent must be integrated.

3.3 Survey Planning and Design

1. The maximum acceptable beam angle is 120 degrees. 90-degree limits (or less) may be required for some sites during stratified conditions. Suitably trained and experienced MBES hydrographers should be present at all times to assess data quality. Survey designs and cost estimates should initially be based on 90-degree "worst-case" conditions.

2. The survey should be designed to provide at least 120% bottom coverage (i.e., full coverage with some overlap between transects). 200% coverage may be desired for some investigations *but is only required for Hard Bottom Navigation and Dredging Surveys (USACE, 2004. Ch. 11).* Note that actual angular limits (swath widths) are constrained by field conditions.

3. Crosslines should be acquired and processed to the same accuracy and data quality standards as required for main scheme lines, and must be included in the grids that are submitted as the final bathymetric product of the survey. Ideally, crosslines should be acquired prior to main scheme data, in areas of gently sloping bottom, and when water levels are as close to survey datum (MLLW) as practicable (see NOS, 2011). Occupation of crosslines first increases the ability of the hydrographer to identify system errors on main scheme lines. Lineal mileage of crosslines must be at least 8% of main scheme mileage.

3.4 Equipment Calibration and Data Acquisition SOP

1. Synchronize a tide gage to the survey acquisition computer. Install the tide gage at a temporary or permanent benchmark near the site. Measurement interval should be 60.0 seconds. Document and photograph gage offsets and benchmark characteristics.

2. Measure offsets between the transducer, GPS antenna, motion sensor, and heading sensor to the nearest 1 cm on installation or change of equipment.

3. Install a sound velocity sensor near the transducer and interface to sonar processor.

4. Program DGPS to beacon update maximum delay = 20 seconds, baud = 19.5 K or greater, minimum satellite elevation = 15°. Refer to product manual for ideal settings regarding signal to noise ratio (SNR).

5. Check DGPS system accuracy at a known point if available. If two or more beacons are available, record and compare static positions using each beacon and compare positions.

6. Program acquisition software to record all DGPS QC data. Alarms should be sent to the hydrographer when horizontal dilution of precision (HDOP) >2.5 or if beacon corrections are lost. Maximum correction age should not exceed 20 seconds without documentation of necessity.

7. Program acquisition software to display a matrix of swath soundings in real-time. Adjust display to facilitate instantaneous identification of compromised data.

8. Check and record transducer static draft using a bar-check of nadir beams at the start and end of each survey day.

9. Perform a daily blunder check of outer beams using a bar or plate suspended athwart ship of the transducer. This may not be possible on some larger vessels.

10. Conduct and process at least two patch tests prior to data acquisition (for a new installation). The average results of the tests should be used as preliminary sensor offsets and entered to acquisition software. Bias resolution of these tests should not exceed 0.1° (roll) or 1° for pitch or yaw. Latency bias resolution should not exceed 0.1 second. Final angular sensor offsets should be calculated using the results of at least four patch tests for each equipment installation. Confidence increases with calibration redundancy.

11. Performance tests (comparison of MBES data to a reference surface surveyed using VBES or nadir beam) may not be possible for most DAMOS cruises. When possible, a small reference surface should be established in shallow depths (<100 feet) over smooth bottom by surveying a closely spaced set of transects. Only the nadir soundings from these lines will be retained. The width of the surface should be at least 3.4 × water depth. A pair of opposing full-swath width (120°) passes should be made perpendicular to the nadir tracklines.

12. Collect and evaluate sound velocity profiles as frequently as practical with intervals not to exceed 2 hours. Sound velocity corrections should not be applied during acquisition unless refraction artifacts are observed and interfere with real-time data QC.

13. Maximum survey speed shall not exceed 10 knots to ensure full bottom coverage. USACE default is 5–10 kt.

14. Pause survey after completing the first survey transect. Apply sound velocity profile and review digital data to ensure adequate data quality across planned angle limits. If data in outer beams appear compromised, redesign survey to match field conditions. This exercise should be performed at all opportunities (scheduled breaks, etc.).

3.5 Data Processing and Delivery SOP

1. Generate tide correction and sound velocity adjustment files. Compare in-situ tides to nearest NOAA Station to check NOAA Station applicability. If necessary, calculate site-specific range and time correctors. Coordinate with NOAA CO-OPS.

2. Apply tide, sound velocity and final angular corrections. Remove outlying soundings associated with water column or system interferences. Minimize the use of automatic filters for investigations for which the mission objectives include object detection.

3. Assess nadir cross-tie data to identify tide or draft biases. Report uncertainty at 95^{th} percentile confidence interval per USACE method.

4. Assess performance test data (if available). Identify and screen beams (angles) which should be eliminated from further processing.

5. If possible, filter data based on performance test results.

6. Set output grid resolution to 0.5 m (or less) in depths less than 20 m, and to not greater than 5% of the water depth in waters 20 m and deeper.

7. Apply the average sounding solution within grid cells as the final node elevation.

8. Export the standard deviation calculated for tide corrected soundings within each cell as a separate ASCII file and use to calculate and plot 95% C.I. data uncertainty relative to USACE (<80 feet) and/or NOS/IHO Performance Standards.

9. Generate grids of elevation and uncertainty surfaces in ASCII and Floating Point Raster formats.

10. Generate elevation contours using an interval greater than the average uncertainty for the survey. Export in SHP and DXF formats.

11. Generate surface and relief maps using scales required for feature depiction. Document scale and light position angles (vertical and horizontal). For relief models/maps, document reflection algorithm.

3.6 References for Additional Guidance

U.S. Army Corps of Engineers. April 1, 2004. Engineering and Design - Hydrographic Surveying. Manual No. 1110-2-1003.

NOAA/NOS. April 2011. Hydrographic Surveys Specifications and Deliverables. U.S. Department of Commerce. National Oceanic and Atmospheric Administration.

NOAA/NOS Office of Coast Survey. May 2011. Field Procedures Manual National Oceanic and Atmospheric Administration.

4.0 SEDIMENT-PROFILE AND PLAN-VIEW SPECIFICATIONS AND STANDARD OPERATING PROCEDURES

The specifications and standard operating procedures (SOPs) described below were adapted from Germano et al., (2011) and Germano & Associates' DAMOS and offshore project experience.

4.1 Training

The users of this SOP should have the training provided by experienced SPI operators at Germano & Associates, Inc. or by the equipment manufacturer (Ocean Imaging Systems, North Falmouth, MA).

4.2 Equipment and Survey Vessel Specifications

1. The Nikon DSLR inside each camera housing should be set to record raw (NEF) files.
2. The navigation system should be capable of real-time sub-meter horizontal accuracy. As many DAMOS sites are distant from shore, RTK DGPS is often impossible or unnecessary due to acoustic limitations.
3. The vessel should be surveyed by a Registered Land Surveyor. Reference points should be documented and archived.

4.3 Survey Planning and Design

1. A minimum of three replicate camera drops should be made at each target station location; vessel should obtain replicate images within a 7.5 m radius of the target location.
2. The camera wire angle should not exceed 20° off the vertical during deployment.
3. Assuming reasonable weather, surveys should be planned for a station acquisition rate of 30–35 stations daily.

4.4 Equipment Calibration and Data Acquisition SOP

1. Fill prism with distilled water (assuming air temperatures are above freezing); insure that no bubbles are adhering to lens port or faceplate prior to survey operations.

2. Measure offsets between the A-frame sheave and GPS antenna on installation or change of equipment if GPS antennae cannot be mounted on top of A-frame at deployment point.

3. Format SD card(s) in both DSLRs prior to sealing the housing.

4. Check voltage output of both SPI and PV batteries to make sure they are at manufacturer's standard (12 V for SPI, 25 V for PV).

5. Check DGPS system accuracy at a known point if available. If two or more beacons are available, record and compare static positions using each beacon and compare positions.

6. Insure lenses on each camera are taped to proper focal distance so that lens cannot rotate accidently during installation or due to camera vibration.

7. Photograph Kodak Q-13 standard through SPI camera before survey starts.

8. Check and calibrate position of lasers on PV camera to insure separation of 26 cm.

9. Perform a daily frame count check of SPI camera at start and end of each survey day.

10. Conduct and process at least one SPI and PV image for proper ISO and f-stop setting; these will vary from location to location depending on sediment albedo (SPI) and water clarity (PV).

11. Check frame count on SPI internal LED display whenever camera is back on board (typically after every station) to insure strobe has fired the requisite number of times.

12. Visual and hand tighten check of all nuts/bolts on SPI/PV camera frame to make sure nothing has vibrated loose during survey.

4.5 Data Processing and Delivery SOP

1. Adjust brightness levels of all raw (NEF) digital image files to maximize histogram in either Adobe Photoshop or Nikon Capture NX2 and re-save in high-resolution jpg format.
2. Convert all RAW digital image files to Adobe DNG format and save on external server for archive.
3. Calibrate image analysis software measurements to color card shot on SPI images or laser scaling dots on PV images.

4.6 Reference for Additional Guidance

Germano, J. D., D. C. Rhoads, R. M. Valente, D. A. Carey, and M. Solan. 2011. The use of Sediment Profile Imaging (SPI) for environmental impact assessments and monitoring studies: Lessons learned from the past four decades. Oceanography and Marine Biology: An Annual Review 49: 247-310.

Appendix SOP A: Certifications

American Congress on Surveying and Mapping

This attests that

Christopher Wright

has met the requirements established by
the American Congress on Surveying and Mapping
Hydrographer Certification Board
for certification as

Hydrographer

by Authority of the Board of Directors

Chairman, Certification Board	Executive Director
Certificate Number 266	Date April 25, 2011

HYSWEEP® CERTIFIED HYDROGRAPHER

Christopher Wright
CR Environmental, Inc.

For successfully completing the
2010 HYSWEEP Certification Test
on 10/13/2010.

Patrick Sanders, President, HYPACK

HYPACK® CERTIFIED HYDROGRAPHER

Christopher Wright
CR Environmental, Inc.

For successfully completing the
2010 HYPACK Certification Test
on 10/13/2010.

Patrick Sanders, President, HYPACK

Appendix SOP B: Forms

SPI and PV Imaging Specifications and SOP Check List

This document summarizes Standard Operating Procedures followed during a SPI and PV Imaging Surveys that must be followed prior to, during and after a field survey is completed, to conform with the DAMOSVision SOP.

Equipment and Survey Vessel Specifications	☐ The Nikon DSLR inside each camera housing set to record raw (NEF) files. ☐ The navigation system capable of real-time sub-meter horizontal accuracy.
Equipment and Survey Vessel Specifications	Signature ____________ Date Completed ____________
Equipment Calibration and Data Acquisition SOP	☐ Fill prism with distilled water (assuming air temperatures are above freezing); insure that no bubbles are adhering to lens port or faceplate prior to survey operations. ☐ Measure offsets between the A-frame sheave and GPS antenna on installation or change of equipment if GPS antennae cannot be mounted on top of A-frame at deployment point. ☐ Format SD card(s) in both DSLRs prior to sealing the housing. ☐ Check voltage output of both SPI and PV batteries to make sure they are at manufacturer's standard (12 V for SPI, 25 V for PV). ☐ Check DGPS system accuracy at a known point if available. If two or more beacons are available, record and compare static positions using each beacon and compare positions. ☐ Insure lenses on each camera are taped to proper focal distance so that lens cannot rotate accidently during installation or due to camera vibration. ☐ Photograph Kodak Q-13 standard through SPI camera before survey starts.

SPI and PV Imaging Specifications and SOP Check List

	☐ Check and calibrate position of lasers on PV camera to insure separation of 26 cm. ☐ Perform a daily frame count check of SPI camera at start and end of each survey day. ☐ Conduct and process at least one SPI and PV image for proper ISO and f-stop setting; these will vary from location to location depending on sediment albedo (SPI) and water clarity (PV). ☐ Check frame count on SPI internal LED display whenever camera is back on board (typically after every station) to insure strobe has fired the requisite number of times. ☐ Visual and hand tighten check of all nuts/bolts on SPI/PV camera frame to make sure nothing has vibrated loose during survey.
Equipment Calibration and Data Acquisition SOP	______________ Signature ______________ Date Completed
Survey Planning and Design	☐ A minimum of three replicate camera drops made at each target station location; replicate images obtained within a 7.5 m radius of the target location. ☐ The camera wire angle did not exceed 20° off the vertical during deployment.
Survey Planning and Design	______________ Signature ______________ Date Completed

SPI and PV Imaging Specifications and SOP Check List	
Data Processing and Delivery SOP	☐ Adjust brightness levels of all raw (NEF) digital image files to maximize histogram in either Adobe Photoshop or Nikon Capture NX2 and re-save in high-resolution jpg format. ☐ Convert all RAW digital image files to Adobe DNG format and save on external server for archive. ☐ Calibrate image analysis software measurements to color card shot on SPI images or laser scaling dots on PV images.
Data Processing and Delivery SOP	________________ Signature ________________ Date Completed

DAMOS
DISPOSAL AREA MONITORING SYSTEM

Multibeam Sonar Survey SOP Check List

This document summarizes Standard Operating Procedures followed during a Multibeam Sonar Survey that must be followed prior to, during and after a field survey is completed, to conform to the DAMOSVision SOP.

Equipment and Survey Vessel Specifications	☐ The Multibeam Echo Sounder (MBES) system frequency approximately 200 kHz if backscatter data will be acquired. Frequencies >300 kHz are not currently supported and are severely constrained by wavelength. ☐ The MBES System capable of recording both backscatter ("Snippets") and side scan, unless otherwise directed. ☐ The motion sensor provides a 20-Hz stream of dynamic roll and pitch measurements with an accuracy of 0.05° or better. ☐ The heading sensor accurate to at least 0.1° RMS (root mean square). ☐ Heave corrections accurate to 0.2 feet or 5% of heave amplitude, whichever is greater. ☐ The navigation system capable of real-time sub-meter horizontal accuracy. ☐ The vessel surveyed by a Registered Land Surveyor. Reference points should be documented and archived. ☐ A squat/settlement calibration of the survey vessel performed annually using either NOS or USACE methods. ☐ PPS (pulse per second) timing or equivalent integrated.
Equipment and Survey Vessel Specifications	__________________ Signature __________________ Date Completed

Multibeam Sonar Survey SOP Check List

Survey Planning and Design	☐ The maximum acceptable beam angle is 120°s. 90-degree limits (or less) may be required for some sites during stratified conditions. Suitably trained and experienced MBES hydrographer present at all times to assess data quality. Survey designs and cost estimates initially be based on 90-degree "worst-case" conditions. ☐ The survey designed to provide at least 120% bottom coverage (i.e., full coverage with some overlap between transects). Note that actual angular limits (swath widths) are constrained by field conditions. ☐ Crosslines acquired and processed to the same accuracy and data quality standards as required for main scheme lines, and included in the grids that are submitted as the final bathymetric product of the survey. Lineal mileage of crosslines at least 8% of main scheme mileage.
Survey Planning and Design	____________________ Signature ____________________ Date Completed
Equipment Calibration and Data Acquisition SOP	☐ Synchronize a tide gage to the survey acquisition computer. Install the tide gage at a temporary or permanent benchmark near the site. Measurement interval should be 60.0 seconds. Document and photograph gage offsets and benchmark characteristics. ☐ Measure offsets between the transducer, GPS antenna, motion sensor, and heading sensor to the nearest 1 cm on installation or change of equipment. ☐ Install a sound velocity sensor near the transducer and interface to sonar processor. ☐ Program DGPS to beacon update maximum delay = 20 seconds, baud = 19.5 K or greater, minimum satellite elevation = 15°. Refer to product manual for ideal settings regarding signal to noise ratio (SNR).

Multibeam Sonar Survey SOP Check List

- ☐ Check DGPS system accuracy at a known point if available. If two or more beacons are available, record and compare static positions using each beacon and compare positions.

- ☐ Program acquisition software to record all DGPS QC data. Alarms should be sent to the hydrographer when horizontal dilution of precision (HDOP) >2.5 or if beacon corrections are lost. Maximum correction age should not exceed 20 seconds without documentation of necessity.

- ☐ Program acquisition software to display a matrix of swath soundings in real-time. Adjust display to facilitate instantaneous identification of compromised data.

- ☐ Check and record transducer static draft using a bar-check of nadir beams at the start and end of each survey day.

- ☐ Perform a daily blunder check of outer beams using a bar or plate suspended athwart ship of the transducer. This may not be possible on some larger vessels.

- ☐ Conduct and process at least two patch tests prior to data acquisition (for a new installation). The average results of the tests should be used as preliminary sensor offsets and entered to acquisition software. Bias resolution of these tests should not exceed 0.1° (roll) or 1° for pitch or yaw. Latency bias resolution should not exceed 0.1 second. Final angular sensor offsets should be calculated using the results of at least four patch tests for each equipment installation. Confidence increases with calibration redundancy.

- ☐ Performance tests (comparison of MBES data to a reference surface surveyed using VBES or nadir beam) may not be possible for most DAMOS cruises. When possible, a small reference surface should be established in shallow depths (<100 feet) over smooth bottom by surveying a closely spaced set of transects. Only the nadir soundings from these lines will be retained. The width of the surface should be at least 3.4 × water depth. A pair of opposing full-swath width (120°) passes should be made perpendicular to the nadir tracklines.

Multibeam Sonar Survey SOP Check List

	☐ Collect and evaluate sound velocity profiles as frequently as practical with intervals not to exceed 2 hours. Sound velocity corrections should not be applied during acquisition unless refraction artifacts interfere with real-time QC. ☐ Maximum survey speed should not exceed 10 knots to ensure full bottom coverage. ☐ Pause survey after completing the first survey transect. Apply sound velocity profile and review digital data to ensure adequate data quality across planned angle limits. If data in outer beams appear compromised, redesign survey to match field conditions. This exercise should be performed at all opportunities (scheduled breaks, etc.).
Equipment Calibration and Data Acquisition SOP	____________________ Signature ____________________ Date Completed
Data Processing and Delivery SOP	☐ Generate tide correction and sound velocity adjustment files. Compare in-situ tides to nearest NOAA Station to check NOAA Station applicability. If necessary, calculate site-specific range and time correctors. Coordinate with NOAA CO-OPS as necessary. ☐ Apply tide, sound velocity and final angular corrections. Remove outlying soundings associated with water column or system interferences. Minimize the use of automatic filters for investigations for which the mission objectives include object detection. ☐ Assess nadir cross-tie data to identify tide or draft biases. Report uncertainty at 95^{th} percentile confidence interval per USACE method. ☐ Assess performance test data (if available). Identify and screen beams (angles) which should be eliminated from further processing. ☐ If possible, filter data based on performance test results.

Multibeam Sonar Survey SOP Check List

	☐ Set output grid resolution to 0.5 m (or less) in depths less than 20 m, and to not greater than 5% of the water depth in waters 20 m and deeper. ☐ Apply the average sounding solution within grid cells as the final node elevation. ☐ Export the standard deviation calculated for tide corrected soundings within each cell as a separate ASCII file and use to calculate and plot 95% C.I. data uncertainty relative to USACE (<80 feet) and/or NOS/IHO Performance Standards. ☐ Generate grids of elevation and uncertainty surfaces in ASCII and Floating Point Raster formats. ☐ Generate elevation contours using an interval greater than the average uncertainty for the survey. Export in SHP and DXF formats. ☐ Generate surface and relief maps using scales required for feature depiction. Document scale and light position angles (vertical and horizontal). For relief models/maps, document reflection algorithm.
Data Processing and Delivery SOP	____________________ Signature ____________________ Date Completed

APPENDIX B

SEDIMENT-PROFILE IMAGE ANALYSIS RESULTS FOR MBDS SURVEY, SEPTEMBER/OCTOBER 2012

Sediment-Profile Image Analysis Results for MBDS Survey, September/October 2012

Location	Station	Replicate	Date	Time	Stop Collar Setting (in)	# of Weights (per side)	Water Depth (ft)	Calibration Constant	Grain Size Major Mode (phi)	Grain Size Maximum (phi)	Grain Size Minimum (phi)	Penetration Area (sq. cm)	Penetration Mean (cm)	Penetration Minimum (cm)	Penetration Maximum (cm)	Boundary Roughness (cm)	Boundary Roughness Type	aRpd Area (sq. cm)	Mean aRpd (cm)
MBDS-G	01	E	10/18/2012	9:22:55	15.5	3	265	14.541135	>4	>4	2	116.2	8.0	6.1	8.7	2.6	physical	ind	ind
MBDS-G	01	G	10/18/2012	9:25:32	15.5	3	265	14.541135	>4	>4	2	153.2	10.5	9.4	11.7	2.3	biogenic	23.7	1.6
MBDS-G	01	H	10/18/2012	9:26:59	15.5	3	265	14.541135	>4	>4	2	166.3	11.4	8.9	14.0	5.1	biogenic	13.2	0.9
MBDS-G	02	B	10/18/2012	9:49:32	16.5	3	271	14.541135	>4	>4	2	138.5	9.5	8.2	12.3	4.2	physical	15.8	1.1
MBDS-G	02	C	10/18/2012	9:50:42	16.5	3	271	14.541135	>4	>4	0	189.6	13.0	12.8	13.3	0.5	biogenic	31.1	2.1
MBDS-G	02	D	10/18/2012	9:51:52	16.5	3	271	14.541135	>4	>4	2	198.3	13.6	13.3	13.8	0.6	biogenic	21.3	1.5
MBDS-G	03	A	10/18/2012	11:21:54	14	2	280	14.541135	>4	>4	1	174.4	12.0	11.6	12.5	0.8	biogenic	29.4	2.0
MBDS-G	03	C	10/18/2012	11:23:52	14	2	280	14.541135	>4	>4	1	206.1	14.2	13.6	14.7	1.1	biogenic	23.2	1.6
MBDS-G	03	D	10/18/2012	11:24:50	14	2	280	14.541135	>4	>4	1	207.9	14.3	13.1	15.4	2.4	biogenic	42.9	2.9
MBDS-G	04	B	10/18/2012	11:00:45	14	2	295	14.541135	>4	>4	2	28.0	1.9	19.3	20.5	1.2	biogenic	39.4	2.7
MBDS-G	04	C	10/18/2012	11:01:58	14	2	295	14.541135	>4	>4	2	300.9	20.7	20.6	20.9	0.3	biogenic	49.0	3.4
MBDS-G	04	D	10/18/2012	11:03:14	14	2	295	14.541135	>4	>4	2	263.4	18.1	17.6	18.7	1.1	biogenic	64.8	4.5
MBDS-G	05	A	10/18/2012	10:08:28	16.5	3	280	14.541135	>4	>4	1	196.2	13.5	13.1	14.2	1.1	biogenic	42.2	2.9
MBDS-G	05	B	10/18/2012	10:09:45	16.5	3	280	14.541135	>4	>4	1	225.2	15.5	15.0	15.8	0.8	biogenic	28.9	2.0
MBDS-G	05	D	10/18/2012	10:11:57	16.5	3	280	14.541135	>4	>4	2	279.8	19.2	19.0	19.7	0.7	biogenic	40.7	2.8
MBDS-G	06	J	10/18/2012	11:59:33	12	0	288	14.541135	>4	>4	2	248.3	17.1	16.3	18.1	1.8	biogenic	32.8	2.3
MBDS-G	06	K	10/18/2012	12:00:44	12	0	288	14.541135	>4	>4	0	224.5	15.4	15.0	16.0	1.0	biogenic	50.2	3.5
MBDS-G	06	L	10/18/2012	12:02:09	12	0	288	14.541135	>4	>4	1	200.2	13.8	13.3	14.4	1.0	biogenic	44.1	3.0
MBDS-G	07	A	10/18/2012	9:54:55	16.5	3	270	14.541135	>4	>4	1	180.6	12.4	8.7	12.8	4.2	biogenic	16.1	1.1
MBDS-G	07	C	10/18/2012	9:57:20	16.5	3	270	14.541135	>4	>4	1	170.5	11.7	10.2	13.4	3.3	physical	15.2	1.0

Sediment-Profile Image Analysis Results for MBDS Survey, September/October 2012

Location	Station	Replicate	Date	Time	Stop Collar Setting (in)	# of Weights (per side)	Water Depth (ft)	Calibration Constant	Grain Size Major Mode (phi)	Grain Size Maximum (phi)	Grain Size Minimum (phi)	Penetration Area (sq. cm)	Penetration Mean (cm)	Penetration Minimum (cm)	Penetration Maximum (cm)	Boundary Roughness (cm)	Boundary Roughness Type	aRpd Area (sq. cm)	Mean aRpd (cm)
MBDS-G	07	D	10/18/2012	9:58:22	16.5	3	270	14.541135	>4	>4	0	131.1	9.0	8.6	9.6	0.9	biogenic	16.4	1.1
MBDS-G	08	A	10/18/2012	11:14:40	14	2	295	14.541135	>4	>4	2	246.8	17.0	16.5	17.5	1.0	biogenic	41.1	2.8
MBDS-G	08	C	10/18/2012	11:16:57	14	2	295	14.541135	>4	>4	2	254.4	17.5	17.2	17.8	0.6	biogenic	67.3	4.6
MBDS-G	08	D	10/18/2012	11:18:03	14	2	295	14.541135	>4	>4	1	267.7	18.4	18.1	18.6	0.5	biogenic	49.6	3.4
MBDS-G	09	A	10/18/2012	10:52:44	14	2	294	14.541135	>4	>4	2	280.7	19.3	18.1	20.4	2.3	biogenic	65.6	4.5
MBDS-G	09	B	10/18/2012	10:53:34	14	2	294	14.541135	>4	>4	0	255.8	17.6	16.4	18.8	2.4	biogenic	37.1	2.6
MBDS-G	09	C	10/18/2012	10:54:37	14	2	294	14.541135	>4	>4	1	277.4	19.1	17.9	19.6	1.7	biogenic	41.8	2.9
MBDS-G	10	A	10/18/2012	11:06:06	14	2	287	14.541135	>4	>4	2	269.3	18.5	17.9	19.1	1.2	biogenic	52.0	3.6
MBDS-G	10	B	10/18/2012	11:07:05	14	2	287	14.541135	>4	>4	2	286.2	19.7	17.4	21.0	3.7	biogenic	35.1	2.4
MBDS-G	10	D	10/18/2012	11:09:37	14	2	287	14.541135	>4	>4	1	309.9	21.3	21.3	21.3	ind	ind	ind	ind
MBDS-G	11	A	10/18/2012	10:02:10	16.5	3	286	14.541135	>4	>4	2	109.5	7.5	5.5	8.9	3.4	physical	10.7	0.7
MBDS-G	11	B	10/18/2012	10:03:10	16.5	3	286	14.541135	>4	>4	2	115.1	7.9	6.5	9.1	2.6	physical	17.4	1.2
MBDS-G	11	D	10/18/2012	10:05:17	16.5	3	286	14.541135	>4	>4	2	120.5	8.3	6.6	10.1	3.4	physical	7.2	0.5
MBDS-G	12	A	10/18/2012	11:27:50	14	2	292	14.541135	>4	>4	1	137.7	9.5	9.1	9.8	0.7	biogenic	24.4	1.7
MBDS-G	12	B	10/18/2012	11:29:49	14	2	292	14.541135	>4	>4	2	160.4	11.0	9.9	11.9	2.0	biogenic	18.8	1.3
MBDS-G	12	D	10/18/2012	11:31:09	14	2	292	14.541135	>4	>4	0	200.5	13.8	13.1	14.2	1.1	biogenic	32.8	2.3
MBDS-H	14	B	10/18/2012	17:08:02	13.5	1	297	14.541135	>4	>4	2	250.2	17.2	16.3	18.5	2.2	biogenic	72.3	5.0
MBDS-H	14	C	10/18/2012	17:08:56	13.5	1	297	14.541135	>4	>4	1	285.7	19.7	19.0	20.1	1.1	biogenic	63.0	4.3
MBDS-H	14	D	10/18/2012	17:09:45	13.5	1	297	14.541135	>4	>4	2	307.4	21.1	20.4	21.4	ind	biogenic	ind	ind
MBDS-H	17	A	10/18/2012	16:58:07	13.5	1	297	14.541135	>4	>4	2	258.1	17.8	17.5	17.9	0.4	biogenic	54.2	3.7
MBDS-H	17	B	10/18/2012	16:59:03	13.5	1	297	14.541135	>4	>4	1	222.2	15.3	14.1	16.6	2.5	biogenic	29.3	2.0

Sediment-Profile Image Analysis Results for MBDS Survey, September/October 2012

Location	Station	Replicate	Date	Time	Stop Collar Setting (in)	# of Weights (per side)	Water Depth (ft)	Calibration Constant	Grain Size Major Mode (phi)	Grain Size Maximum (phi)	Grain Size Minimum (phi)	Penetration Area (sq. cm)	Penetration Mean (cm)	Penetration Minimum (cm)	Penetration Maximum (cm)	Boundary Roughness (cm)	Boundary Roughness Type	aRpd Area (sq. cm)	Mean aRpd (cm)
MBDS-H	17	C	10/18/2012	16:59:58	13.5	1	297	14.541135	>4	>4	1	245.1	16.9	15.9	18.5	2.6	physical	31.2	2.1
MBDS-H	20	B	10/18/2012	16:48:05	13.5	1	298	14.541135	>4	>4	1	237.0	16.3	15.4	16.9	1.6	biogenic	58.3	4.0
MBDS-H	20	C	10/18/2012	16:48:58	13.5	1	298	14.541135	>4	>4	1	298.1	20.5	19.1	20.7	ind	ind	ind	ind
MBDS-H	20	D	10/18/2012	16:50:01	13.5	1	298	14.541135	>4	>4	1	280.9	19.3	18.7	19.9	1.2	biogenic	42.6	2.9
MBDS-H	22	A	10/18/2012	17:13:24	13.5	1	296	14.541135	>4	>4	1	280.0	19.3	18.6	20.3	1.7	biogenic	45.2	3.1
MBDS-H	22	C	10/18/2012	17:15:26	13.5	1	296	14.541135	>4	>4	2	284.4	19.6	19.3	19.9	0.6	biogenic	57.1	3.9
MBDS-H	22	D	10/18/2012	17:16:38	13.5	1	296	14.541135	>4	>4	1	276.1	19.0	18.5	19.6	1.1	biogenic	31.6	2.2
MBDS-I	30	A	10/18/2012	16:15:41	13.5	1	292	14.541135	4-3/>4	>4	0	177.6	12.2	8.6	17.3	8.7	physical	57.0	3.9
MBDS-I	30	B	10/18/2012	16:16:41	13.5	1	292	14.541135	>4	>4	1	209.3	14.4	11.2	16.0	4.8	physical	26.3	1.8
MBDS-I	30	C	10/18/2012	16:17:36	13.5	1	292	14.541135	4-3/>4	>4	0	162.7	11.2	9.1	13.1	3.9	physical	ind	2.6
MBDS-I	31	A	10/18/2012	16:22:24	13.5	1	292	14.541135	4-3	>4	-2	65.2	4.5	3.5	5.5	2.0	physical	ind	1.4
MBDS-I	31	C	10/18/2012	16:23:26	13.5	1	292	14.541135	>4	>4	-1	119.3	8.2	7.6	9.2	1.6	biogenic	19.2	1.3
MBDS-I	31	D	10/18/2012	15:24:39	13.5	1	292	14.541135	4-3	>4	0	40.6	2.8	2.0	3.4	1.5	physical	ind	ind
MBDS-I	34	A	10/18/2012	16:08:51	13.5	1	297	14.541135	4-3	>4	0	93.4	6.4	5.6	7.9	2.3	biogenic	14.2	1.0
MBDS-I	34	B	10/18/2012	16:09:41	13.5	1	297	14.541135	4-3	>4	0	69.5	4.8	3.4	5.2	1.9	biogenic	33.5	2.3
MBDS-I	34	D	10/18/2012	16:12:08	13.5	1	297	14.541135	4-3	>4	0	97.7	6.7	6.3	7.4	1.1	biogenic	32.0	2.2
MBDS-I	36	A	10/18/2012	16:27:24	13.5	1	296	14.541135	1-0/4-3	>4	0	86.7	6.0	4.8	6.7	2.0	biogenic	86.7	6.0
MBDS-I	36	B	10/18/2012	16:28:31	13.5	1	296	14.541135	4-3	>4	-2	76.1	5.2	4.6	5.5	1.0	biogenic	7.2	0.5
MBDS-I	-36	C	10/18/2012	16:29:49	13.5	1	296	14.541135	4-3	>4	0	112.1	7.7	7.1	8.5	1.4	biogenic	32.7	2.2
MBD-REF	37A	A	10/18/2012	14:49:11	13.5	1	299	14.541135	>4	>4	2	254.7	17.5	17.1	17.8	0.7	biogenic	60.2	4.1
MBD-REF	37A	C	10/18/2012	14:51:35	13.5	1	299	14.541135	>4	>4	2	247.0	17.0	16.4	17.4	0.9	biogenic	52.6	3.6

Sediment-Profile Image Analysis Results for MBDS Survey, September/October 2012

Location	Station	Replicate	Date	Time	Stop Collar Setting (in)	# of Weights (per side)	Water Depth (ft)	Calibration Constant	Grain Size Major Mode (phi)	Grain Size Maximum (phi)	Grain Size Minimum (phi)	Penetration Area (sq. cm)	Penetration Mean (cm)	Penetration Minimum (cm)	Penetration Maximum (cm)	Boundary Roughness (cm)	Boundary Roughness Type	aRpd Area (sq. cm)	Mean aRpd (cm)
MBD-REF	37A	D	10/18/2012	14:53:09	13.5	1	299	14.541135	>4	>4	2	233.7	16.1	14.4	17.2	2.8	biogenic	18.3	1.3
MBD-REF	38	B	10/18/2012	14:12:37	13.5	1	296	14.541135	>4	>4	0	139.1	9.6	8.7	10.0	1.3	biogenic	24.1	1.7
MBD-REF	38	C	10/18/2012	14:13:47	13.5	1	296	14.541135	>4	>4	1	189.1	13.0	11.6	13.8	2.2	biogenic	19.7	1.4
MBD-REF	38	D	10/18/2012	14:14:54	13.5	1	296	14.541135	>4	>4	2	112.6	7.7	6.1	9.0	2.9	biogenic	20.4	1.4
MBD-REF	39	A	10/18/2012	13:58:28	13.5	1	299	14.541135	>4	>4	2	241.9	16.6	16.2	17.5	1.2	biogenic	22.2	1.5
MBD-REF	39	B	10/18/2012	13:59:40	13.5	1	299	14.541135	>4	>4	1	278.4	19.1	18.5	20.1	1.6	biogenic	29.7	2.0
MBD-REF	39	C	10/18/2012	14:00:47	13.5	1	299	14.541135	>4	>4	2	254.9	17.5	16.8	18.4	1.6	biogenic	30.6	2.1
MBD-REF	40	A	10/18/2012	14:27:18	13.5	1	299	14.541135	>4	>4	2	255.1	17.5	17.0	18.4	1.4	biogenic	31.5	2.2
MBD-REF	40	B	10/18/2012	14:28:23	13.5	1	299	14.541135	>4	>4	1	226.5	15.6	15.1	16.4	1.3	biogenic	29.7	2.0
MBD-REF	40	D	10/18/2012	14:30:14	13.5	1	299	14.541135	>4	>4	0	276.8	19.0	18.6	19.4	0.8	biogenic	31.6	2.2
FG-23	41	B	10/18/2012	15:17:20	13.5	1	289	14.541135	>4	>4	2	243.3	16.7	15.8	17.4	1.6	biogenic	41.7	2.9
FG-23	41	C	10/18/2012	15:18:23	13.5	1	289	14.541135	>4	>4	2	235.4	16.2	15.4	16.7	1.3	biogenic	52.5	3.6
FG-23	41	D	10/18/2012	15:19:28	13.5	1	289	14.541135	>4	>4	1	243.1	16.7	16.3	17.2	0.8	biogenic	40.7	2.8
FG-23	42	A	10/18/2012	15:23:11	13.5	1	293	14.541135	>4	>4	2	253.7	17.5	16.9	18.0	1.1	physical	20.3	1.4
FG-23	42	C	10/18/2012	15:25:05	13.5	1	293	14.541135	>4	>4	2	273.4	18.8	16.9	19.3	2.4	biogenic	39.6	2.7
FG-23	42	D	10/18/2012	15:25:57	13.5	1	293	14.541135	>4	>4	3	253.3	17.4	16.7	18.2	1.4	biogenic	32.7	2.2
FG-23	43	A	10/18/2012	15:39:08	13.5	1	290	14.541135	>4	>4	2	253.2	17.4	17.1	17.8	0.7	biogenic	34.4	2.4
FG-23	43	B	10/18/2012	15:40:14	13.5	1	290	14.541135	>4	>4	3	242.3	16.7	15.9	17.1	1.2	biogenic	35.4	2.4
FG-23	43	C	10/18/2012	15:41:12	13.5	1	290	14.541135	>4	>4	2	222.9	15.3	15.0	15.6	0.7	biogenic	35.9	2.5
FG-23	44	A	10/18/2012	15:30:34	13.5	1	290	14.541135	>4	>4	2	235.4	16.2	15.5	16.8	1.3	biogenic	23.7	1.6
FG-23	44	B	10/18/2012	15:31:55	13.5	1	290	14.541135	>4	>4	2	241.0	16.6	16.3	17.1	0.8	biogenic	27.0	1.9

Sediment-Profile Image Analysis Results for MBDS Survey, September/October 2012

Location	Station	Replicate	Date	Time	Stop Collar Setting (in)	# of Weights (per side)	Water Depth (ft)	Calibration Constant	Grain Size Major Mode (phi)	Grain Size Maximum (phi)	Grain Size Minimum (phi)	Penetration Area (sq. cm)	Penetration Mean (cm)	Penetration Minimum (cm)	Penetration Maximum (cm)	Boundary Roughness (cm)	Boundary Roughness Type	aRpd Area (sq. cm)	Mean aRpd (cm)
FG-23	44	C	10/18/2012	15:32:55	13.5	1	290	14.541135	>4	>4	2	251.7	17.3	16.9	17.6	0.7	biogenic	31.0	2.1
SE-REF	45	A	10/18/2012	13:24:34	14	2	304	14.541135	>4	>4	2	255.7	17.6	17.3	18.3	1.0	biogenic	33.6	2.3
SE-REF	45	B	10/18/2012	13:25:33	14	2	304	14.541135	>4	>4	2	288.9	19.9	17.3	20.3	3.0	biogenic	36.6	2.5
SE-REF	45	D	10/18/2012	13:27:53	14	2	304	14.541135	>4	>4	1	241.9	16.6	15.9	18.2	2.3	biogenic	23.9	1.6
SE-REF	46	B	10/18/2012	12:55:50	14	2	303	14.541135	>4	>4	2	247.9	17.1	16.6	18.2	1.6	biogenic	40.2	2.8
SE-REF	46	C	10/18/2012	12:56:52	14	2	303	14.541135	>4	>4	2	267.4	18.4	17.7	18.8	1.1	biogenic	39.8	2.7
SE-REF	46	D	10/18/2012	12:57:56	14	2	303	14.541135	>4	>4	2	264.7	18.2	17.8	18.7	0.9	biogenic	40.1	2.8
SE-REF	47	A	10/18/2012	13:06:25	14	2	297	14.541135	>4	>4	1	307.6	21.2	20.8	21.3	ind	ind	ind	ind
SE-REF	47	B	10/18/2012	13:07:36	14	2	297	14.541135	>4	>4	2	307.9	21.2	20.6	21.4	ind	ind	ind	ind
SE-REF	47	D	10/18/2012	13:10:22	14	2	297	14.541135	>4	>4	1	245.0	16.9	16.4	17.5	1.1	biogenic	36.5	2.5
SE-REF	48	A	10/18/2012	13:16:38	14	2	303	14.541135	>4	>4	2	248.1	17.1	16.1	17.9	1.8	biogenic	39.3	2.7
SE-REF	48	C	10/18/2012	13:18:57	14	2	303	14.541135	>4	>4	2	278.7	19.2	18.8	19.6	0.8	biogenic	38.0	2.6
SE-REF	48	D	10/18/2012	13:20:25	14	2	303	14.541135	>4	>4	2	289.4	19.9	18.8	21.0	2.2	biogenic	43.8	3.0

Sediment-Profile Image Analysis Results for MBDS Survey, September/October 2012

Location	Station	Replicate	Mud Clast Number	Mud Clast State	Methane?	Low DO?	Comment	# of Feeding Voids	Void Minimum Depth (cm)	Void Maximum Depth (cm)	Void Average Depth (cm)	Successional Stage
MBDS-G	01	E	>20	both	n	n	DM > pen depth; gray silty DM in consolidated clasts; partial voids, some filled in; open burrow against faceplate, clam siphons & polychaete tubes at surface	3	2.8	7.9	5.4	2 on 3
MBDS-G	01	G	5	both	n	n	DM> pen depth; mud clasts @ SWI are wiper blade artifacts; transected vertical burrow, 0.5 - 1 cm thick layer of fecal pellets at surface	1	4.9	5.4	5.1	1 on 3
MBDS-G	01	H	0		n	n	DM > pen depth; silty sand; large depression in middle of SWI; long thick tubes on surface; bio reworked surface; possible burrowing anemone arms in background on right; DM> penetration, voids and transected burrows at depth, large tubes at SWI, pit appears to be part of large burrow opening (see PV image)	2	9.0	9.7	9.3	1 on 3
MBDS-G	02	B	6	both	n	n	DM > penetration, reduced ribbon clasts are wiper blade artifacts, multiple tubes @ SWI, consolidated clay inclusions at depth	2	1.8	7.6	4.7	1 on 3
MBDS-G	02	C	0		n	n	DM > pen depth; very fine sandy fraction in upper layer, evidence of burrowing through aRPD and at depth	0				1 on 3
MBDS-G	02	D	4	both	n	n	DM > penetration, large tubes at SWI, biogenic reworking extends beyond prism penetration depth	5	6.4	13.0	9.7	1 on 3
MBDS-G	03	A	0		n	n	DM > penetration; multiple polychaetes visible against faceplate, evidence of burrowing at depth, 0.5 -1 cm surface layer of fecal pellets	2	7.2	11.0	9.1	1 on 3
MBDS-G	03	C	0		n	n	DM > penetration; segments of polychaetes visible against faceplate, evidence of burrowing at depth, enhanced fraction of very fine sand along with fecal pellets in surface layer	2	5.1	5.9	5.5	1 on 3
MBDS-G	03	D	0		n	n	DM > pen depth, some clay inclusions in dragdown; silty sand at surface; one large void with transected burrows at depth	3	4.6	12.5	8.5	1 on 3
MBDS-G	04	B	0		n	n	DM > pen depth, ribbon of reduced sediment at SWI is artifact from wiper blade; few tubes at surface in background on left; burrowing through aRPD, relict aRPD a depth; few worms against faceplate near base on aRPD- one is capitellid	0				1 on 3
MBDS-G	04	C	0		n	n	DM > pen depth, gray at depth, few clay artifacts at surface; only bit of SWI visible; burrowing in aRPD; evidence of burrowing to depth	1	16.6	17.1	16.9	1 on 3
MBDS-G	04	D	0		n	n	DM > pen depth, patchy at depth, silty sand at surface; small tubes at surface; debris on surface at right; burrowing through aRPD; bits of worms against faceplate near base of aRPD; old voids at depth	0				1 on 3

Sediment-Profile Image Analysis Results for MBDS Survey, September/October 2012

Location	Station	Replicate	Mud Clast Number	Mud Clast State	Methane?	Low DO?	Comment	# of Feeding Voids	Void Minimum Depth (cm)	Void Maximum Depth (cm)	Void Average Depth (cm)	Successional Stage
MBDS-G	05	A	4	reduced	n	n	DM > pen depth, gray DM mixed with dark low DO sed at depth on right; silty very fine sand over silt; wiper blade clay clast artifacts on surface, tubes on surface and one incorporated in upper cm; burrowing in upper cms of aRPD; relict aRPD; thin worm on left; voids at depth .	2	8.7	13.9	11.3	1 on 3
MBDS-G	05	B	0		n	n	DM > pen depth, gray silt at depth and throughout; patchy dark sed below aRPD; relict aRPD; burrows in aRPD; one longer burrow extending below aRPD on left; few thin polychaetes, evidence of old voids at depth.	0				1 on 3
MBDS-G	05	D	0		n	n	DM > pen depth, gray slit at depth in chunks; patchy dark sed below aRPD; fecal pellet layer on surface; burrows in aRPD; one worm below aRPD; voids on right.	2	8.2	12.9	10.5	1 on 3
MBDS-G	06	J	1	oxidized	n	n	Silty very fine sand at surface with mall tubes at SWI; small worms visible burrowing in upper cms, evidence of burrowing at depth	0				1 on 3
MBDS-G	06	K	0		n	n	Silt to silty very fine sand in upper layer; evidence of burrowing through aRPD; evidence of old voids at depth	0				1 on 3
MBDS-G	06	L	6	oxidized	n	n	Silty very fine sand over silt/clay; tubes on surface; bits of clumped sediment incorporated in upper 0.5 cm; burrowing in aRPD; voids at base of aRPD	2	5.3	5.8	5.5	1 on 3
MBDS-G	07	A	0		n	n	DM > pen depth; mostly silt, topped with thin layer of silty sand; large gray clay DM chunk on left stuck to faceplate; shallow burrows in upper cm; large burrow connected to surface at left edge of frame; few worms below aRPD, possible capitellids.	2	6.1	12.5	9.3	1 on 3
MBDS-G	07	C	3	reduced	n	n	DM > pen depth; chunk of gray DM from replicate A still stuck to faceplate, thin clasts on surface are wiper blade artifacts; burrowing through aRPD; relict aRPD; part of worm visible at base of aRPD	1	8.9	9.4	9.2	1 on 3
MBDS-G	07	D	0		n	n	DM > pen depth; most of pen depth is gray DM , chunk from replicate A is still stuck to faceplate; silt topped with thin layer of silty sand; collapsed tubes in pit at right edge; ampeliscid tube on surface in background; evidence of burrowing at depth.	0				1 on 3
MBDS-G	08	A	0		n	n	DM at depth, > pen depth; algal debris on surface; portion of shrimp above SWI, tube on left; relict aRPD; burrowing through aRPD; larger long polychaete below relict aRPD at depth against faceplate; void at base of relict aRPD	1	4.5	4.9	4.7	1 on 3
MBDS-G	08	C	0		n	n	DM at depth, >pen depth; silty very fine sand over silt clay; burrowing through aRPD; worms visible against faceplate	0				1 on 3

Sediment-Profile Image Analysis Results for MBDS Survey, September/October 2012

Location	Station	Replicate	Mud Clast Number	Mud Clast State	Methane?	Low DO?	Comment	# of Feeding Voids	Void Minimum Depth (cm)	Void Maximum Depth (cm)	Void Average Depth (cm)	Successional Stage
MBDS-G	08	D	0		n	n	DM at depth, >pen depth; silty very fine sand over silt clay; burrowing through aRPD; worms visible against faceplate, evidence of burrowing at depth	1	12.8	13.0	12.9	1 on 3
MBDS-G	09	A	0		n	n	DM at depth, > pen depth; silty very fine sand over silt/clay; high density of small tubes at SWI; burrowing through aRPD; relict aRPD;	1	9.1	9.4	9.3	1 on 3
MBDS-G	09	B	0		n	n	DM > penetration, burrowing in aRPD; relict aRPD, 1-2 cm of fecal pellets at surface	0				1 on 3
MBDS-G	09	C	0		n	n	Silty DM > penetration with higher fraction of very fine sand at surface. pronounced fecal pellet layer at surface; burrowing in aRPD; relict aRPD; three polychaetes visible at depth- one fat, two thin, one may be capitellid; void is vertically-oriented and looks more like a burrow sliced in half by faceplate	1	14.4	15.3	14.8	1 on 3
MBDS-G	10	A	0		n	n	DM at depth, > pen depth; tubes at surface; bit of algal debris on surface; burrowing and thin worms in aRPD.	1	7.8	8.8	8.3	1 on 3
MBDS-G	10	B	0		n	n	Silty very fine sand over silt/clay with gray DM at depth near base of image, patchy; surface slopes to right; bits of DM on surface; burrowing in aRPD; relict aRPD; thin worm below aRPD; indication of old voids below aRPD	0				1 on 3
MBDS-G	10	D	ind		n	n	Over-penetration; DM at depth, > pen depth; burrowing in aRPD, void below aRPD	1	ind	ind	ind	3
MBDS-G	11	A	0		n	n	DM entire pen depth and > pen depth; tubes on surface; clumps of gray DM on surface in background; thin polychaetes in center below aRPD, evidence of burrowing at depth	0				1 on 3
MBDS-G	11	B	4	reduced	n	n	DM entire pen depth and > pen depth; clumps of gray DM on surface; discontinuous oxy sed; possible oil droplets in upper cms at center, transected burrows at depth	0				3
MBDS-G	11	D	0		n	n	DM entire pen depth and > pen depth; few thin polychaetes against faceplate, transected burrows at depth	3	5.1	7.7	6.4	1 on 3
MBDS-G	12	A	0		n	n	DM > pen depth, large clay inclusion on left below few cms; silt and silty sand; tubes on surface; burrowing in upper cms; relict aRPD	0				1 on 3
MBDS-G	12	B	0		n	n	DM > pen depth, some clay artifacts on surface; burrowing in aRPD; relict aRPD; void below aRPD; worm at depth	1	3.7	4.5	4.1	1 on 3
MBDS-G	12	D	2	reduced	n	n	DM > pen depth, burrowing in aRPD; relict aRPD, biogenic reworking beyond penetration depth	1	6.6	7.4	7.0	1 on 3

Sediment-Profile Image Analysis Results for MBDS Survey, September/October 2012

Location	Station	Replicate	Mud Clast Number	Mud Clast State	Methane?	Low DO?	Comment	# of Feeding Voids	Void Minimum Depth (cm)	Void Maximum Depth (cm)	Void Average Depth (cm)	Successional Stage
MBDS-H	14	B	0		n	n	DM > pen; Silt; fecal pellets; worm against faceplate at base of aRPD on right; burrowing through aRPD; multiple voids at depth	3	8.4	11.4	9.9	1 on 3
MBDS-H	14	C	0		n	n	DM > pen; Silt; fecal pellets; algal debris on left; small void at base of aRPD; vertical transected burrow	2	7.5	15.9	11.7	1 on 3
MBDS-H	14	D	0		n	n	DM > pen; Over-penetration, for all but right few cms; silt; DM clast sed at depth; relict aRPD; evidence of reworking throughout profile	0				3
MBDS-H	17	A	0		n	n	DM > pen; Silt; fecal pellets; evidence of burrowing through aRPD; large polychaete (nereid) against faceplate at depth	0				1 on 3
MBDS-H	17	B	4	both	n	n	DM > pen; Silt; uneven surface; small tubes & small mud clasts at SWI; clay inclusion at depth, with void and worm	1	7.8	8.1	8.0	1 on 3
MBDS-H	17	C	0		n	n	DM > pen; Silt; uneven surface; tubes on surface; shrimp at surface; small clay inclusions on right in aRPD and dragdown	0				1 on 3
MBDS-H	20	B	0		n	n	DM > pen; Silt, with small worms in aRPD; evidence of burrowing at depth	0				1 on 3
MBDS-H	20	C	0		n	n	DM > pen; Silt; over-penetration on right side; tube on surface; deep relict aRPD with patches of red sed; voids filled with sed	2	12.7	15.4	14.1	1 on 3
MBDS-H	20	D	0		n	n	DM > pen; Silt, clay inclusions at depth on left; burrowing through aRPD; voids at depth.	2	7.8	9.9	8.9	1 on 3
MBDS-H	22	A	1	oxidized	n	n	DM > pen; silt, some gray clay inclusions at depth; mud clasts and tubes on surface; burrowing through aRPD, polychaete against faceplate at ~3.5 cm	1	7.1	7.8	7.5	1 on 3
MBDS-H	22	C	0		n	n	Silty DM > pen; burrowing through aRPD; one tube visible at ~2 cm; voids below aRPD	2	8.8	12.9	10.9	1 on 3
MBDS-H	22	D	3	reduced	n	n	Silty DM > pen; wider burrow on right ~2-3 cm relict aRPD; voids at depth	2	11.1	16.0	13.5	1 on 3
MBDS-I	30	A	0		n	n	Silty very fine sand with gray clay DM (large clasts visible in PV); homogeneous sediment texture at depth, thoroughly re-worked, all DM	0				3
MBDS-I	30	B	0		n	n	Gray silt, some sand in upper cms; bits of clay at depth, DM > pen, shells and debris on surface; signs of void ~4 cm on right, small tubes @ SWI	1	3.6	5.2	4.4	1 on 3
MBDS-I	30	C	0		n	n	DM > pen, aRPD estimate from linear measurement to left of large gray clay inclusion which is smeared over profile in right half of image; large transected burrow at depth	1	8.2	13.0	10.6	1 on 3
MBDS-I	31	A	0		n	n	Poorly-sorted silty sand, coarser on surface; DM > penetration, transected burrows and evidence of deposit-feeders at depth	0				3

Sediment-Profile Image Analysis Results for MBDS Survey, September/October 2012

Location	Station	Replicate	Mud Clast Number	Mud Clast State	Methane?	Low DO?	Comment	# of Feeding Voids	Void Minimum Depth (cm)	Void Maximum Depth (cm)	Void Average Depth (cm)	Successional Stage
MBDS-I	31	C	0		n	n	Silty sand; as with previous rep, DM > pen and gray DM from surface smeared down faceplate; tubicolous fauna on surface; voids at depth	2	5.8	6.7	6.3	1 on 3
MBDS-I	31	D	0		n	n	Poorly-sorted silty sand with DM > pen, debris on surface; tube on surface, transected burrows at depth	0				1 on 3
MBDS-I	34	A	0		n	n	Poorly sorted silty fine to medium sand, DM > pen, tubicolous fauna at surface; relict aRPD; part of shrimp above sed on far right; burrowing at depth	1	5.6	6.0	5.8	1 on 3
MBDS-I	34	B	0		n	n	Poorly-sorted silty sand with DM > pen, transected burrows at depth	0				1 on 3
MBDS-I	34	D	0		n	n	Poorly-sorted silty sand with DM > pen, transected burrows at depth	1	3.3	5.2	4.2	1 on 3
MBDS-I	36	A	0		n	n	Poorly-sorted silty sand with aRPD and DM > pen, transected burrows at depth	1	2.9	4.6	3.7	1 on 3
MBDS-I	36	B	1	reduced	n	n	Poorly-sorted silty sand with DM > pen, transected burrows at depth	0				1 on 3
MBDS-I	36	C	0		n	n	Poorly-sorted silty sand with DM > pen, transected burrows at depth, dense small tubes @ SWI	2	2.1	5.3	3.7	1 on 3
MBD-REF	37A	A	0		n	n	Silt; tubes on surface; burrowing through aRPD; evidence of large burrows at depth	0				1 on 3
MBD-REF	37A	C	2	reduced	n	n	Silt, tubes on surface; burrowing in aRPD and throughout profile; polychaetes visible at depth	0				1 on 3
MBD-REF	37A	D	0		n	n	Silt; relict aRPD; void at depth	1	12.8	13.1	13.0	1 on 3
MBD-REF	38	B	0		n	n	Silt; lots of tubes on surface; algal debris; end of larger burrow at depth	0				1 on 3
MBD-REF	38	C	1	oxidized	n	n	Silt; tubes on surface, some laying on surface; shallow burrowing; void at depth	1	6.0	6.4	6.2	1 on 3
MBD-REF	38	D	0		n	n	Silt; tubes on surface; thin polychaetes (likely capitellids) connected to burrowing in aRPD	0				1 on 3
MBD-REF	39	A	0		n	n	Silt; tubes laying on surface; organic debris on surface; thin polychaete below aRPD;	0				1 on 3
MBD-REF	39	B	2	reduced	n	n	Silt; few tubes on surface; evidence of burrowing at depth	0				1 on 3
MBD-REF	39	C	4	reduced	n	n	Silt; clasts are from prism & wiper blade; small tubes on surface; burrowing in aRPD	0				1 on 3
MBD-REF	40	A	0		n	n	Silt with multiple small tubes at SWI; evidence of burrowing at depth	0				1 on 3
MBD-REF	40	B	8	reduced	n	n	Silt; clasts are from SPI frame and wiper blade; small tubes at SWI; burrowing through aRPD; worm at depth	0				1 on 3
MBD-REF	40	D	16	both	n	n	Silt; fecal pellets; clasts are from SPI frame; burrows through aRPD; evidence of burrowing at depth	0				1 on 3

Sediment-Profile Image Analysis Results for MBDS Survey, September/October 2012

Location	Station	Replicate	Mud Clast Number	Mud Clast State	Methane?	Low DO?	Comment	# of Feeding Voids	Void Minimum Depth (cm)	Void Maximum Depth (cm)	Void Average Depth (cm)	Successional Stage
FG-23	41	B	8	both	n	n	Silt/clay with mud clasts (artifacts) from SPI frame; worms visible against faceplate as well as transected burrows at depth.	0				1 on 3
FG-23	41	C	3	reduced	n	n	Silt/clay with mud clasts (artifacts) from SPI frame; evidence of burrowing at depth.	0				1 on 3
FG-23	41	D	1	reduced	n	n	Silt/clay with large and small tubes @ SWI; burrowing in aRPD; v thin polychaete below aRPD	0				1 on 3
FG-23	42	A	8	reduced	n	n	Silt/clay; patchy aRPD; patchy areas of gray red sed in contact with SWI; clastic sed throughout; tubes laying on surface, looks like disturbed bottom (trawling or disposal)	0				1 on 3
FG-23	42	C	6	both	n	n	Silt/clay; clasts and tubes on surface; algal debris; void and parts of small worms in aRPD; PV image shows evidence of trawling disturbance	1	3.8	4.2	4.0	1 on 3
FG-23	42	D	1	reduced	n	n	Silt/clay; clast is artifact from SPI frame; tube structures visible in aRPD; one void is at base of aRPD; evidence of burrowing at depth	2	4.2	9.6	6.9	1 on 3
FG-23	43	A	0		n	n	Silt/clay with small tubes at surface; polychaetes below aRPD; evidence of burrowing at depth	0				1 on 3
FG-23	43	B	6	both	n	n	Silt/clay with mud clasts artifacts from SPI frame; large tube on far right; burrowing through aRPD; worm below aRPD on right;	0				1 on 3
FG-23	43	C	1	reduced	n	n	Silt/clay with wiper blade artifact clast @ SWI; small tubes on surface; burrowing through aRPD; voids just below aRPD	2	2.6	3.8	3.2	1 on 3
FG-23	44	A	1	oxidized	n	n	Silt/clay with burrowing through aRPD; bits of worms against faceplate at depth; large void at base	1	14.0	16.3	15.2	1 on 3
FG-23	44	B	1	oxidized	n	n	Silt/clay with small tubes at surface; tubes incorporated in aRPD to ~2 cm; two voids are small at base on aRPD, bisected vertical burrow with dark red sed at bottom; parts of worms against faceplate at depth	3	2.0	11.3	6.6	1 on 3
FG-23	44	C	7	both	n	n	Silt/clay with mud clast artifacts from SPI frame; burrowing in upper cms; few v thin worms against faceplate at various depths	0				1 on 3
SE-REF	45	A	2	reduced	n	n	Silt/clay with mud clast artifacts from SPI frame; tubes incorporated in upper cm and visible against faceplate at ~2 cm; burrowing through aRPD; thin polychaete at depth	0				1 on 3
SE-REF	45	B	3	reduced	n	n	Silt/clay with clast artifacts from SPI frame; many tubes on surface, most on the edge of a large burrow at the right edge of the image; worm visible at depth	0				1 on 3
SE-REF	45	D	3	reduced	n	n	Silt/clay with dense tubes @ SWI, transected burrows at depth.	3	2.7	5.1	3.9	1 on 3

Sediment-Profile Image Analysis Results for MBDS Survey, September/October 2012

Location	Station	Replicate	Mud Clast Number	Mud Clast State	Methane?	Low DO?	Comment	# of Feeding Voids	Void Minimum Depth (cm)	Void Maximum Depth (cm)	Void Average Depth (cm)	Successional Stage
SE-REF	46	B	11	reduced	n	n	Silt/clay with clast artifacts from SPI frame; transected burrow at depth.	0				1 on 3
SE-REF	46	C	8	both	n	n	Silt/clay with clast artifacts from SPI frame; debris on surface; tubes @ SWI with burrowing through aRPD; worm near base of aRPD; small void at depth	1	16.6	17.2	16.9	1 on 3
SE-REF	46	D	4	both	n	n	Silt/clay with clast artifacts from SPI frame; v thin polychaetes in aRPD, evidence of burrowing at depth	0				1 on 3
SE-REF	47	A	ind		n	n	Over-penetration; all but deepest void are small; worm against faceplate	5	2.8	18.7	10.7	1 on 3
SE-REF	47	B	ind		n	n	Over-penetration; burrowing in aRPD; small void at below aRPD	1	5.0	5.1	5.0	1 on 3
SE-REF	47	D	4	reduced	n	n	Silt/clay; burrowing through aRPD; evidence of void at depth on left;	0				1 on 3
SE-REF	48	A	0		n	n	Silt/clay; burrowing through aRPD; closed end of burrow below aRPD on left; v thin polychaete at depth	0				1 on 3
SE-REF	48	C	4	reduced	n	n	Silt/clay with clast artifacts from SPI frame; burrowing in aRPD; relict aRPD; one portions of polychaetes visible at depth	0				1 on 3
SE-REF	48	D	3	reduced	n	n	Silt/clay with clast artifact from SPI frame; burrowing in aRPD; one void right below aRPD; polychaete at depth	2	5.1	18.9	12.0	1 on 3

APPENDIX C

PLAN-VIEW IMAGE ANALYSIS RESULTS FOR MBDS SURVEY, SEPTEMBER/OCTOBER 2012

Plan-View Image Analysis Results for MBDS Survey, September/October 2012

Location	Station	Replicate	Date	Time	Image Width (cm)	Image Height (cm)	Field-of-View imaged (m2)	Sediment Type	Bedforms	Burrows	Tubes	Tracks	Epifauna	Mud Clasts	Debris	Comment
MBDS-G	PV-01	E	10/18/2012	9:23:20	111.7	74.0	0.8	sandy mud with chunks of DM clay on surface	n	y	y	y	n	y	y	sandy mud with lots of clumpy DM in diffuse pile in center of image; small burrows; many tubes on surface; some debris (algal, shell)
MBDS-G	PV-01	G	10/18/2012	9:25:55	114.7	76.0	0.9	sandy mud with chunks of DM clay on surface	n	y	y	n	n	y	y	sandy mud with lots of large chunks of clumpy DM in upper right; small burrows; many tubes on surface; some debris (algal, shell)
MBDS-G	PV-01	H	10/18/2012	9:26:00	NA	NA	only left visible	sandy mud with chunks of DM clay on surface	n	y	y	y	n	n	y	turbidity obscuring much of image; sandy mud with DM layer on left; medium burrows in upper left; small burrows; some tubes
MBDS-G	PV-02	A	10/18/2012	9:48:44	118.2	78.3	0.9	sandy mud with DM	n	y	y	y	y	y	y	sandy mud with large chunks of gray DM in upper area and layer throughout; many small burrows, some tubes; short tracks in upper left; shrimp on surface; bits of algal debris
MBDS-G	PV-02	B	10/18/2012	9:49:56	115.1	76.2	0.9	sandy mud with DM	n	y	y	y	n	n	y	sandy mud with hints of gray DM under surface; many small burrows, some medium; lots of tubes on surface; regular track marks across width of image; bits of algal debris
MBDS-G	PV-02	C	10/18/2012	9:51:06	121.9	80.7	1.0	sandy mud	n	y	y	n	y	n	y	sandy mud; many small burrows; tubes on surface; bits of algal debris, shrimp in left half of image
MBDS-G	PV-03	A	10/18/2012	11:22:19	112.3	74.4	0.8	sandy mud with DM	n	y	y	y	y	n	y	sandy mud with gray DM near surface in lower right and upper left; small burrows; tubes; short tracks; algal and shell debris; shrimp; burrowing anemone at far right
MBDS-G	PV-04	A	10/18/2012	11:00:17	122.6	81.2	1.0	sandy mud	n	y	y	n	y	n	y	sandy mud; small and medium burrows; tubes; multiple shrimp on surface; some depressions on surface; bits of algal debris

Plan-View Image Analysis Results for MBDS Survey, September/October 2012

Location	Station	Replicate	Date	Time	Image Width (cm)	Image Height (cm)	Field-of-View imaged (m2)	Sediment Type	Bedforms	Burrows	Tubes	Tracks	Epifauna	Mud Clasts	Debris	Comment
MBDS-G	PV-04	D	10/18/2012	11:03:36	123.4	81.8	1.0	sandy mud	n	y	y	n	n	n	y	sandy mud; lots of small and medium burrows; tubes; some depressions on surface; bits of algal debris
MBDS-G	PV-05	A	10/18/2012	10:08:53	115.2	76.3	0.9	sandy mud with DM	n	y	y	y	y	y	y	sandy mud with gray DM near surface and in chunks at left corner; small burrows, one med; tubes; few short tracks; algal debris; shrimp
MBDS-G	PV-05	B	10/18/2012	10:10:06	113.8	75.4	0.9	sandy mud with DM	n	y	y	y	y	n	y	sandy mud with gray DM near surface; small to med burrows; tubes long track marks; bits of algal debris; shrimp
MBDS-G	PV-05	D	10/18/2012	10:12:23	110.0	72.8	0.8	sandy mud with chunks of DM clay on surface	n	y	y	y	y	y	y	sandy mud with gray DM chunks on surface; small burrows; tubes; few thin tracks; algal debris; shrimp
MBDS-G	PV-06	G	10/18/2012	10:43:52	124.0	82.2	1.0	sandy mud	n	y	y	y	y	n	y	sandy mud with some 'pockmarks' in upper left, probably from deeper burrows; med burrows; short tracks; shrimp; bits of algal debris
MBDS-G	PV-06	I	10/18/2012	11:58:40	117.7	77.9	0.9	sandy mud	n	y	y	y	y	n	y	sandy mud with some 'pockmarks' , probably from deeper burrows; med burrows; tubes on surface; multiple shrimp; bits of algal debris
MBDS-G	PV-06	J	10/18/2012	11:59:56	117.0	77.5	0.9	sandy mud	n	y	y	y	y	n	n	sandy mud with some 'pockmarks' in line across top, med burrows; tubes; shrimp
MBDS-G	PV-07	A	10/18/2012	9:55:20	128.9	85.4	1.1	sandy mud with DM	n	y	y	y	n	n	y	sandy mud with gray DM near surface at center; small and med burrows; shell frag in upper right
MBDS-G	PV-07	B	10/18/2012	9:56:21	116.5	77.1	0.9	sandy mud	n	y	y	n	y	ind	y	half obscured by suspended sed; sandy mud; possible burrows; tubes; two demersal fish
MBDS-G	PV-08	A	10/18/2012	11:15:06	119.7	79.3	0.9	sandy mud	n	y	y	y	y	n	y	sandy mud; small burrows; short track marks; tubes; multiple shrimp; bits of algal debris

Plan-View Image Analysis Results for MBDS Survey, September/October 2012

Location	Station	Replicate	Date	Time	Image Width (cm)	Image Height (cm)	Field-of-View imaged (m2)	Sediment Type	Bedforms	Burrows	Tubes	Tracks	Epifauna	Mud Clasts	Debris	Comment
MBDS-G	PV-08	B	10/18/2012	11:16:08	126.1	83.5	1.1	sandy mud	n	y	y	y	y	n	y	rel. poor visibility; sandy mud; small burrows, one larger one pit near back; shrimp at bottom of image; bits of algal debris
MBDS-G	PV-09	A	10/18/2012	10:53:08	116.5	77.1	0.9	sandy mud	n	y	y	y	y	n	y	sandy mud; med burrows; short tracks; shrimp; algal debris
MBDS-G	PV-09	B	10/18/2012	10:53:58	119.4	79.1	0.9	sandy mud	n	y	y	y	y	n	y	sandy mud; small to med burrows; couple pits; shrimp; algal debris
MBDS-G	PV-10	A	10/18/2012	11:06:30	108.2	71.7	0.8	sandy mud	n	y	y	n	y	n	y	sandy mud; small burrows; tubes; algal debris; multiple shrimp
MBDS-G	PV-11	A	10/18/2012	10:02:31	143.3	94.9	1.4	sandy mud with chunks of DM clay on surface	n	y	y	n	n	n	ind	sandy mud with gray DM chunks on surface; few burrows visible; red fish
MBDS-G	PV-11	B	10/18/2012	10:03:33	118.7	78.7	0.9	sandy mud with chunks of DM clay on surface	n	y	y	y	n	y	y	sandy mud with chunks of DM on surface in lower right and center; lots of small and medium burrows; short track marks; tubes on surface
MBDS-G	PV-11	C	10/18/2012	10:44:44	125.7	83.3	1.0	sandy mud with chunks of DM clay on surface	n	y	y	n	n	ind	y	sandy mud with chunks of DM on surface; small burrows; relatively poor visibility; bit of wood debris(?) on left
MBDS-G	PV-12	A	10/18/2012	11:28:15	116.4	77.1	0.9	sandy mud	n	y	y	y	ind	ind	ind	turbidity obscuring much of image; sandy mud
MBDS-G	PV-12	C	10/18/2012	11:30:12	111.7	74.0	0.8	sandy mud	n	y	y	y	y	n	n	sandy mud; small burrows; tubes; few tracks; either polychaete tentacles or tops of burrowing anemones
MBDS-H	PV-14	A	10/18/2012	17:07:18	104.1	68.9	0.7	sandy mud	n	y	y	y	y	n	y	sandy mud; small to med-large burrows; tubes on surface; shrimp; algal debris
MBDS-H	PV-14	D	10/18/2012	17:09:20	113.9	75.4	0.9	sandy mud	n	y	y	y	y	n	y	sandy mud; large wide burrows; tubes; shrimp; various debris
MBDS-H	PV-17	A	10/18/2012	16:58:28	114.5	75.8	0.9	silty mud	n	y	y	y	y	y	ind	silty mud; lots of small burrows; med-large burrows giving surface a pockmarked look; dark, reduced sediment at surface at upper center from burrow excavation; shrimp

Plan-View Image Analysis Results for MBDS Survey, September/October 2012

Location	Station	Replicate	Date	Time	Image Width (cm)	Image Height (cm)	Field-of-View imaged (m2)	Sediment Type	Bedforms	Burrows	Tubes	Tracks	Epifauna	Mud Clasts	Debris	Comment
MBDS-H	PV-20	A	10/18/2012	16:47:31	115.6	76.6	0.9	silty mud	n	y	y	y	n	n	ind	relatively poor resolution due to particles in water column; silty mud; lots of small burrows, couple large burrows; tracks in upper right
MBDS-H	PV-22	A	10/18/2012	17:13:48	111.0	73.5	0.8	silty mud	n	y	y	y	y	n	n	silty mud; gray reduced sed on surface around two large burrows in upper left; small burrows; tracks; shrimp
MBDS-H	PV-22	B	10/18/2012	17:14:43	116.3	77.0	0.9	silty mud	n	y	y	y	n	n	y	silty mud; thin layer of gray reduced sed on surface across center; burrows; tracks
MBDS-H	PV-22	C	10/18/2012	17:15:50	113.0	74.8	0.8	silty mud	n	y	y	y	n	n	n	silty mud; burrows, few large ones in the upper right and center; tubes; tracks
MBDS-I	PV-30	A	10/18/2012	16:16:05	132.2	87.6	1.2	sandy mud with chunks of DM and gravel	n	y	y	y	n	y	y	sandy mud with large chunks of DM, gravel; few small burrows; tubes
MBDS-I	PV-30	B	10/18/2012	16:17:04	125.6	83.2	1.0	sandy mud with debris and chunks of DM	n	y	y	n	y	y	y	sandy mud with large chunks of DM, gravel; stick across bottom left; few burrows, crab in upper right
MBDS-I	PV-30	C	10/18/2012	16:18:00	109.6	72.6	0.8	sandy mud with chunks of DM, gravel, one boulder	n	n	y	y	n	y	y	sandy mud with large chunks of DM, gravel, large boulder; tracks upper left; shell frag at surface
MBDS-I	PV-31	A	10/18/2012	16:21:34	112.0	74.2	0.8	sandy mud with large mound of DM	n	y	y	n	n	y	y	sandy mud with large mound of DM; med burrows (fauna in one at far right)
MBDS-I	PV-31	B	10/18/2012	16:22:47	126.5	83.8	1.1	sandy mud	n	y	y	n	n	n	y	sandy mud with some gray sediment on surface; pockmarked surface; few med burrows
MBDS-I	PV-31	C	10/18/2012	16:23:48	115.3	76.4	0.9	sandy mud	n	y	y	n	n	y	y	sandy mud, bit of gray sed on surface at upper left; burrows, tubes
MBDS-I	PV-34	A	10/18/2012	16:09:15	122.1	80.9	1.0	sandy mud with chunk of DM	n	y	y	n	y	y	y	sandy mud with large chunk of DM at base; small to med burrows; tubes; shrimp

Plan-View Image Analysis Results for MBDS Survey, September/October 2012

Location	Station	Replicate	Date	Time	Image Width (cm)	Image Height (cm)	Field-of-View imaged (m2)	Sediment Type	Bedforms	Burrows	Tubes	Tracks	Epifauna	Mud Clasts	Debris	Comment
MBDS-I	PV-34	B	10/18/2012	16:10:06	NA	NA	not visible	sandy mud with chunks of DM	n	n	y	ind	ind	y	ind	sandy mud with large chunks of DM; fish; relatively poor image resolution from particles in water column
MBDS-I	PV-34	D	10/18/2012	16:12:31	128.9	85.4	1.1	sandy mud with boulders	n	y	y	n	y	y	ind	sandy mud with large boulders; fish; small burrows, tubes
MBDS-I	PV-36	A	10/18/2012	16:27:48	116.8	77.4	0.9	sandy mud	n	ind	y	n	ind	ind	y	silty mud, pockmarked surface; tubes
MBDS-I	PV-36	B	10/18/2012	16:28:57	117.8	78.0	0.9	sandy mud	n	y	y	n	y	y	y	silty mud, some pockmarks on surface; few small burrows; tubes; shrimp
MBDS-I	PV-36	C	10/18/2012	16:30:13	117.3	77.7	0.9	sandy mud	n	y	y	y	y	n	y	silty mud, pockmarks on surface; few small burrows; tubes; shrimp
MBD-REF	PV-37A	A	10/18/2012	14:49:36	117.7	77.9	0.9	silty mud	n	y	y	n	y	y	n	silty mud, few pockmarks; med burrows; tubes; shrimp
MBD-REF	PV-37A	B	10/18/2012	14:50:52	110.1	72.9	0.8	silty mud	n	y	y	y	y	y	y	silty mud; small to large burrows; tubes; tracks; algal debris
MBD-REF	PV-38	A	10/18/2012	14:12:00	109.5	72.5	0.8	silty mud	n	y	y	n	y	n	n	silty mud; burrowing anemones; burrows; tubes
MBD-REF	PV-38	B	10/18/2012	14:13:02	111.2	73.7	0.8	silty mud	n	y	y	y	y	y	ind	silty mud; burrowing anemones; burrows; tubes; shrimp
MBD-REF	PV-38	C	10/18/2012	14:14:09	NA	NA	not visible	silty mud	n	y	y	y	y	ind	ind	silty mud; burrowing anemones; much of image is obscured by suspended sed
MBD-REF	PV-39	A	10/18/2012	13:58:49	107.9	71.5	0.8	silty mud	n	y	y	n	n	y	y	silty mud; small to large burrows; algal debris
MBD-REF	PV-39	C	10/18/2012	14:01:09	113.9	75.4	0.9	silty mud	n	y	y	n	y	n	y	silty mud; small to large burrows; v. large 'pit' on right edge; shrimp
MBD-REF	PV-39	D	10/18/2012	14:02:26	111.4	73.8	0.8	silty mud	n	y	y	n	n	n	y	silty mud; small to large burrows; algal debris
MBD-REF	PV-40	B	10/18/2012	14:27:43	109.4	72.5	0.8	sandy mud	n	y	y	n	y	y	y	sandy mud; med to large burrows; shrimp; algal debris
MBD-REF	PV-40	C	10/18/2012	14:28:45	108.6	71.9	0.8	sandy mud	n	y	y	y	n	n	y	sandy mud; small to med burrows; relatively low resolution
MBD-REF	PV-40	D	10/18/2012	14:29:41	110.1	72.9	0.8	sandy mud	n	y	y	y	n	y	y	sandy mud; small to large burrows; tubes

Plan-View Image Analysis Results for MBDS Survey, September/October 2012

Location	Station	Replicate	Date	Time	Image Width (cm)	Image Height (cm)	Field-of-View imaged (m2)	Sediment Type	Bedforms	Burrows	Tubes	Tracks	Epifauna	Mud Clasts	Debris	Comment
FG-23	PV-41	B	10/18/2012	15:17:44	114.5	75.8	0.9	silty mud	n	y	y	y	y	y	y	silty mud; small burrows, med-large burrows; tracks; tubes; algal debris, shrimp
FG-23	PV-41	C	10/18/2012	15:18:45	117.3	77.7	0.9	silty mud	n	y	y	y	n	y	y	silty mud; small burrows, med burrows; tubes; algal debris
FG-23	PV-41	D	10/18/2012	15:19:52	106.5	70.5	0.8	silty mud	n	y	y	y	y	y	y	silty mud; many small burrows; med and large burrows; tubes; algal debris; shrimp; mud sea star
FG-23	PV-42	A	10/18/2012	15:23:37	119.5	79.2	0.9	silty mud	n	y	y	y	y	y	n	silty mud; chunks of possible DM or trawling disturbance on surface; small to large burrows; tubes; burrowing anemone
FG-23	PV-42	C	10/18/2012	15:25:30	109.3	72.4	0.8	silty mud	n	y	y	y	n	n	y	silty mud; many tubes; small to large burrows, downslope furrow in upper left indicates trawling scar
FG-23	PV-42	D	10/18/2012	15:26:22	107.7	71.3	0.8	silty mud	y	y	y	y	y	n	y	silty mud; many small burrows, several large; tubes
FG-23	PV-43	A	10/18/2012	15:39:32	109.0	72.2	0.8	silty mud	n	y	y	y	y	n	y	silty mud; small to large burrows; tracks; shrimp
FG-23	PV-43	B	10/18/2012	15:40:36	111.4	73.8	0.8	silty mud	n	y	y	y	n	y	y	silty mud; small to med burrows; tracks; cloud of suspended sed
FG-23	PV-43	C	10/18/2012	15:41:37	118.4	78.4	0.9	silty mud	n	y	y	n	n	y	n	silty mud; small to large burrows; tubes; mud from SPI frame in view
FG-23	PV-44	A	10/18/2012	15:30:59	119.2	78.9	0.9	silty mud	n	y	y	y	n	n	y	silty mud; small to large burrows; tubes
FG-23	PV-44	B	10/18/2012	15:32:18	111.9	74.1	0.8	silty mud	n	y	y	y	y	n	y	silty mud; small to med-large burrows; tubes; algal debris; shrimp
FG-23	PV-44	C	10/18/2012	15:33:20	121.6	80.5	1.0	silty mud	n	y	y	y	n	n	y	silty mud; small to large burrows; tracks; algal debris
SE-REF	PV-45	A	10/18/2012	13:24:57	115.3	76.4	0.9	silty mud	n	y	y	n	y	y	y	silty mud; small infaunal to very large lobster burrows; tubes; shrimp; algal debris
SE-REF	PV-45	B	10/18/2012	13:25:59	109.9	72.8	0.8	silty mud	n	y	y	n	y	y	y	silty mud; small to large burrows; tubes; shrimp; algal debris
SE-REF	PV-45	D	10/18/2012	13:28:18	118.5	78.5	0.9	silty mud	n	y	y	n	n	y	y	silty mud; small to med-large burrows; tubes; algal debris

Plan-View Image Analysis Results for MBDS Survey, September/October 2012

Location	Station	Replicate	Date	Time	Image Width (cm)	Image Height (cm)	Field-of-View imaged (m2)	Sediment Type	Bedforms	Burrows	Tubes	Tracks	Epifauna	Mud Clasts	Debris	Comment
SE-REF	PV-46	B	10/18/2012	12:56:14	112.3	74.4	0.8	silty mud	n	y	y	y	y	y	y	silty mud; small and very large burrows; tracks; tubes; algal debris
SE-REF	PV-46	C	10/18/2012	12:57:17	105.1	69.6	0.7	silty mud	n	ind	y	y	y	y	ind	silty mud; v fine suspended sed from previous rep obscures most of image; tubes and clasts visible; shrimp
SE-REF	PV-46	D	10/18/2012	12:58:18	109.6	72.6	0.8	silty mud	n	y	y	y	y	n	y	silty mud; small to large burrows; tracks; tubes; algal debris
SE-REF	PV-47	A	10/18/2012	13:06:49	108.2	71.7	0.8	silty mud	n	y	y	n	n	n	y	silty mud; med-large burrows; tubes; algal debris, fish
SE-REF	PV-47	B	10/18/2012	13:07:59	112.0	74.2	0.8	silty mud	n	y	y	n	n	n	y	silty mud; small to large burrows; clasts; algal debris
SE-REF	PV-47	D	10/18/2012	13:10:47	106.6	70.6	0.8	silty mud	n	y	y	y	y	n	y	silty mud; small to large burrows; tubes; short tracks; shrimp
SE-REF	PV-48	A	10/18/2012	13:17:02	106.5	70.5	0.8	silty mud	n	y	y	y	n	n	y	silty mud; small to med burrows; tubes; algal debris
SE-REF	PV-48	C	10/18/2012	13:19:22	111.0	73.5	0.8	silty mud	n	y	y	y	n	n	y	silty mud; small to large burrows; tubes; algal debris
SE-REF	PV-48	D	10/18/2012	13:20:49	109.0	72.2	0.8	silty mud	n	y	y	y	n	n	y	silty mud; small to med burrows; tubes; algal debris

APPENDIX D

GRAIN SIZE SCALE FOR SEDIMENTS

APPENDIX D

Grain Size Scale for Sediments

Phi size	Size range (mm)	Size class (Wentworth class)
<-1	>2	Gravel
0 to −1	1 to 2	Very coarse sand
1 to 0	0.5 to 1	Coarse sand
2 to 1	0.25 to 0.5	Medium sand
3 to 2	0.125 to 0.25	Fine sand
4 to 3	0.0625 to 0.125	Very fine sand
>4	<0.0625	Silt/clay

APPENDIX E

TABLE OF COMMON CONVERSIONS

APPENDIX E

Table of Common Conversions

Metric Unit Conversion to English Unit		English Unit Conversion to Metric Unit	
1 meter 1 m	3.2808399 ft	1 foot 1 ft	0.3048 m
1 square meter 1 m^2	10.7639104 ft^2	1 square foot 1 ft^2	0.09290304 m^2
1 kilometer 1 km	0.621371192 mi	1 mile 1 mi	1.609344 km
1 cubic meter 1 m^3	1.30795062 yd^3	1 cubic yard 1 yd^3	0.764554858 m^3
1 centimeter 1 cm	0.393700787 in	1 inch 1 in	2.54 cm